MODELLING SAND BYPASS SCHEMES ON THE KWAZULU-NATAL COASTLINE

Calvin Paul Wells

Submitted in fulfilment of the requirements for the degree of
Master of Science in Engineering
In the
Civil Engineering programme
University of KwaZulu-Natal
Durban
2015

Supervisors: Professor D. D. Stretch
Dr S. Corbella

ABSTRACT

Coastal structures such as breakwaters cause a disruption of longshore sediment transport along coastlines. The result of this disruption creates sand accumulation up-drift and beach erosion down-drift of these structures. Therefore, sediment bypass schemes are implemented by dredging the sand out of the sand trap up-drift of the structures and nourishing the beach down-drift of them. The beach north of the Richards Bay harbour entrance in KZN, South Africa was used as a case study to model and compare alternative nourishment schemes to alleviate chronic beach erosion due to disruption of the longshore sediment supply.

This study used the Delft3D 2DH sediment transport models to investigate the nourishment schemes and a calibration study was done to test the capability of the models to maintain a theoretical equilibrium profile over a long term simulation. Subsequently the model was used to investigate and compare three nourishment schemes at a case study site over a period of a year to determine the beach response to the nourishment. The sediment budget for the nourishment schemes was limited to 1 000 000 m^3 per year. The first scheme comprised of a continuous steady nourishment throughout the year and the second scheme was a bulk nourishment where the sediment is dumped onto the beach at the maximum dredging capacity, in this case 10 000 m^3/day. The last was a bimonthly sediment nourishment scheme.

The model calibration results revealed that a single wave related transport factor governs the cross-shore movement direction. A single set of parameters does not produce offshore sediment movement during large wave events and onshore movement during smaller wave events as observed in reality. Therefore, the model was unable to reproduce a quasi-equilibrium behaviour unless the cross-shore transport factors are allowed to vary as a function of wave height. It was possible to define a cross-shore factor within the Van Rijn transport model that limited the cross-shore movement over a long term morphological simulation resulting in only the longshore transport affecting the morphology within the model. This model setup was used for the case study since a lack of sediment supply was the main focus of this study. The continuous steady nourishment results showed a natural longshore shore movement of sediment down-drift of the harbour entrance and a uniform beach width increase along the entire beach. The bimonthly nourishment closely emulated the continuous nourishment resulting in a net increase of beach width along the modelled coastline. The bulk nourishment revealed significant differences to the previous cases. The sheltering effect of the northern breakwater kept the main recreational beach in a nourished state while the northern beach outside of the breakwater's shadow-zone returned to its initial sand starved state.

COLLEGE OF AGRICULTURE, ENGINEERING AND SCIENCE

DECLARATION - PLAGIARISM

I, Calvin Paul Wells declare that

1. The research reported in this thesis, except where otherwise indicated, is my original research.

2. This thesis has not been submitted for any degree or examination at any other university.

3. This thesis does not contain other persons' data, pictures, graphs or other information, unless specifically acknowledged as being sourced from other persons.

4. This thesis does not contain other persons' writing, unless specifically acknowledged as being sourced from other researchers. Where other written sources have been quoted, then:
    a. Their words have been re-written but the general information attributed to them has been referenced
    b. Where their exact words have been used, then their writing has been placed in italics and inside quotation marks, and referenced.

5. This thesis does not contain text, graphics or tables copied and pasted from the Internet, unless specifically acknowledged, and the source being detailed in the thesis and in the References sections.

Signed

…… ……

C. P. Wells Date

…… ……

D. D. Stretch Date

ACKNOWLEDGEMENTS

I would like to express my acknowledgement of the following:

Firstly to Professor D.D. Stretch, whose door was always open and his continual advice was always appreciated. I would also like to thank him for the subsistence funding which made this research possible.

Secondly I would like to thank Stefano Corbella, who always had time to listen to my ideas and give me a push in the right direction when I needed it most.

I would also like to thank the Durban Municipality for funding the surveys which were crucial to this study and Clinton Crystal.

Last but not least I would like to thank my family and friends for their constant support throughout the year. They kept me on track and always believed in me.

TABLE OF CONTENTS

LIST OF FIGURES

LIST OF TABLES

LIST OF SYMBOLS

A	=	Equilibrium profile shape parameter.
A_{fac}	=	Bijker wave asymmetry factor.
c	=	Wave celerity (m/s).
D_{50}	=	Median grain size (µm).
D_{90}	=	Ninetieth percentile of the grain size (µm).
E	=	Wave energy (J/m^2).
F_y	=	Longshore driving force (N/m^2).
f_{sus}	=	van Rijn wave related suspended transport factor.
g	=	Gravitational acceleration (m/s^2).
γ	=	Wave breaking index.
α_b	=	Beach steepness.
H	=	Wave height (m).
H_b	=	Breaking wave height (m).
H_s	=	Significant wave height (m).
H_0	=	Deep water wave height (m).
h	=	Water depth (m).
h_b	=	Breaking wave water depth (m).
δ	=	Iribarren Number.
k	=	Wave number (m^{-1}).

L = Wave length (m).

L_0 = Deep water wave length (m).

Q = Bulk longshore sediment transport rate (m^3/s).

ρ = Density of water (kg/m^3).

ρ_s = Density of sediment (kg/m^3).

θ = Direction of wave propagation (^{o}).

T = Wave period (s).

τ = Bottom stress (N/m^2).

U_{on} = Onshore near bed orbital velocity (m/s).

U_{off} = Offshore near bed orbital velocity (m/s).

$\bar{u}$ = Depth averaged velocity (m/s).

w = Particle settling velocity (m/s).

CHAPTER 1

Introduction

1.1 Motivation

Coastal structures such as breakwaters are a common engineering practice that protect the harbour bays from energetic wave climates. However, these structures cause a disruption of the longshore sediment transport along the coastline. This disruption traps sand which causes sediment accumulation up-drift and beach erosion down-drift of the structure. Therefore sediment bypass schemes are implemented by dredging the sand out of the sand trap and nourishing the beach down-drift of the harbour entrance. Ineffective bypass schemes have many negative impacts including too much sediment accumulating in the sand trap and spilling into the harbour entrance. It can also cause significant loss of beach down-draft of the breakwater due to longshore sediment transport and a lack of sediment supply from the sand trap (Dean, 2002).

The energetic wave climate along the east coast of South Africa (Corbella & Stretch, 2012) results in a dynamic coastline experiencing morphological changes and longshore sediment movement up to 1 000 000 m^3 per year (Schoonees, 2000). The beaches north of Richards Bay in KwaZulu-Natal, South Africa are a typical example of how anthropogenic coastal activities such as harbour entrances have an impact on the morphological evolution of coastlines down-drift of hard engineering coastal structures (Figure 1.1)

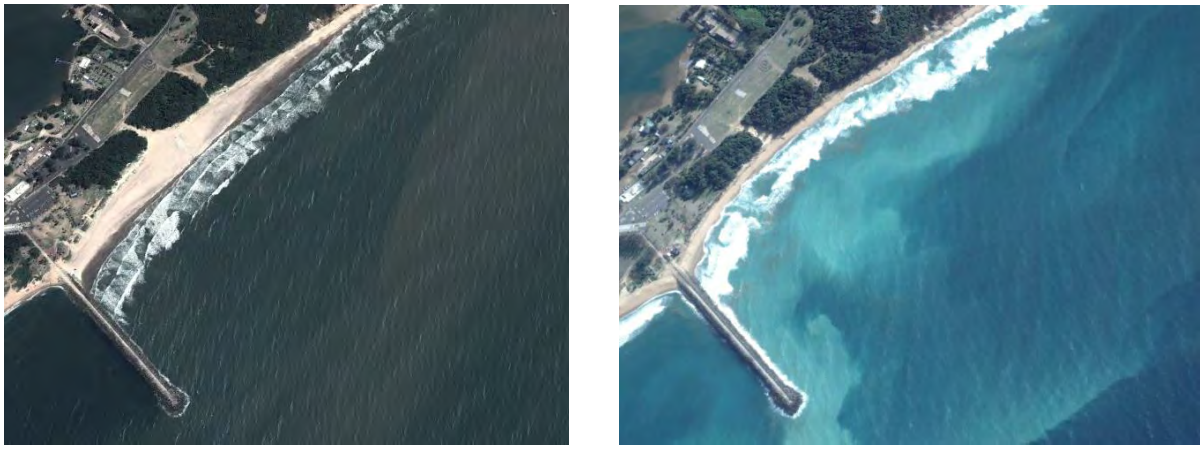

Figure 1.1: a) Aerial photograph of post nourished beach Alkantstrand (Google Earth, 2011). b) Aerial photograph of sand starved beach Alkantstrand (Google Earth, 2015) .

This shoreline retreat and the influence of sea level rise, estimated at 3mm per year (Mather & Stretch, 2012), increases the vulnerability of both coastal structures in lowlands and coastal wetlands due to storm surges and wave action. This has both environmental and economic impacts resulting from damage to the coastal structures and salt water advancing landward. This can inundate agriculture, estuaries and water supplies. It also causes a reduction in beach width resulting in a negative impact on tourism and recreational benefits of the beach (IPCC, 1990).

Due to environmental concerns, coastal engineering is shifting away from hard structures such as breakwaters and groynes and moving towards soft engineering solutions. Bypass schemes that involve beach sand nourishment is a soft engineering solution used to reduce coastal vulnerability as well as reduce the negative impacts down-drift of hard engineering structures along coastlines. Implemented correctly, sand nourishment schemes can be a cost effective solution to coastal vulnerability with environmental and economic benefits while reducing storm damage. Increased beach widths enhance recreational activities along the beach and it has been observed that the value of properties upland of beach nourishment schemes can increase up to 20%. It also provides a constructive use for sediment dredged out of harbour breakwater sand traps. (Dean, 2002).

This thesis investigates alternative sediment bypass schemes and compares the beach response of three different sand nourishment techniques along the coast down-drift of the Richards Bay harbour. The cross-shore sediment movement is expected to have a seasonal effect of erosive conditions during storms and accretion conditions during calm periods effectively maintaining an equilibrium cross-shore profile. Therefore, the beach loss north of the Richards Bay harbour is a result of longshore sediment transport and a lack of sediment supply was the main focus of this study.

Delft3D is a coastal process based modelling software which has the ability to model spectral waves, hydrodynamics and sediment transport making it an ideal tool to investigate beach nourishment through use of a case study. Previous research into the capabilities of the Deflt3D sediment transport models revealed that these models are capable of being calibrated to accurately represent the longshore sediment transport along the eastern coast of South Africa as well as simulating specific cross-shore erosion or accretion events. However, there is limited research on long term cross-shore morphology modelling along the South African coastline. Along most coastlines, beaches exhibit a seasonal cross-shore movement of sediment experiencing erosion during larger waves and accretion during smaller waves that typically act over a longer period (Figure 1.2) (Dean & Dalrymple, 2004).

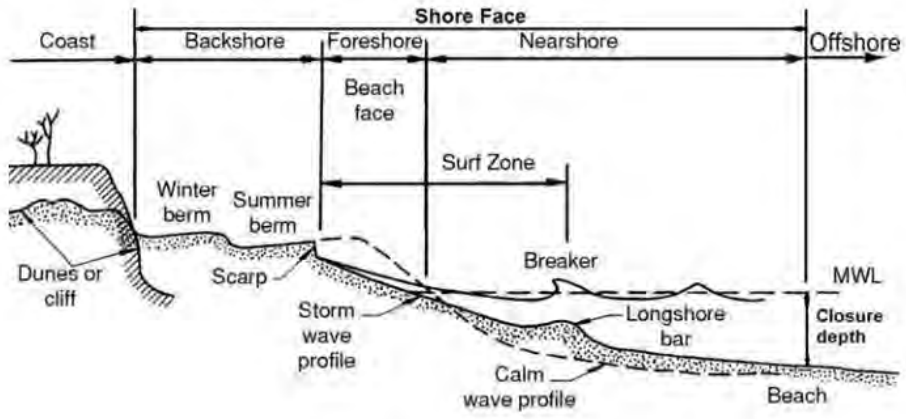

Figure 1.2: Cross-section showing the seasonal changes in beach profile *(Ataei, et al., 2014)*.

The Deflt3D sediment transport models utilised in this study are coupled with the 2 Dimensional Horizontal (2DH) hydrodynamic model which does not directly model the 3D (Three Dimensional) effects that occur in the surf-zone. These 3D effects, such as undertow, are the main drivers of the cross-shore sediment transport that occur in the surf-zone and are therefore parameterized by user-defined parameters within the depth averaged Deflt3D sediment transport models. In reality, beach profiles tend to erode away from and accrete towards a quasi-equilibrium profile dependent on the energy within the coastal system. Therefore, it is important to determine whether the Delft3D coastal sediment models are capable of reproducing this quasi-equilibrium cross-shore behaviour over a long term simulation with the calibration of the parameters influencing the cross-shore sediment transport. The calibration of the cross-shore sediment transport parameters will aid in a better understanding of how the models analyse the cross-shore sediment movement and how the models can be improved to more accurately represent the morphological changes experienced along the South African coastline.

1.2 Research Questions

This research poses two questions. The first question concerns the capability of Delft3D and relates to the methodology for addressing the second question.

Can the Delft3D depth averaged coastal sediment transport models be calibrated to predict beach erosion during storm wave events and beach recovery during smaller wave events resulting in an equilibrium cross-shore profile over time?

How does a beach down-drift of a harbour entrance respond to beach nourishment due to alternative sand bypass schemes over a period of a year?

1.3 Aim

To investigate whether the Delft3D depth averaged sediment transport models are capable of reproducing an equilibrium cross-shore profile with the calibration of the wave related factors influencing the cross-shore sediment transport.

Evaluate and compare alternative sand nourishment schemes along a sand depleted beach as a result of alternative sediment bypass schemes.

1.4 Objectives

To determine the capabilities of the Delft3D sediment transport models with respect to the cross-shore movement of sand, the following objectives need to be achieved:

1. To become proficient in Delft3D coastal process modelling software including curvilinear grid generation and spectral wave modelling coupled with the 2 DH and sediment transport model.
2. Understand and determine how waves influence the cross-shore movement of sediment along a coastline in reality.
3. Understand the physics involved in the Deflt3D coastal sediment transport models and how the calibration of the models affects the cross-shore movement of sediment.
4. Test whether the sediment transport models used are capable of maintaining an equilibrium profile by predicting offshore movement of sediment during large wave events and onshore movement during smaller wave events.
5. Provide recommendations on how to improve the realism of the cross-shore movement prediction within the Delft3D sediment transport models over a long term period.

In order to evaluate and compare alternative beach nourishment schemes the following objectives focus on setting up a case study at Richards Bay with the aim of simulating alternative sediment pumping rates onto Alkantstrand and comparing the predicted beach response to the different schemes using Delft3D:

1. Collecting relevant morphological and wave data for Richards Bay in order to set up a model in Delft3D for the case study.
2. Calibrate the model to predict realistic sediment transport rates for a period of one year.
3. Implement alternative beach nourishment schemes along the area of interest as a result of the sediment bypass using the sediment nourishment function within Delft3D.
4. Analyse and compare the beach response to the alternative nourishment schemes.
5. Make recommendations with regards to the most effective bypass scheme for beaches along the east coast of South Africa taking both economic and environmental impacts into consideration.

1.5 Dissertation Outline

This dissertation contains the following chapters:

Chapter 2 is a literature review pertaining to the theory of coastal processes and previous research done on coastal morphology and beach nourishment. Ocean waves and how they relate to surf-zone hydrodynamics are discussed as well as the drivers of sediment transport in a coastal system. The review includes an analysis of the coastal process models used and empirical research done on sediment transport.

Chapter 3 outlines and describes the Richards Bay case study beach. It includes a description of the location, relevant wave, tide and morphological data available, current dredging infrastructure and why it is a suitable location for a beach nourishment case study.

Chapter 4 discusses the methods used to test the cross-shore sediment transport capability of the Delft3D depth averaged models. It also discusses the model setup for the sediment bypass case study and the analysis to be undertaken.

Chapter 5 presents the results of the cross-shore transport model capability study. It discusses how the calibration coefficients for the sediment transport models affect the predicted morphology. Recommendations are then presented on how to improve the realism of the cross-shore sediment transport predicted by the Delft3D depth averaged models. This chapter also provides a recommendation for the choice of sediment transport model used in the case study.

Chapter 6 discusses the results of the Richards Bay sediment bypass case study. It presents modelled results of the beach response and sediment distribution for alternative nourishment schemes and morphological changes over the period of a year. It also discusses the economic considerations and environmental impacts associated with the different schemes.

Chapter 7 presents the conclusions drawn by both the Delft3D cross-shore sediment transport capability study and the sediment bypass case study. It offers recommendations on improving morphological modelling using Delft3D and the implementation of beach nourishment schemes. Recommendations are made regarding further research.

CHAPTER 2

Literature Review

2.1 Wind-Generated Waves

Ocean waves are considered to be the oscillations of the water which propagate along the ocean's surface away from the area of wave generation (Bosboom & Stive, 2012). Airy (1845) developed a simple linear wave theory (Figure 2.1) used to describe the displacement of the water surface η (x, t) due to these oscillations:

$$\eta(x,t) = \frac{H}{2}\cos k(x - Ct) \tag{2-1}$$

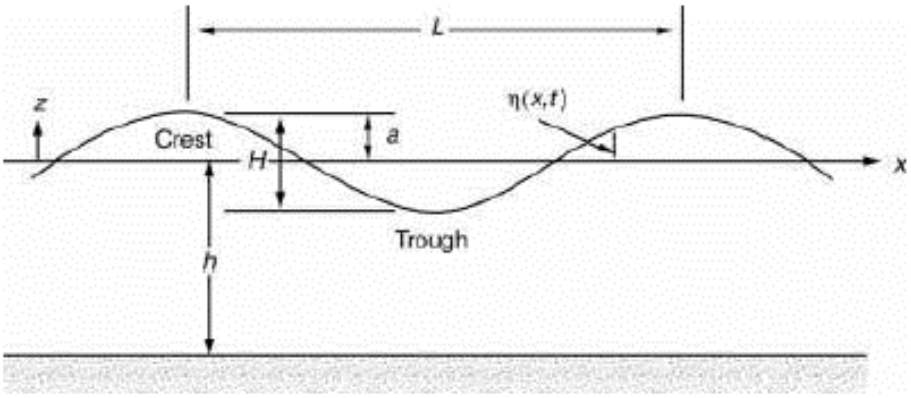

Figure 2.1: Schematic of a wind generated wave *(Dean & Dalrymple, 2004)*

In which:

H = Wave Height

k = $\frac{2\pi}{CT}$

L = Wave Length

C = Wave Celerity

The height of the wave can be interpreted as indicative of the energy per unit surface area.

The wave energy per unit area can be defined as:

$$E = \frac{1}{8}\rho g H^2 \tag{2-2}$$

where ρ is the water density, g is the acceleration of gravity and H is the wave height (Dean & Dalrymple, 2004).

Wind blowing over the ocean creates a frictional stress on the water surface. This frictional stress causes a transfer of momentum and energy resulting in the disturbance of water particles from their original position in the water column. Gravity then acts as the restoring force which dampens the wave motion by restoring the water particles to their natural position in the water column. The principle restoring force is gravity, therefore the waves generated are known as gravity waves (Wright, et al., 1999). According to Jeffreys (1925), wind waves gain energy through the sheltering effect of wave crests from the wind. The rear face of the wave will experience a higher pressure due to the force of the wind against it and air eddies at the front face of the wave will cause a low pressure in front of the wave (Figure 2.2). This difference in pressure will push the wave and result in the wave gaining energy (Jefferys, 1925).

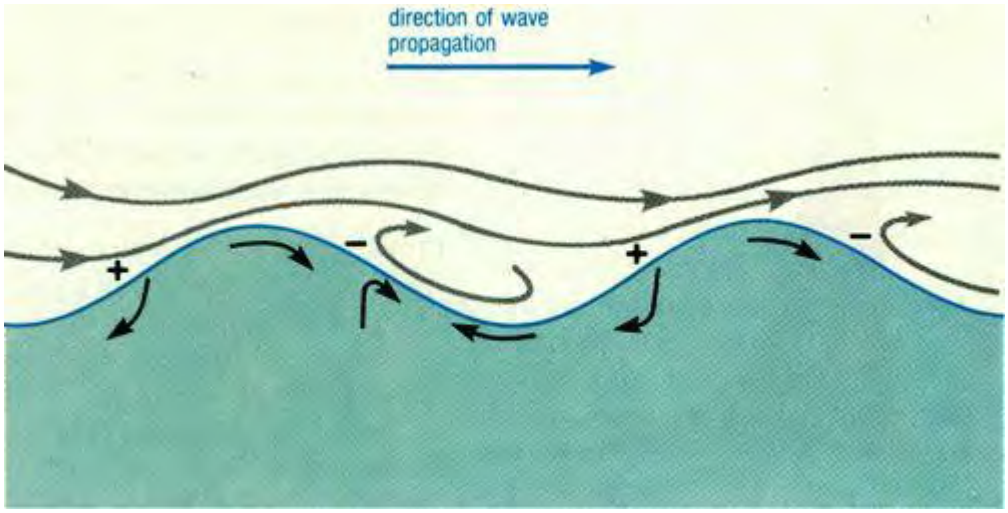

Figure 2.2: Jefferys' sheltering wave generation theory. (High pressure indicated with a positive sign and low pressure indicated with a negative sign)

For Jefferys' theory to hold true, wind speeds must exceed one meter per second as well as the wave speed and the waves had to be steep enough to create a sheltering effect (Thomson, 1981).

A local wind field or storm over the ocean create short, random and irregular waves called sea. The wave size in deep water is dependent on wind speed, length of time the wind blows and fetch, which is the distance of unobstructed sea over which the wind blows. Due to variations in wind over the

ocean, a fully developed sea is made up of varying wave heights and lengths which is known as a wave field (Wright, et al., 1999).

Waves can travel away from the point of generation over long distances before reaching the coastline. In doing so, they become longer, faster and more regular and are referred to as swell. This transformation is caused by shorter waves filtering out through dissipation processes such as white-capping and currents which have a larger effect on shorter waves (Bosboom & Stive, 2012). According to Bosboom and Stive (2012), the spectrum of swell is narrow in both direction and frequency as it approaches a coastline. Both sea and swell are primary suppliers of energy to a coastal system (Bosboom & Stive, 2012). Therefore an accurate analysis and schematisation of the wave climate along the coastline of interest is required in order to accurately determine the sediment transport.

2.2 Wave Transformations

1. Shoaling

As waves propagate into shallower water, the waves will be influenced by the seabed when the depth of water becomes approximately less than half the wave length. As the depth decreases, so will the wavelength as stated by the dispersion relationship of waves (Dean & Dalrymple, 2004):

$$L = \frac{g}{2\pi} T^2 \tanh(kh) \qquad (2\text{-}3)$$

In which:

T = Wave Period

Due to the wave period being constant, this will result in a decrease of wave length and velocity and an increase in wave height as shoaling occurs. This causes non-linearity of waves in shallow water (Bosboom and Stive, 2012). Shoaling will result in wave asymmetry which is an important factor influencing the onshore movement of sediment.

This transformation would occur along the majority of Southern Africa's coastal systems as the waves propagate into shallower water and interact with the sea bed. The increase in wave height along with the decrease in depth will lead to the breaking of the waves which is the predominant cause of sediment transport along the South African coastline.

2. Refraction

As a wave approaches the shore at an angle to the rising seabed contours, the crest of the wave in deeper water moves faster than the crest of the wave in shallower water. The faster part of the wave in deeper water will try catch up with the shallower section and will result in the crest of the wave turning towards the depth contours as seen in Figure 2.3. This change in wave propagation angle is called refraction (Bosboom and Stive, 2012).

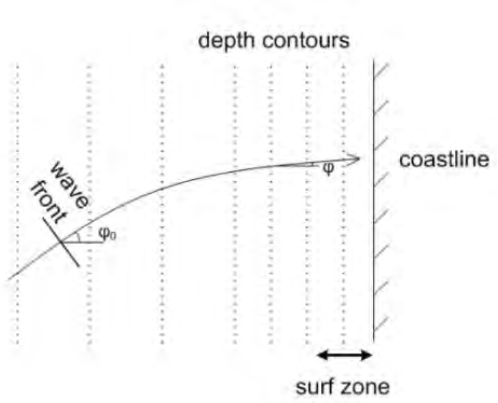

Figure 2.3: Obliquely Incident Waves Propagating on Uniform Depth Contours *(Dean & Dalrymple, 2004)*.

The change in wave direction proportional to the wave speed can be expressed by Snell's Law:

$$\frac{sin\varphi_1}{c_1} = \frac{sin\varphi_2}{c_2} \tag{2-4}$$

where φ_1 is the deep water wave direction, φ_2 is the nearshore refracted wave direction, c_1 is the deep water wave celerity and c_2 is the nearshore refracted wave celerity.

Refraction has a significant effect on the angle at which waves approach the shoreline. Therefore, the effect of refraction has to be carefully considered in this research due to sediment transport. The sediment transport formulas are sensitive to the angle at which the waves approach the shore. A decrease in the angle between the incoming wave direction and the normal of the beach results in a decrease in the longshore sediment transport. This means that wave refraction can cause a decrease in longshore sediment transport dependent on the deep water wave approach direction.

3. Diffraction

Diffraction occurs due to the transfer of energy along the wave crests when a propagating wave encounters an obstruction, such as a breakwater (Bosboom and Stive, 2012). When a propagating

wave encounters an obstruction or sudden change in bottom contours, there is an abrupt change in the wave energy along the wave crest resulting in wave height and direction changes. This causes the waves to turn and propagate into a shadow zone created by the obstruction (Figure 2.4) (Dean and Dalrymple, 2004).

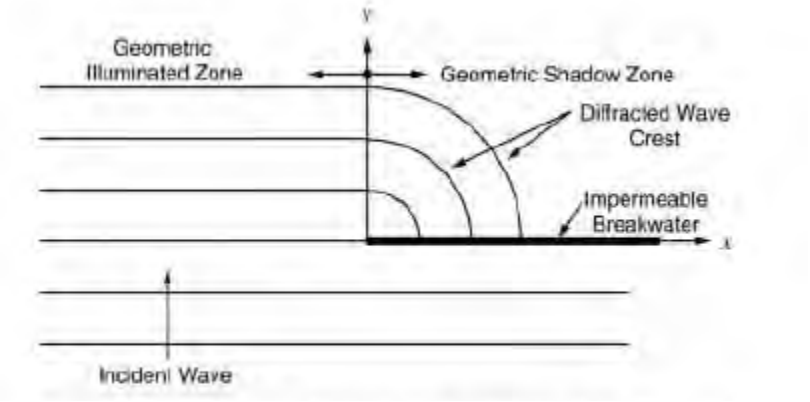

Figure 2.4: Diffraction of waves around a breakwater *(Dean & Dalrymple, 2004)*

Due to the lateral energy transfer of the wave as it bends into the shadow zone, the wave heights in the shadow zone will be lower than the incident wave (Bosboom and Stive, 2012).

4. Wave Breaking

Shoaling describes the increase in wave heights as depth decreases. However, there is a limit to this due to instability caused by wave steepness when the particle velocity becomes greater than the wave celerity. This results in the wave breaking. This limiting of wave steepness was expressed by Miche (1944) using a breaker index based on Stoke's wave theory (Bosboom & Stive, 2012). It states that in shallow water using a non-linear wave theory:

$$[\frac{H}{L}]_{max} = 0.142\frac{2\pi h}{L} \approx 0.78\frac{h}{L} \quad (2\text{-}5)$$

which is equivalent to:

$$\gamma = \frac{H_b}{h_b} \approx 0.78 \quad (2\text{-}6)$$

where γ is the breaker index, H_b is the wave height when it breaks, h_b is the depth at which the wave breaks, h is water depth and L is the wave length. When $\frac{H_b}{h_b}$ becomes greater than the breaker index,

the wave will break. The breaker index value of 0.78 is an approximate value that may vary dependent on the specific beach or coastline considered. However, 0.78 is a realistic value for most generic coastlines based on monochromatic waves (Bosboom & Stive, 2012).

Battjies (1974) showed that the type of wave breaking occurring along a coast can be expressed as a non-dimensional number; the Iribarren number. This is given by the ratio of the beach slope to the square root of the wave steepness:

$$\delta = \tan\beta / \sqrt{H_0 / L_0} \qquad (2\text{-}7)$$

Where δ is the Iribarren number, $\tan\beta$ is the beach slope, H_0 is the deep water wave height and L_0 is the deep water wave length. The Iribarren number categorises the type of wave breaking into the following wave categories as shown in figure 2.5:

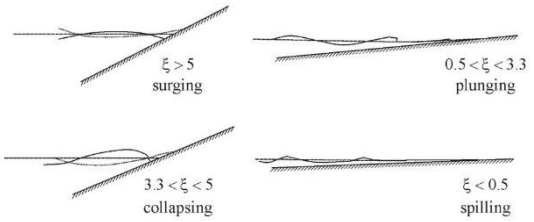

Figure 2.5: Four types of breaking waves based on the Irribaren number *(Bosboom & Stive, 2012)*.

2.3 Wave Induced Hydrodynamics

2.3.1 Radiation Stresses

There is a mean transport of water particles in the direction of wave propagation that is not defined in linear wave theories. This mass transport of water results in a momentum flux in the water column (Figure 2.6) which is known as radiation stress and can be defined as (Dean & Dalrymple, 2004):

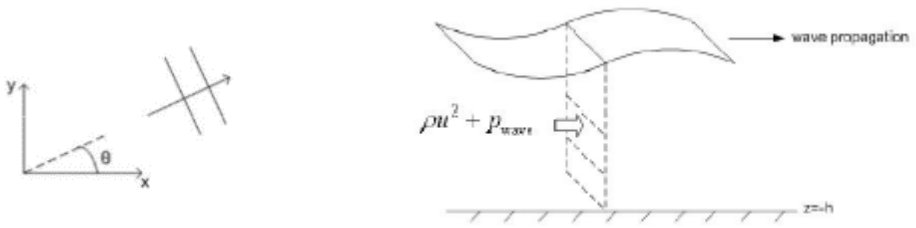

Figure 2.6: Horizontal transport of wave-induced momentum through a vertical plan of unit width perpendicular to the wave propagation direction *(Bosboom & Stive, 2012)*.

Waves approaching the coastline obliquely result in three different radiation stresses.

S_{xx} - Normal stress acting in the x direction.

S_{yy} - Normal stress acting in the y direction.

S_{xy} - Transport of x momentum in the y direction which acts as a shear stress on the plane.

$$S_{xx} = \overline{\int_{-h_0}^{n} (\rho u_x) u_x \, dz} + \overline{\int_{-h_0}^{n} p_{wave} dz} \quad (2\text{-}8)$$

$$S_{yy} = \overline{\int_{-h_0}^{n} (\rho u_y) u_y \, dz} + \overline{\int_{-h_0}^{n} p_{wave} dz} \quad (2\text{-}9)$$

$$S_{xy} = \overline{\int_{-h_0}^{n} (\rho u_x) u_y \, dz} \quad (2\text{-}10)$$

Where n is the water level, h_0 is the water depth, ρ is water density, u_x is velocity and p_{wave} is the pressure caused by the wave. When waves break, there is a change in the wave-induced momentum flux and this gradient in the radiation stress has a significant effect on the nearshore hydrodynamics. This change in the radiation stress results in set-down, which is the lowering of the mean water level where shoaling occurs. It also causes set-up, which is an increase in mean water level in the surf zone and the generation of an alongshore current due to waves approaching the shore at an oblique angle (Bosboom & Stive, 2012).

Using linear wave theory, these radiation stresses can be generalised and represented by the following formulae (Bosboom & Stive, 2012):

$$S_{xx} = E[n(cos^2\theta + 1) - \tfrac{1}{2}] \quad (2\text{-}11)$$

$$S_{yy} = E[n(sin^2\theta + 1) - \tfrac{1}{2}] \quad (2\text{-}12)$$

$$S_{xy} = E[nC\ cos\theta \left(\frac{sin\theta}{C}\right)] \quad (2\text{-}13)$$

where E is the wave energy per unit area, n is the water level at a point along the wave, C is the wave celerity and θ is the wave direction. The gradient of the radiation stresses, that can drive flows, are related to the wave energy gradient due to shoaling and dissipation.

It is also possible to use the wave energy dissipation terms to drive the currents in the hydrodynamic model. Battjies and Janssen (1978) proposed the following model to describe energy dissipation due to wave breaking:

$$D_w = Q_b \frac{1}{4} \rho g \alpha f_p H_{max}^2 \tag{2-14}$$

where D_w is the energy dissipation rate per area, ρ is density, g is acceleration due to gravity, f_p is the peak wave frequency, H_{max} is the maximum wave height, α is a calibration coefficient generally in the order of 1 and Q_b describes the fraction of breaking waves given by the implicit relation:

$$Q_b = \exp\left(-\left(\frac{H_{max}^2}{H_{rms}^2}(1 - Q_b)\right)\right) \tag{2-15}$$

where H_{max} is the root mean square wave height. In this study the hydrodynamic driving forces were based on the dissipation rates as radiation stresses can often be numerically unstable and result in unrealistic spurious flow patterns (Roelvink & Reniers, 2012).

2.3.2 Cross-shore Hydrodynamics

The cross-shore momentum balance states that when waves break, the momentum flux decreases rapidly creating a force in the onshore direction. For equilibrium purposes this force therefore has to be balanced by a hydrostatic force resulting in the water column at the landward side being higher than at the seaward side. This phenomenon is known as wave setup (Bosboom & Stive, 2012). There is also a slight reduction of the water level behind the breaker zone to maintain equilibrium when wave energy increases due to shoaling known as wave set-down.

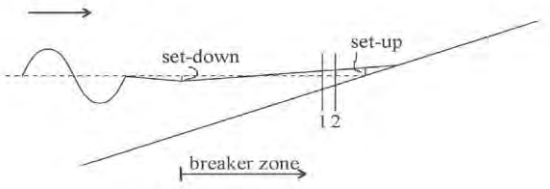

Figure 2.7: Cross section of surf zone showing set-up and set-down *(Bosboom & Stive, 2012)*.

The second important cross-shore process that has a significant impact on sediment transport is undertow. Undertow is an offshore flow near the bottom of the water column in the surf zone to maintain the equilibrium of mass transport. This occurs because there can be no net onshore flow of water particles due to the presence of a sloped beach (Dean & Dalrymple, 2004). A 2DH model has difficulty reproducing this cross-shore flow in the surf zone due to the hydrodynamics being based on depth-averaged shallow water equations (Trouw, et al., 2012). Three-dimensional hydrodynamic models can more accurately represent the effect of breaking waves on the cross-shore flow but the computation time of these models increases significantly and therefore is not always a viable option. Generally, the 2DH models do account for a mean return flow that acts in the direction of the decreasing bathymetry contours resulting in a net offshore flow in the surf zone. Therefore careful calibration of the 2DH morphological models are required when analysing the cross-shore movement of sediment in the surf zone (Roelvink & Reniers, 2012)

Near bed orbital velocities generated by waves have a significant influence on the flow in a water column which in turn has a significant influence in the sediment transport in the direction of the incoming waves. These near bed orbital velocities act in an onshore direction under the wave crest and in an offshore direction under the wave trough and can be determined using a parameterization of the fifth-order Stokes wave theory.
This states that:

$$U_w = \frac{\pi H}{T sinh(2kh)} \tag{2-16}$$

where H is the wave height, T is wave period, h is the water depth and $k = \frac{2\pi}{L}$. Both the onshore and offshore near bed velocities can be computed from U_w.

$$U_{on} = U_w \tag{2-17}$$

$$U_{off} = U_w[1 - r_2 \exp\left(-\frac{r_3 h}{L_0}\right)] \tag{2-18}$$

In which:

$$r_2 = 3 * 2(\frac{H_0}{L_0})^{0.65} \tag{2-19}$$

$$r_3 = 27 \log\left(\frac{H_0}{L_0}\right) - 17 \tag{2-20}$$

where U_{on} represents the near bead orbital velocity in the direction of wave propagation which is onshore and U_{off} represents the near bed orbital velocity in the offshore direction. H_0 is the deep water wave height and L_0 is the deep water wave length. This means that U_{off} can be up to 1.5 times smaller than U_{on} resulting in a net onshore near bed orbital velocity in the direction of wave propagation. Therefore these near bed orbital velocities are important for analysing the onshore movement of sediment and are incorporated within the Delft3D Van Rijn sediment transport model (Soulsby, 1987).

2.3.3 Longshore Currents

The change in the S_{xy} radiation stress in the surf zone results in a transfer of momentum in the alongshore direction of wave propagation creating currents in the longshore direction. Unlike in the cross-shore direction, a pressure gradient cannot be developed in the longshore direction to balance the gradients in radiation stress in the surf zone. Therefore currents in the longshore direction will develop bed shear stress that act as the equilibrium restoring force (Dean & Dalrymple, 2004).
Bowen (1969), Thronton (1970) and Longuet-Higgins (1970) describe the following balance of momentum in the longshore direction using the following equation:

$$F_y = \frac{dS_{yx}}{dx} = \bar{\tau}_{b,y} \tag{2-21}$$

where F_y is the force in the y direction, S_{yx} is the radiation stress and $\bar{\tau}_{b,y}$ is the bed shear stress in the y direction. This means that for a longshore current to develop along an uninterrupted stretch of coastline, the driving force F_y must be greater than the bed shear stress created by friction.

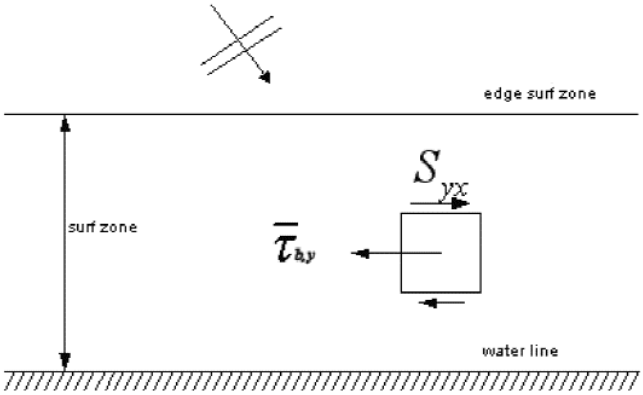

Figure 2.8: Forces acting on a water column that induce a longshore current *(Bosboom & Stive, 2012)*.

2.4 Sediment Transport

Sediment transport along the coast can be described as the movement of sediment particles due to coastal processes such as currents and waves. This occurs when the water exerts a velocity or shear stress on the sediment particles that exceeds the sediment's critical velocity or shear strength. This causes the sediment to move either as bed load along the bottom or suspended load in the water column (Wright, et al., 1999).

2.4.1 Sediment Properties

The most critical sediment properties affecting sediment transport according to Wright, et al (1999) are the sediment grain size and cohesiveness. This study investigates the movement of sediment along the eastern coastline of South Africa which mainly comprises of medium to fine non-cohesive sand. Therefore, the sediment grain size is one of the most important sediment parameters with respect to sediment transport. Erosion or initial sediment movement is affected due to the grain size being directly proportional to the critical bed shear stress required for incipient sediment motion (Dean & Dalrymple, 2004). Once sediment is being transported in suspension, the deposition of that sediment is dependent on the fall velocity of the sediment. This fall velocity is also directly proportional to the sediment grain size resulting in large particles having a greater fall velocity (Ponce, 1989).

2.4.2 Cross-shore Transport

Cross-shore transport of sediment along the coastline is the movement of sand towards and away from the shore predominantly cause by wave actions. During large wave or storm events, the wave action is considered a destructive force. Due to high turbulence in the surf zone and strong undertow currents generated by large waves, sediment will be eroded from the beach and deposited offshore in the form of a sand bar. Gravity and beach slope also have an effect on destructive forces of waves and the offshore movement of sand due to beaches with shallow slopes distributing the breaking wave energy over a greater cross-shore distance (Dean & Dalrymple, 2004). Corbella and Stretch (2012) define an erosion event as a storm period that produces significant wave heights greater than 3,5m.

Constructive forces occur as a result of smaller waves which move sand towards the shore and aid in beach recover after storm events. According to Corbella and Stretch (2012), this beach recovery due to smaller waves is a slow process and can take up to two years on average to reach its pre-storm profile after an erosive storm event. These constructive forces occur as a result of net onshore shear stresses created by near bed orbital velocities and asymmetry of shallow-water waves.

Studies have been conducted both in wave flumes as well as case studies to predict the wave parameters that determine erosion and accretion events. Dean (1973) proposed a simple heuristic model that states if:

$$\frac{H_S}{\omega T} < 3.2 \qquad \text{(accretion)} \qquad \text{(2-22)}$$

$$\frac{H_S}{\omega T} > 3.2 \qquad \text{(erosion)} \qquad \text{(2-23)}$$

where H_S is the significant deep water wave height, ω is the sediment fall velocity and T is the wave period. Kraus (1992) then expanded on this model through use of empirical field data (Figure 2.9) and developed a non-dimensional plot to determine whether a wave condition would cause erosion or accretion:

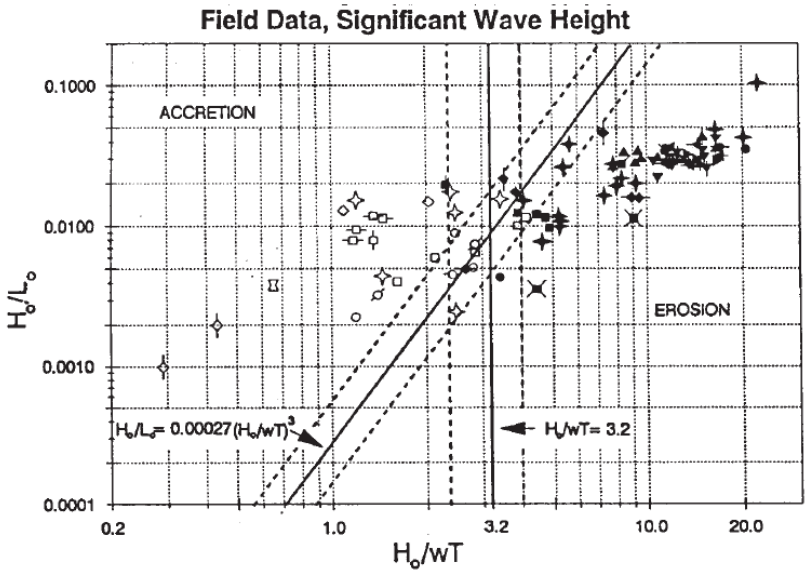

Figure 2.9: Erosion and accretion predictor by field data reproduced from *(Kraus, 1992)*.

Hyong (2008) tested this in a wave flume with an artificial beach with a uniform slope. A series of expected accretion and erosion wave conditions were simulated in the wave flume and the cross-shore sediment movement in this study was in agreement with prior literature. However an equilibrium profile was not reached which may have been caused by a large decay of wave height over

the surf zone caused by the bar forming a great distance from the shore. This on and off shore movement of sediment is an important factor in the evolution of nearshore morphology, therefore it is important to test the Delft3D sediment transport models' capability of reproducing these erosion and accretion events as a function of wave height.

Previous studies have been done analysing Delft3D's sediment transport models capability to hindcast specific storm events and offshore bar migration. van Son (2009) compared the van Rijn sediment transport model's capability to reproduce the flattening of an offshore bar that was monitored during a storm event in 2008 along the Dutch coast. The results revealed that the van Rijn model showed a similar offshore migration as physically monitored however the model predicted a greater flattening of the bar than actually occurred in reality. A major limitation of this study was that the simulation was done over the period of a few days only investigating erosion. The study did not test whether the model could reproduce onshore migration of the bar if the investigation covered a longer time period.

2.4.3 Equilibrium Beach Profiles

The theory of equilibrium beach profiles was introduced by Keulegan and Krumbein (1919). The theory states that over time the erosive and accretive wave forces along most beaches will be balanced and the beach will erode away from and accrete towards a quasi-equilibrium profile.

Bruun (1954) empirically determined a formula to quantitatively calculate the shape of a specific beach's equilibrium profile. The field study monitored beach profiles along the coast of Montery Bay in California, USA and observed that many natural beaches are concave in shape and the depth varies as a function of the two thirds power law. It was also found that the steepness of the equilibrium profile was related to the size of the sediment along the coast. The following generalized power law was proposed:

$$h = Ax^{2/3} \tag{2.24}$$

where h is the depth calculated, A is a profile shape parameter based on sediment grain size and x is the distance from the shore. Further studies by Dean, et al. (2001) compiled a summary of profile shape parameters relating to specific sediment grain diameters as shown in Table 2.1.

Table 2.1: Summary of recommended profile shape parameter values relative to median grain size (Dean, et al. 2001).

d (mm)	0.00	0.01	0.02	0.03	0.04	0.05	0.06	0.07	0.08	0.09
0.1	0.063	0.0672	0.0714	0.0756	0.0798	0.084	0.0872	0.0904	0.0936	0.0968
0.2	0.100	0.103	0.106	0.109	0.112	0.115	0.117	0.119	0.121	0.123
0.3	0.125	0.127	0.129	0.131	0.133	0.135	0.137	0.139	0.141	0.143
0.4	0.145	0.1466	0.1482	0.1498	0.1514	0.153	0.1546	0.1562	0.1578	0.1594
0.5	0.161	0.1622	0.1634	0.1646	0.1658	0.167	0.1682	0.1694	0.1706	0.1718
0.6	0.173	0.1742	0.1754	0.1766	0.1778	0.179	0.1802	0.1814	0.1826	0.1838
0.7	0.185	0.1859	0.1868	0.1877	0.1886	0.1895	0.1904	0.1913	0.1922	0.1931
0.8	0.194	0.1948	0.1956	0.1964	0.1972	0.198	0.1988	0.1996	0.2004	0.2012
0.9	0.202	0.2028	0.2036	0.2044	0.2052	0.206	0.2068	0.2076	0.2084	0.2092
1.0	0.210	0.2108	0.2116	0.2124	0.2132	0.2140	0.2148	0.2156	0.2164	0.2172

Corbella and Stretch (2012) analyse 37 years of beach profile data along the east coast of South Africa. Their study revealed that after severe erosive storm events, beach recovery did occur and took an average of two years for the beach to return to its pre-storm state. This indicates that the beaches along the east coast of South Africa do experience cyclic offshore and onshore sediment movement and oscillate around a quasi-equilibrium profile. Therefore it is important to determine whether the process based morphological models available are capable of reproducing this cyclic onshore and offshore movement in order to accurately capture the cross-shore evolution over time which will maintain this equilibrium profile observed in reality.

2.4.4 Longshore Transport

Longshore sediment transport occurs when the shear stress of the longshore current generated by obliquely incident waves in the surf zone is greater than the critical shear stress of the sediment. This will cause sediment to either move along the bottom as bed load or lifted into the water column and transported as suspended load in the longshore direction of the incoming wave. An empirical study of the effects shear velocity has on the transport of non-cohesive sediment showed that the amount of suspended sediment in the water column will increase with the increase of shear velocity and will result in coarser grains being lifted into suspension (Wright, et al., 1999).

Figure 2.10 shows that uniform coastlines with a constant supply of sediment will experience a zero gradient in the longshore transport and the coast will remain stable. Coastal structures such as breakwaters disrupt the longshore sediment transport creating a positive gradient down-drift and a negative gradient up-drift of the structure. This causes accumulation of sand up-drift of the structure and erosion down-drift. Figure 2.11 shows this along sandy coastlines where ports have been constructed using breakwaters that extended seaward past the surf zone (Bosboom & Stive, 2012).

Left unattended, this can cause negative impacts which include the accumulated sand reaching the end of the breakwater and spilling into the port entrance channel and significant loss of beach down-drift of the port due to a lack of sediment supply. This is an important component of this study because a firm understanding of the longshore transport along a coastline is needed to implement a successful bypass scheme, involving dredging and beach nourishment, to mitigate this effect that occurs around coastal structures.

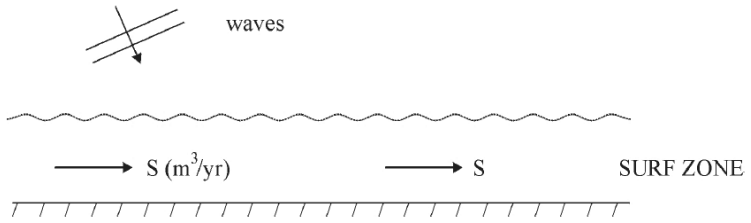

Figure 2.10: Plan view of longshore sediment transport along a uniform coastline *(Bosboom & Stive, 2012)*.

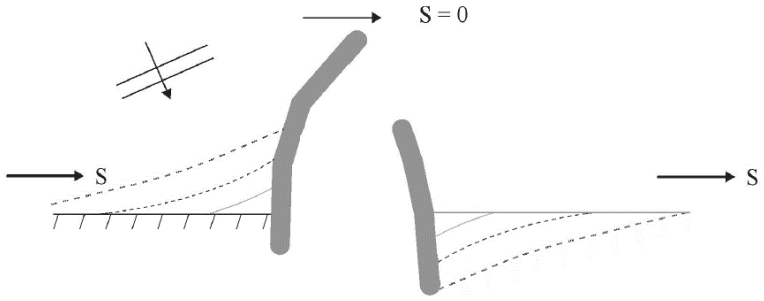

Figure 2.11: Plan view of longshore disruption caused by port breakwaters (note updrift accretion and down-drift erosion *(Bosboom & Stive, 2012)*.

Schoonees (1992) analysed the net longshore transport rates along the coast of South Africa using Durban and Richards Bay as case study locations. Sediment transport data was inferred from surveyed beach profiles, bathymetry volumetric differences and sand accumulation in the harbour sand traps between 1979 and 1993. His results revealed that the mean net longshore sediment transport along the coast of Richards Bay was in the order of 850000 m^3/year while Durban experienced a lower mean transport rate of 500000 m^3/year. This study was important for longshore calibration purposes of the sediment transport model used in this investigation.

2.5 Sediment Transport Models

In order to understand and predict the movement of sediment within a coastal system, a number of semi empirical models have been developed. A large amount of research has been done testing the capability of these models and either proving or disproving their validity against field data. The models discussed in this review will be limited to the bulk longshore transport models used for calibration purposes and the appropriate process based coastal sediment transport models within Delft3D.

2.5.1 Bulk Transport Models

The bulk sediment transport models considered in this study use wave conditions such as height and incoming direction to estimate the longshore transport rate. These models could utilize the wave data gathered from the Richards Bay wave rider buoy to estimate the annual longshore transport which can be compared to Schoonees' (1992) study of the measured longshore transport. Therefore the longshore transport rates can be calibrated within the Delft3D model. The *Shoreline Protection Manual* (U. S. Army Corps of Engineers, 1984) recommends the use of the CERC (Coastal Engineering Research Centre) model developed by Inman and Bagnold (1963):

$$Q = \frac{K}{16\sqrt{\gamma}}\rho g^{3/2} {H_b}^{5/2}\sin(2\theta) \qquad (2\text{-}25)$$

where Q is the total longshore sediment transport, γ is the breaker index, ρ is the density of water, g is gravitational acceleration, H_b is the height of the breaking wave, θ is the angle of the incoming wave and K is an empirical coefficient. Initially a K coefficient of 0.77 was proposed by Komar and Inman (1970), however this greatly overestimates the total longshore transport and further field measurements determined an approximate K value of 0.2 (Schoonees & Theron, 1993). Wang, et al. (2002) tested the accuracy of the CERC equation and concluded that the longshore transports are still greatly overestimated with the new recommended K value. The empirical coefficient has to be significantly calibrated for the CERC equation to give realistic results. Wang (2002) determined that the Kamphuis equation was a more accurate representation of the realistic measured longshore sediment transport rates.

Kamphuis (1991) proposed that the total longshore sediment transport could be derived from using the breaking wave height, period and angle as the main driving factors of the sediment transport as

well as considering the beach slope and sediment grain size as important factors influencing the longshore transport. Kamphuis derived the following equation:

$$Q = 2.27{H_b}^2 T^{1.5} (tan\alpha_b)^{0.75} d^{-0.25} sin^{0.6}(2\theta) \quad (2\text{-}26)$$

where Q is the total longshore sediment transport, T is the wave period, α_b is the surf zone beach slope and d is the sediment grain diameter. Olij (2015) tested the accuracy of these two bulk transport formulae along the coast of Durban in KwaZulu-Natal, South Africa (approximately 200km south of Richards Bay). Compared to the measured transport, Olij's results also revealed that the CERC model produced an unrealistically large annual net longshore sediment transport rate while the Kamphuis model estimated a more accurate net annual transport rate along the east coast of KwaZulu-Natal.

2.5.2 2DH Process Based Models

The three process based sediment transport models considered in this study were the van Rijn model (van Rijn, 1993), the Bijker model (Bijker, 1971) and the Soulsby-van Rijn model (Soulsby, 1997). All three models take into account the effect of both currents and waves to determine the bed load and suspended sediment transports making them applicable for modelling coastal morphology. The models are incorporated into the Delft3D software and can be coupled online with the Delft3D FLOW module. Therefore the bathymetry used in the spectral wave and hydrodynamic simulations will be updated due to the sediment transport. Due to Delft3D simulating the hydrodynamics in two-dimensions as a depth averaged flow to save computation time, these models have parameterizations to account for the three dimensional processes that occur in the surf zone.

The van Rijn model was originally developed in 1984 which was commonly used to model fine sediment transport without the effect of waves. This formula was adapted in 1993 to include the effect of waves making it more applicable for modelling sediment transport and morphological evolution in coastal areas. It is now used as the default model for modelling non-cohesive sediment transport within Deflt3D. The van Rijn model allows for extensive calibration of both the current and wave related sediment transport which makes it an effective tool for hindcasting morphological events and for studies where the sediment transport rates are known. The cross-shore movement of sediment is sensitive to the wave related transport factors within the model. Without correct calibration the default parameters are too high and over predict the onshore movement of sediment due to waves. This results in an unrealistic steepening of the beach face (Trouw, et al., 2012). Therefore without

calibrating the model, the van Rijn model is not an effective forecasting model. However, sediment transport data is available for this study for calibration purposes. This means that the Van Rijn model would be an effective model for this investigation comparing alternative nourishment schemes along the case study beach if calibrated correctly. Trouw, et al. (2012) states that it is possible to minimize the cross-shore sediment transport by lowering the wave related transport factors which will result in no significant erosion or accretion during the simulation. By limiting the cross-shore evolution the focus can be put on the longshore sediment transport without the concern of unrealistic cross-shore processes effecting the results of the study.

The Bijker formula is widely used in coastal areas and is also able to include wave asymmetry and bed slope effects using the Bailard (1981) approach. This is important for the cross-shore sediment transport calibration of this model. Increasing wave asymmetry results in an increase in sediment transport in the direction of the wave which translates to onshore movement of sand. Increasing the bed slope effect causes increased offshore sediment transport (Deltares, 2011). However, Olij (2015) found that a simulation using the Bijker formula in a case study along the east coast of South Africa predicted unrealistically small longshore transport rates when compared to empirical data.

The Soulsby-van Rijn model is an adaptation of the van Rijn (1993) model. Unlike the other models, there are fewer user-defined calibration parameters allowing the adjustment of only the D_{90}/D_{50} ratio, bed roughness height (m) and a total sediment transport calibration coefficient effecting the overall magnitude of the sediment transport. This model was used by Olij (2015) to investigate input reduction techniques and sequencing since it reproduced the most accurate longshore sediment transports along the coast of Durban in KwaZulu-Natal, South Africa. During large wave events it produced an offshore bar without any cross-shore sediment transport calibration. The study showed that the Soulsby-van Rijn model can reproduce the offshore movement of sediment during storm wave events creating an offshore bar but did not investigate whether the model could predict the onshore migration of the bar due to small waves after the storm.

2.6 Beach Nourishment

The basic concept of beach nourishment is the placement of large quantities of sand on the beach to increase the beach width and advance it seaward. It is a cost effective soft engineering solution used along beaches that experience moderate pervasive erosion (Dean, 2002). As discussed previously,

beaches down-drift of harbour entrance breakwaters experience chronic erosion and require beach nourishment to mitigate this effect to prevent loss of valuable beach width.

Ninety five percent of sediment used for beach nourishment comes from offshore dredged material. The process of dredging is done by collecting sediment from a borrow site through use of a fixed pipeline dredger or a hopper dredger to later dump onto the nourishment site (Dean, 2002). A fixed pipeline dredge involves a floating barge located at the borrow area that uses a ladder to support a suction pipe (Figure 2.12a). The suction pipe makes use of a pumping system to create pressure in order to move a sand and water slurry mixture from the borrow area to the dump site via a pipeline system. A hopper dredger is a ship fitted with a dredge pump and a drag arm that is pulled along the sea bed collecting sediment from the borrow area (Figure 2.12b). The sediment is then stored inside a hopper in the ship and transported and dumped in the nourishment area (Dean, 2002). The sediment is then dumped onto the beach either directly from the hopper dredger through use of the rainbow method or through use of a pump out facility where the dredge will moor and connect to a pipeline which allows it to pump the sediment out of the hull and onto the beach (Bruun & Willekes, 1992). Due to the relative immobility of pipeline dredgers to that of hopper dredgers which can travel between ports, pipeline dredgers are situated in a single borrow area and used in continuous nourishment schemes where they dredge and dump at a constant rate maintaining a constant bypass of sediment. Hopper dredgers are capable of dumping larger volumes of sediment relative to time and therefore generally do not stay in a single port and are instead used to supply multiple ports.

The case study site used in this investigation makes use of a hopper dredger, which dredges sediment from the harbour sand trap and moors within the harbour to make use of a pump out pipe system that dumps the sand onto the beach via a buried pipeline.

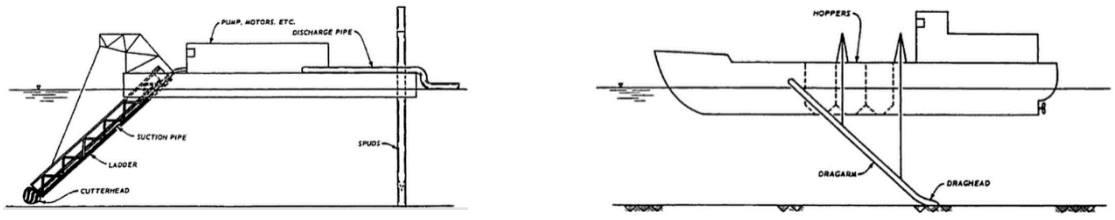

Figure 2.12: a) Schematic of a pipeline dredge. b) Schematic of a hopper dredger (Richardson,1976).

In cases where breakwaters create a disruption in the longshore sediment transport, it is common practice to dredge the sediment from the sand accumulating in the sand trap to nourish the beach down-drift of the structure. The benefits of this bypass scheme is that the sediment accumulated in the sand trap is generally the same grade as the sediment down-drift of the structure. Therefore the quality of the sediment dredged should be of an acceptable quality to dump directly onto the beach requiring the nourishment. It also means that the sediment used for the beach nourishment does not have to be sourced from an external source and transported over large distances. Sediment borrow areas for bypass schemes are generally located close to the nourishment site ranging from around 1km to 20km. Bypass schemes result in beach nourishment down-drift of the coastal structures. Therefore sediment bypass schemes and beach nourishment will be used interchangeably in this thesis.

The sediment accumulating in the sand trap should be equivalent to the sediment being lost down-drift of the structure. In cases where a bypass scheme has not occurred for a period time and sand has been allowed to accumulate in the sand trap, it is necessary to dredge and dump a greater volume than what is being transported along the coastline. This results in the emptying of the sand trap and reclamation the beach down-drift of the structure (Dean, 2002).

The economic benefits of beach nourishment have been investigated and include storm protection, recreational benefits and an increase in upland property appreciation. Dean (1988) investigated the damages caused by Hurricane Eloise along the coastline of Bay County and the damage reduction by advancing the beach width by 50 feet (Figure 2.13). This study also revealed that an increase in beach width can result in an increase in the annual recreational economic benefits due to higher beach visitation rate.

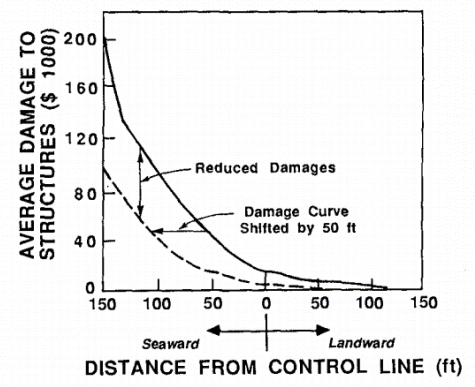

Figure 2.13: Damage reduction due to beach nourishment advancing the profile fifty feet seaward *(Dean, 1988)*.

Stronge (1995) showed that properties along the coast and upland of beach nourishment projects can have an increase in value of up to 20.6% as a result of the beach nourishment.

One of the most well know nourishment schemes is the sand engine project along the Dutch coastline. The project involved a mega nourishment of approximately 20 million cubic meters of sediment dumped along the coastline to form an artificial sand island that will over time nourish the coastline due to longshore transport (Mulder & Tonnon, 2011). Figure 2.15 shows the morphological evolution of the sand engine over a period of 15 years predicted by the van Rijn model within Delft3D.

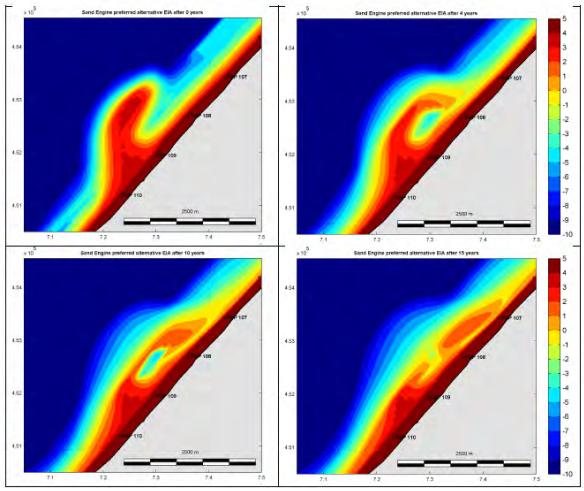

Figure 2.14: Computed morphological development of hook-shaped design with the initial bathymetry in the upper left panel, bathymetry after 5 years in the upper right, 10 years in the lower left and 15 years in the lower right *(Mulder & Tonnon, 2011)*.

This research is fundamentally similar to the current investigation but the wave climate and tidal conditions experienced along the east coast of South Africa are significantly different to those along the coast of the Netherlands. Therefore, while the previous study reveals that Delft3D can be used as a tool to evaluate medium to long term nourishment schemes the specific results cannot be used with confidence to infer beach nourishment performance along the South African.

CHAPTER 3

Case Study Beach Description

3.1 Case Study Location

The Alkantstrand beach north of the Richards Bay (28^{o} 48' 00" South and 32^{o} 06' 00" East) harbour entrance on the east coast of KwaZulu-Natal in South Africa was used as a case study. Figure 3.1b shows the area of interest that extends two kilometres north of the harbour entrance. The direction of the coastline is 45^{o} relative to north and average grain size is D_{50}= 350 µm.

Figure 3.1: Overview of case study location. a) Map of South Africa (Left). b) Aerial image of the Richards Bay Coastline (Right).

There are multiple reasons for the case study location. The first is that it is down-drift of a harbour entrance resulting in the beach being significantly affected by the disruption the entrance causes to the longshore sediment transport. The receding beach width is evident from historic aerial photography with a current beach width of only $\pm$20m. Therefore, this beach can be considered sand starved and should respond rapidly to any simulated nourishment system and give a clear comparison of how the beach responds to alternative nourishment schemes. The second reason is that after the harbour entrance, the beach is straight and the only disruption to the longshore transport is caused by the harbour entrance. The third reason is that there is a wave rider buoy situated at Richards Bay at a depth of 22m supplying wave data for the investigation. The final reason for the use of Richards

Bay as the case study site is that there is an existing bypass nourishment scheme, therefore the model can be set up to simulate the current operating nourishment areas along Alkantstrand to increase the accuracy of the nourishment modelling.

3.2 Data

The three types of data required for this case study are wave, tide and morphological data. The wave data was collected by a Datawell Directional Waverider Mk 4 buoy situated 1,4km off the point of the harbour's southern breakwater. The geographic location of the waverider buoy is 28° 49' 35.40"S and 32° 6' 14.40"E. Data is available between 06/11/1997 and 01/03/2005 in 3 hour intervals. Thereafter data is available between 01/03/2005 and 01/04/2013 in 30 minute intervals. The recorded wave conditions include significant wave height, period, direction and directional spreading. There are 16 years of wave data for the case study.

The tidal data required for the case study was simulated from WXTide. WXTide is an open source tide prediction program based on harmonic analysis of the tide gauge data gathered from the Durban tide gauge. It was used to provide the water level above the lowest astronomical tide for a period of 14 days along the Richards Bay coastline. This period included full spring and neap tides.

Recent detailed bathymetry data was required for the case study beach. The Ethekweni municipality undertook a beach and bathymetric survey to provide the necessary morphology. The measurements were done on 09/07/2015.

Less recent morphological data recorded annually between 1979 and 1993 was used by Schoonees (2000) to estimate annual net longshore sediment transport rates for Richards Bay. These rates were estimated through volumetric differences for the beaches adjacent to the harbour and the volumes of dredged material south of the harbour entrance from the sand trap. This data can be used as an approximation of net longshore sediment transport along the case study beach for calibrating the Delft3D longshore transport.

3.3 Wave Climate

Corbella and Stretch (2012) did a statistical analysis of the wave data collected from the Durban and Richards Bay waverider buoys over the past 18 years. The analysis revealed that along the east coast

of KwaZulu Natal, South Africa the average significant wave height is 1,65m with an average wave direction of 130 degrees and an average peak period of 10 seconds. However, Corbella and Stretch's study revealed that there is a distinct trend in the seasonal distribution of wave parameters (Figure 3.1). Storm events along the South African coastline were defined by wave heights in excess of 3,5m which result in significant erosion along the coast. Autumn is the roughest period of the year and tends to experience the highest frequency of storms as well as the highest significant wave heights. Winter and spring then follow autumn and experience a similar the number of storm events. Winter experiences predominantly southerly incoming swell while the distribution of incoming direction for spring is more spread between easterly and southerly directions (Figure 3.2). Summer is the calmest season with both the fewest events as well as the lowest significant wave heights.

Table 3.1: Seasonal exceedance and maximum, minimum and average Hs of conditionally sampled significant wave heights along the east coast of KwaZulu-Natal using a 3.5m Hs threshold as the condition *(Corbella & Stretch, 2012)*.

Season	Hs > 3.5m (%)	Max Hs (m)	Min Hs (m)	Average Hs (m)
Summer	13.2	4.55	3.52	4.01
Autumn	30.2	8.5	3.59	4.64
Winter	28.3	5.47	3.53	4.12
Spring	28.3	5.64	3.5	4.02

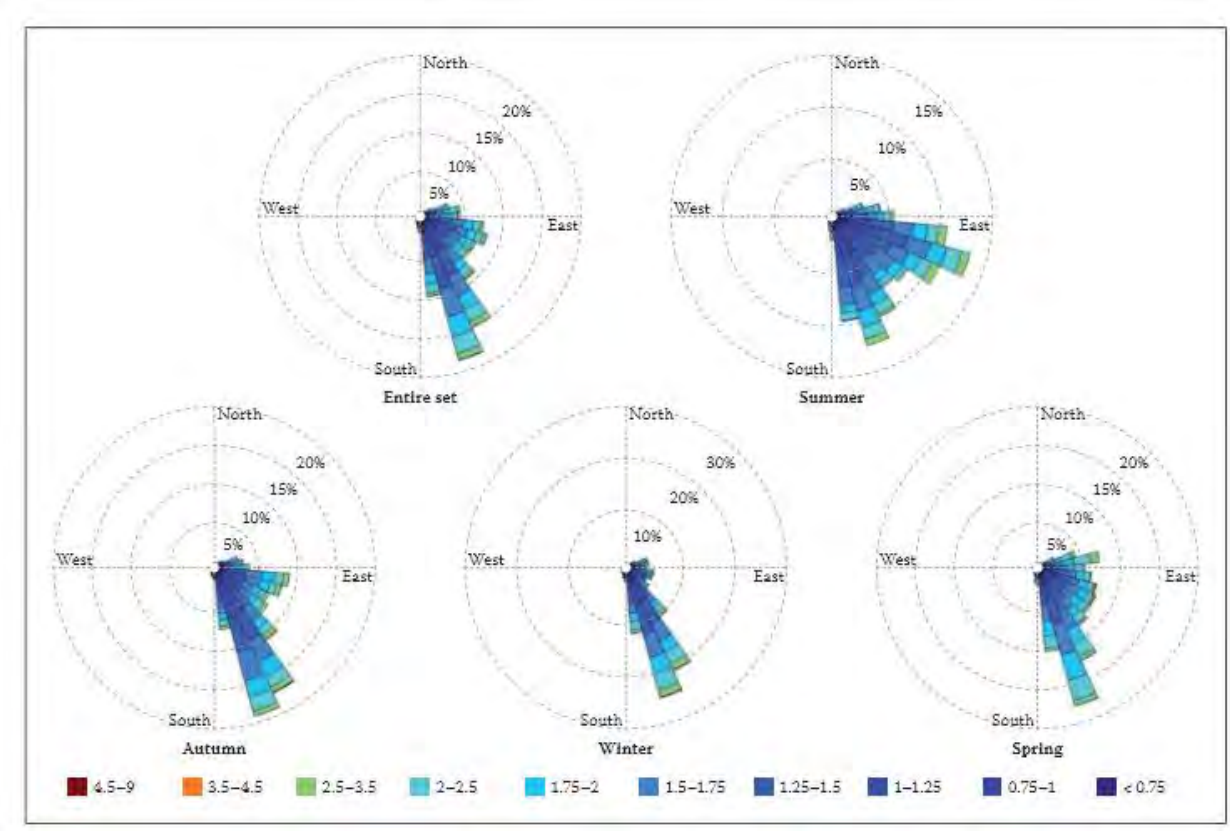

Figure 3.2: Seasonal and combined wave roses for the coast of KwaZulu-Natal, South Africa *(Corbella & Stretch, 2012)*.

A schematization of the Richards Bay wave climate can be done using this formal analysis and recorded wave data in order to effectively reduce the wave climate for a long term morphological model.

3.4 Richards Bay Sediment Transport

The movement of sediment in both the cross-shore and longshore direction have an effect on the morphology of the coastline. Both directions are considered in the evaluation of this case study.

3.4.1 Cross-shore

Due to the dynamic surf zone along the coast of KwaZulu-Natal, the cross-shore movement of sediment will have an effect on the morphology of the case study beach. It has been observed that the east coast of KwaZulu-Natal experiences significant beach erosion after large wave storm events due to strong undertow currents. After these storm events, calmer wave conditions that occur over a longer period of time result in an onshore movement of sediment due to wave asymmetry associated with smaller shorter waves. Over time this accretion balances the erosive wave forces and the beach recovers to its pre-storm state (Corbella and Stretch, 2012). Therefore, beaches along the east coast of KwaZulu-Natal that do not experience an external influence on the longshore sediment supply should erode away from and accrete towards a quasi-equilibrium profile and experience little net cross-shore sediment transport over long periods.

3.4.2 Longshore

The disruption of the longshore sediment transport causes the Alkantstrand beach to be starved of its sediment supply. This means that without artificial beach nourishment, the sediment removed from the beach by longshore transport will cause chronic erosion and a landward migration of the shoreline.

The measured net mean longshore transport rate along the coast of Richards Bay is approximately 850 000 m^3/year and is transported in a northerly direction up the coastline. Annual net longshore transport is difficult to accurately estimate and the coefficient of variation may be up to 50% (Schoonees, 2000). To supplement the measured longshore transport rates, the Kamphuis formula was used along with the Richards Bay wave data to empirically predict the mean net sediment

transport rate per year. Using a beach slope of 1:50 and a median grain size of 350 µm, the Kamphuis formula predicts a net northward longshore sediment transport of 814 815 m^3/year which corresponds to the average measured transport of 850 000 m^3/year. Table 3.2 shows the overall net northward sediment movement predicted by the Kamphuis formula as well as the total gross sediment movement in both the southerly and northerly direction.

Table 3.2: Richards Bay longshore transport rates computed using the Kamphuis bulk longshore transport formula.

Longshore Transport (m^3/year)	Kamphuis Formula
Net	814 815
Gross	2 219 265
Northern	1 517 040
Southern	702 225

An analysis of the longshore bulk sediment transport formulae along the east coast of South Africa, including Kamphuis, done by Olij (2015) revealed that the winter and autumn months have the greatest influence on the sediment transport. This correlates well with the wave climate analysis with winter and autumn experiencing larger waves which would result in greater sediment transport and less longshore transport occurring during the calmer months of the year.

Figure 3.3 shows the lack of sediment supply north of the harbour resulting in a rapidly receding beach width. This receding beach width puts coastal structures in danger of failure as erosion worsens. Figure 3.3 shows the water level within 10m of the local lifeguard tower. Due to the lack of beach as well as bricks being washed away along the eroding beach at high tide, the swimming conditions at high tide are dangerous to bathers.

Figure 3.3: Photograph of significant beach erosion in front of the Richards Bay lifeguard tower due to a lack of sediment supply (Zululand Observer, March 2015).

3.5 Beach Nourishment Capability and Infrastructure

Currently, the hopper dredger Isandlwana is meant to service the port of Richards Bay. The sand bypass scheme involves the Isandlwana dredging the sand trap and docking at the T-jetty inside the port. The dredger is then connected to a sediment discharge pipeline on the T-jetty (Figure 3.4a) which pumps the sand though the pipeline from the hopper directly onto the main recreational beach(Figure 3.4b). The Isandlwana has a hopper capacity of 4200 m^3 (Global Ship Technology, 2015). Considering both dredging time, travel time between the borrow and dump area and the discharge time, a conservative estimate of the daily nourishment rate could be made. It was estimated that the Isandlwana was capable of providing approximately 10000 m^3 of sand onto the beach per day.

Figure 3.4: a) Isandlwana docked at the T-jetty inside Richards Bay port and connected to the discharge pipeline. b) Sand pumped onto Alkantstrand beach through the discharge pipeline (Zululand Observer, 2015).

The pipeline runs underground from the T-jetty to the main recreational beach and discharges the sand onto the beach approximately 400m north of the northern harbour breakwater (Figure 3.5).

Figure 3.5: Plan view and position of the sediment discharge pipeline used to nourish Alkantstrand and coastal infrastructure.

CHAPTER 4

Methodology

This chapter discusses the modelling methodology using the Deltares Delft3D modelling system. First the coastal process based models are described. Secondly the model setup was described together with the approach taken to test the cross-shore capability of the Delft3D depth averaged sediment transport models. This was done to investigate the model's capability of maintaining an equilibrium profile. The last section of this chapter describes the data collection and the simulation of the sediment bypass process.

4.1 Delft3D Model

Delft3D is a process based modelling system developed to simulate and analyse coastal processes. Delft3D was used to compute the spectral wave, hydrodynamics and morphology in the coastal areas (Figure 4.1).

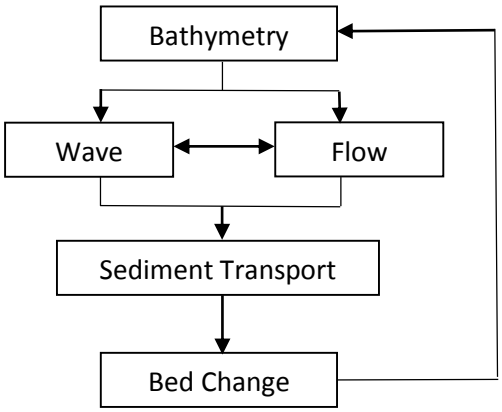

Figure 4.1: Flow diagram of Delft3D morphodynamic model procedure.

4.1.1 Wave Model

The wave transformation was computed using the third generation spectral wave model SWAN. The SWAN model is favoured for morphological studies because it can compute the 2D spectrum evolution

of the wave climate models and it supports curvilinear grids which can be implemented in Delft3D (Roelvink & Reniers, 2012).

A JONSWAP spectrum shape was used in SWAN to analyse the wave spectrum with a peak enhancement factor of 3. Corbella and Stretch (2014) revealed that the JONSWAP distribution best fits the wave spectrum along the east coast of KwaZulu-Natal.

Wave breaking was determined in SWAN by the Battjes and Janssen (1987) depth-induced breaking model. The breaker index was set to 0.7 based on H_s. A breaker index lower than the 0.78 for monochromatic waves is recommended by Roelvink and Reniers (2012) for spectral wave modelling.

The dissipation rate was used to predict the driving forces of the hydrodynamics in the surf zone. It is possible to predict a more accurate wave force directly from the radiation stress gradients as the dissipation rate is only an approximation of the wave force based on radiation stresses. However, Dingemans et al. (1987) showed that generating the wave forces directly from the radiation stresses predicted unrealistic spurious flow patterns. Therefore the model is more numerically stable using the dissipation rates to generate the wave forces in the surf zone.

4.1.2 Flow Model

The Delft3D flow module is a process based hydrodynamic model that can be used to predict the flow in coastal areas. In this investigation the 2DH hydrodynamic model was coupled online with the spectral wave model and used to predict the depth averaged current velocities by solving the Navier Stokes equations for an incompressible fluid and shallow water assumptions.

The model used the dissipation rates from SWAN to produce the nearshore currents. The tidal effects are accounted for as a water level fluctuation defined by the model boundary conditions.

The computational time-step for the hydrodynamic simulation was 6 seconds in order to satisfy a courant number criteria for numerical stability.

The horizontal eddy diffusivity was set to 10 m^2/s. An initial resolution check showed that hydrodynamic grids up to approximately 20m resolution would be resolution independent using this eddy diffusivity.

4.1.3 Morphological Model

In coastal areas, the drivers behind sediment transport are wave forces and currents. The three sediment transport models considered for this investigation were the van Rijn, Bijker and Soulsby-van Rijn models. All three models use the current velocities computed by the hydrodynamic model to predict the suspended and bed load sediment transport.

The change in bed level is then determined by the sediment balance. This bed level change will result in a morphological evolution of the beach and have an effect on both the wave transformations and the hydrodynamics. Due to the sediment transport model being run online with the waves and flow, the bed level changes computed throughout the simulation are reused in SWAN and the hydrodynamic model to account for the changes in the coastal processes due to the morphological evolution.

The morphological changes that occur during the simulation can be scaled up through use of a morphological factor. This factor was included because morphological changes occur on a significantly longer time scale than hydrodynamic changes and long term hydrodynamic simulations are not computationally efficient.

4.2 Delft3D Cross-shore Capability

It is important for the cross-shore transport models to predict realistic transports as the morphological evolution determined by it has an influence on all the coastal processes respectively. As the cross-shore profile changes, so does the wave transformations, hydrodynamics and sediment transport.

4.2.1 Model Domain

1. Cross-shore Profile

Long term cross-shore profile data is not available for Richards Bay but Durban provides a suitable substitute and has the required data. The averaged cross-shore profile data recorded from survey station A within the Durban Bight (see appendix B for survey station location) was used to create the bathymetry used for this study (Figure 4.2). This averaged profile “loosely fits” a theoretical

equilibrium profile proposed by Bruun (1954) with a sediment grain size of 350 µm. Therefore the profile was chosen as a representative equilibrium profile for the east coast of KwaZulu-Natal.

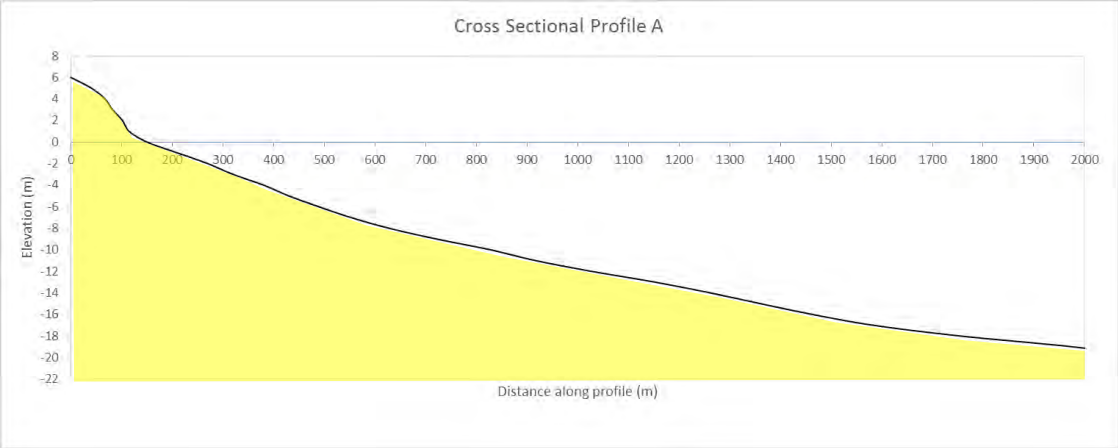

Figure 4.2: Average surveyed cross-shore profile from survey station A in Durban, KwaZulu-Natal.

2. Grid and Bathymetry

The profile was extended laterally to generate a representative beach with a uniform profile bathymetry (Figure 4.3b).

The grid for the wave and flow domain were generated using a curvilinear grid system.

The wave grid extends 4 km in the longshore direction and 1.5 km in the cross-shore direction. The grid has a resolution of 50x50 m at the offshore boundary and increases resolution in the cross-shore direction resulting in a 10x50 m grid resolution in the nearshore zone.

A smaller flow grid is nested within the wave grid to negate the effect of wave energy dead zones near the lateral boundaries in the wave model and reduce computation time. The flow grid extends 150 m in the longshore direction and 1000 m in the cross-shore direction. A longer flow grid is not necessary due to only the cross-shore sediment transport being the main focus of this part of the investigation. The flow grid also has a resolution of 10x50 m in the nearshore zone and a resolution of 20x50 m at the offshore boundary (Figure 4.3a). This grid resolution supports a courant number of 6s and is small enough to give a detailed description of the sediment transport in the cross-shore direction.

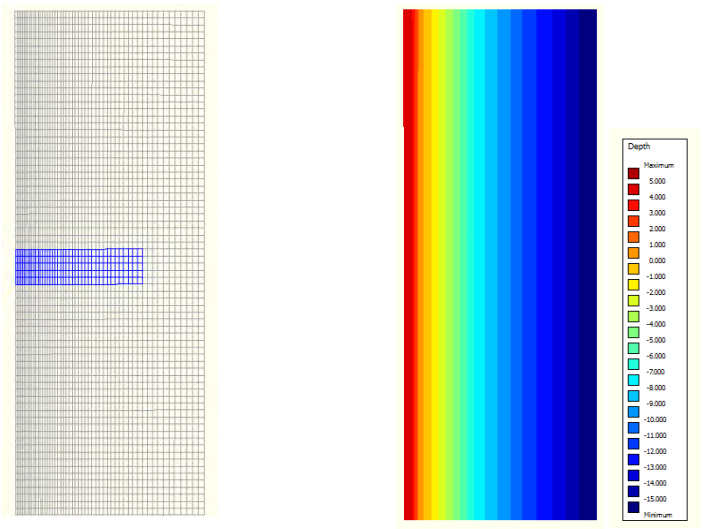

Figure 4.3: a) Flow grid nested inside large wave grid. b) Uniform bathymetry.

4.2.2 Time Frame

The hydrodynamic and morphological simulation was run for a period of two days. This simulation time period allowed a clear representation of the cross-shore sediment transport direction and magnitude. The wave module was coupled with the hydrodynamic and morphological model every three hours (simulation time). No morphological factor was applied to the sediment transport

4.2.3 Wave Conditions

Two wave conditions were considered in this part of the study based on Kraus's (1992) empirical model determining erosion and accretion wave events. Keeping the average wave period of 10 seconds constant and an average grain size of 350 µm, the corresponding wave heights were determined. Wave heights greater than 1.6m would empirically result in offshore sediment transport and wave heights less than 1.6m would result in onshore sediment transport. Therefore a significant wave height H_s = 3m was chosen to represent the erosion wave condition. A significant wave height H_s = 1m was chosen to represent the accretion wave condition.

4.2.4. Boundary Conditions

1. Wave Boundaries

The wave conditions were imposed uniformly along the eastern sea boundary of the model domain. The north and south lateral boundaries were left open. This means that no waves were generated from the lateral wave boundaries.

2. Flow Boundaries

The north and south lateral boundaries were open and defined as zero gradient Neumann boundaries. The eastern sea boundary had a water level boundary condition. The tidal fluctuation of this water level was not included for the cross-shore capability study.

4.2.5 Morphology

1. van Rijn Sediment Transport Model

The first sediment transport model tested was the van Rijn model which incorporates the effects of both current and waves on the suspended and bedload transport.

Within the van Rijn formula, the sediment transport in the direction of the propagating wave (onshore transport) is sensitive to the wave related suspended transport factor (f_{sus}) which is a calibration coefficient (See appendix A Equation A-7). To determine whether a single f_{sus} could be defined to predict erosion for large waves and accretion for smaller waves, five test simulations were conducted on both the 1m (expected accretion) and 3m (expected erosion) wave heights varying the f_{sus} from 0 to 0.2. The f_{sus} value was increased from 0 to 0.2 in steps of 0.05 for each simulation for both wave conditions.

The predicted cross-shore sediment transport direction and rates were recorded and analysed with regard to the change of the f_{sus} value. Cross-shore transport was not sensitive to the wave related bedload transport factor and was set to a default of 0.1 for all simulations.

2. Bijker Sediment Transport Model

The Bijker formula is a robust sediment transport formula that accounts for both the effects of waves and currents on the movement of sand in a coastal area. Without any cross-shore calibration, the Bijker formula tends to produce an offshore bar over a long term morphological simulation.

The Bailard (1981) approach was taken to determine whether the Bijker formula could reproduce onshore movement for small waves and offshore movement for large waves. The Bailard approach involves the inclusion of a wave asymmetry factor (A_{fac}) that influences the amount of onshore movement of sediment due to waves and wave asymmetry in shallow water (See appendix A Equation A-24). From here on this model will be referred to as the Bijker-Bailard model. Five test simulations were conducted on both the H_s = 1m (expected accretion) and H_s = 3m (expected erosion) while varying A_{fac} in the range 0.2 to 1. The A_{fac} value was increased from 0.2 to 1 in steps of 0.2 for each simulation for both wave conditions.

3. Soulsby-van Rijn Sediment Transport Model

The Soulsby-van Rijn is a commonly used coastal sediment transport model. The calibration parameters available in this model are the D_{90}/D_{50} ratio and bed roughness. These have little direct influence on the direction of the cross-shore sediment transport. Therefore the D_{90}/D_{50} ratio was set to 1.3 (based on measured sediment particle sizes along the coast of KwaZulu-Natal) and the bed roughness was left at the default value. The Soulsby-van Rijn model was only run once using these parameters for each wave condition to determine whether the model could reproduce the expected onshore and offshore sediment transport trends.

4.3 Beach Nourishment Case Study

4.3.1 Bathymetric Survey

To set up the model, bathymetry data of the case study site prior to recent beach nourishment was required. A full beach and bathymetric survey was undertaken on 09/07/2015. The survey began immediately north of the Richards Bay harbour entrance and extended 2 km northwards along the coastline and 1 km offshore (Figure 4.4).

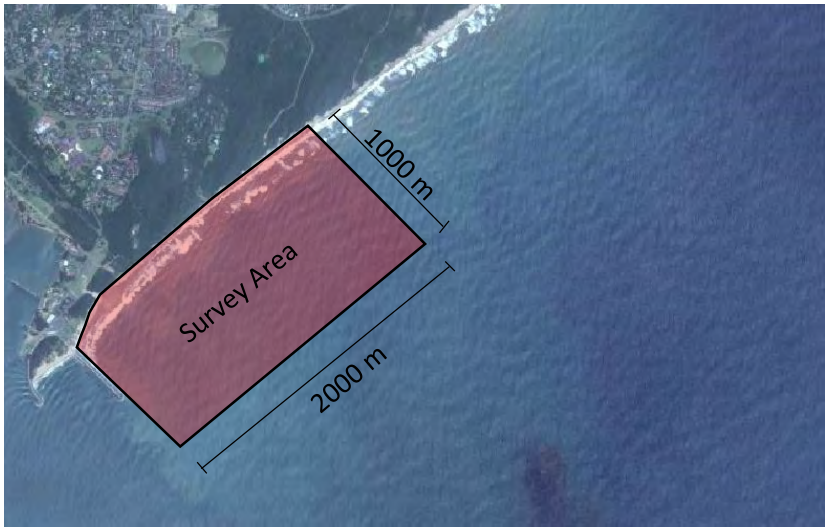

Figure 4.4: Plan view of the surveyed coastline north of the Richards Bay harbour.

1. Beach Survey

A LIDAR (Light Detection and Ranging) and Real Time Kinematic GPS (Global Positioning System) were used to conduct the beach survey. The RTK GPS was wirelessly linked to the Richard's Bay base station run by TrigNet through the GPRS network. Figure 4.5 shows the survey instruments that were attached to an all-terrain vehicle that could travel along the beach barrier effectively and move the instrumentation with ease during the survey.

Figure 4.5: RTK GPS and LIDAR mounted to the all-terrain vehicle used for the beach survey.

2. Bathymetric Survey

The hydrographic survey was conducted using SONAR (Sound Navigation and Ranging) and an RTK GPS mounted to a Waverunner Jetski (Figure 4.6). The Jetski followed pre-planned gridlines spaced 50 m apart along the survey area and recorded a depth reading every 5 seconds. The survey extended

approximately 1km offshore. The RTK GPS was used to correct for the fluctuation of the depth reading due to the effect of waves. A plan of the detailed path followed by the Jetski during the bathymetric survey can be found in Appendix C.

Figure 4.6: Waverunner jetski used for the bathymetric survey.

The surveyed data was post-processed into a XYZ format and used in Delft3D to generate a model domain for the case study.

4.3.2 Case Study Model Domain

The case study model domain consists of a fine curvilinear flow grid nested within a larger coarse wave grid. The wave grid extends 4 km along the coastline and 2 km in the cross-shore direction and has a resolution on 50x50 m. The eastern water depth boundary condition was approximately 20 m which is the same depth at which the Richards Bay waverider buoy is situated which allowed for the consideration of wave transformations that occur as the waves propagate towards the shore.

The flow grid had a finer resolution of 20x20m and extended 2km in the longshore direction and 1km in the cross-shore direction (Figure 4.7). At this resolution the model was numerically stable with a time step of 6 seconds and resolution independent with an eddy diffusivity of 10 m^2/s. This means that a smaller grid resolution would not predict a different flow field. The bathymetry for the flow grid was generated from the XYZ coordinates obtained from the beach and bathymetric survey (Figure 4.8).

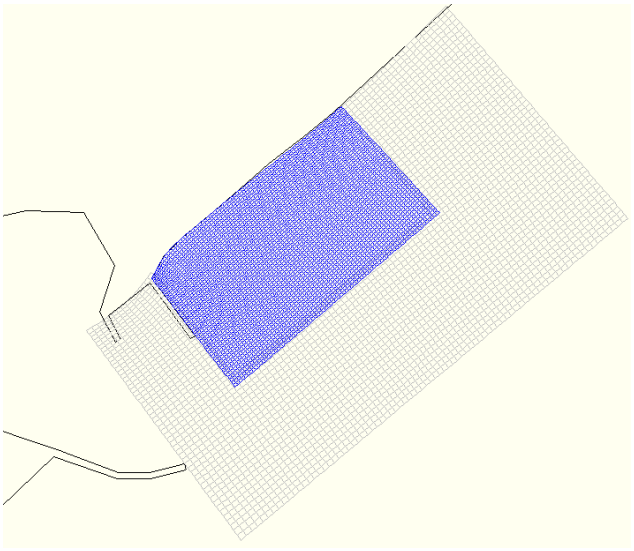

Figure 4.7: Flow and morphological grid nested inside the larger wave grid.

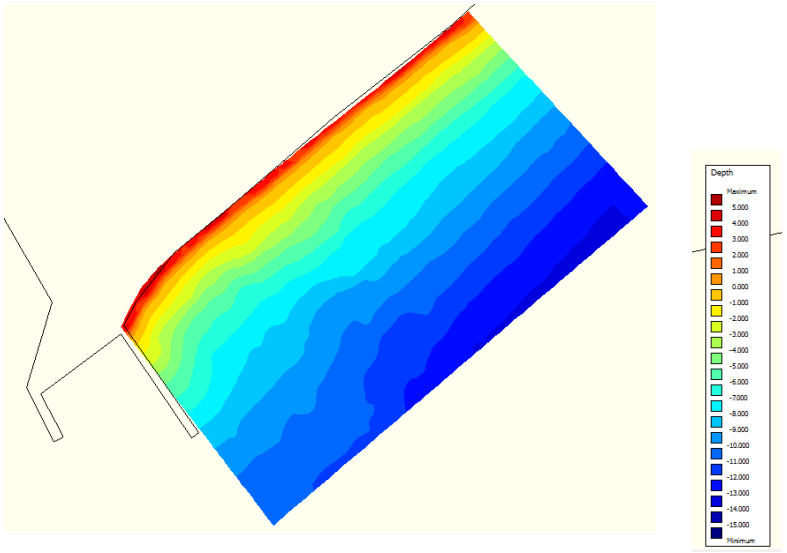

Figure 4.8: Initial bathymetry used in Delft3D investigation (m MSL).

4.3.3 Time Frame

The hydrodynamic model was run for a simulation time of 14 days with morphology. This allowed for a full tidal cycle to be considered in the hydrodynamic model. The spectral wave model was coupled

with the hydrodynamic model every three hours (simulation time). A morphological factor of 26 was applied to the sediment transport model. This scaled up the simulated morphological changes to the period of a full morphological year.

4.3.4 Wave Climate Reduction

Including all recorded wave conditions for a medium to long term morphological numerical model becomes too computationally expensive to be a practical morphological prediction technique. Therefore the technique of wave reduction was used on the wave data collected from the Richards Bay Waverider to reduce the wave climate down to 15 representative wave conditions.

The first step in reducing the wave climate was to determine the frequency of each wave condition measured and the sediment transport rate that corresponded to each wave condition. The Kamphuis bulk sediment transport formula was used to determine the sediment transport rates. The frequency was then combined with the transport rates to determine the contribution each possible wave condition had on the total cumulative sediment transport. Figure 4.9 shows the results of the above described wave climate reduction and the 15 wave conditions with the highest contribution that were chosen for the reduced wave climate. The choice of wave conditions included waves resulting in both northerly and southerly longshore sediment movement as well as a storm event. For a detailed description of input wave reduction techniques see Walstra, et al. (2013) and Olij (2015).

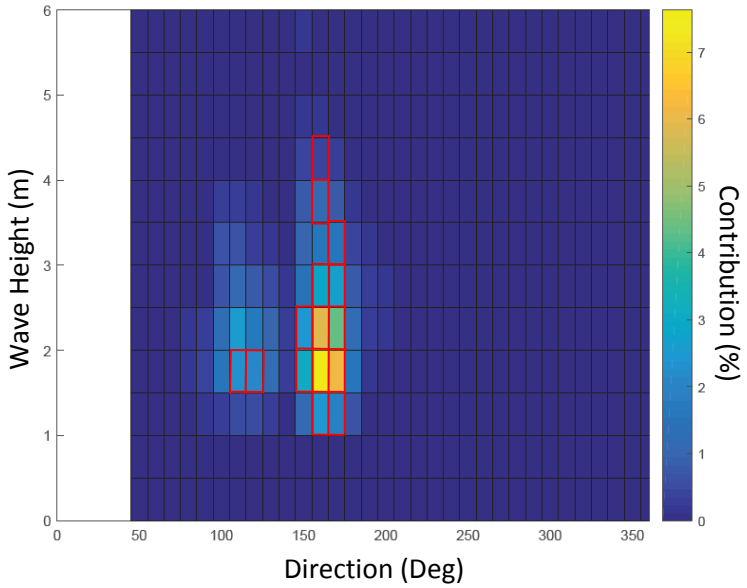

Figure 4.9: Sediment transport contribution relative to wave height and direction determined using the Kamphuis formula and wave reduction technique.

The reduced wave climate can be sequenced in various ways, which include sequencing based on wave height, Markov chain sequencing and 4th variable sequencing investigated by Olij (2015). For this study, the sequencing was based on the seasonal wave climate trends analysed by Corbella and Stretch (2012). Assuming the morphological model starts in January and acts over the period of a year, the wave conditions were sequenced so that the autumn and winter periods of the morphological simulation experienced the highest wave heights from the southerly directions. Spring and summer experience a greater directional spread of wave energy with summer experiencing the calmest wave conditions. The wave reduction and sequencing yielded the following wave climate used for the beach nourishment case study:

Table 4.1: Reduced Richards Bay wave climate used for case study.

Wave Condition	H_{m0} (m)	Period (s)	Direction (Deg)	Time (%)
1	2	11.8	150	5.1
2	1	12.6	160	11.0
3	1.5	9.4	110	5.0
4	1.5	11.9	150	13.0
5	2.5	12.1	170	2.1
6	4	13.2	160	0.2
7	3.5	13.1	160	0.5
8	1.5	12.5	170	13.5
9	2.5	12.5	160	2.5
10	3	12.5	170	0.8
11	2	12	170	6.5
12	1	12.5	170	7.6
13	1.5	9.9	120	4.0
14	2	12.5	160	8.1
15	1.5	12.7	160	18.1

4.3.5 Boundary Conditions

1. Wave Boundaries

The reduced wave climate was imposed uniformly along the eastern sea boundary of the model domain. The reduced wave climate was also imposed along part of the southern boundary from the eastern sea boundary till where the southern breakwater ends. This was done to compensate for the sheltering effect the breakwater has along the coastline north of the harbour entrance.

2. Flow Boundaries

The north and south lateral boundaries for the hydrodynamic model were open and defined as zero gradient Neumann boundaries. The eastern sea boundary had a varying water level boundary condition as a function of time. The varying water level at this boundary was used to reproduce the effect the tide had on the mean sea level over the 14 day simulation. The two weeks of tidal data was extracted from WX Tide and included a full spring and neap tidal range (Appendix C).

3. Sediment Transport Boundaries

Zero gradient Neumann boundary conditions were used for the sediment transport model. This meant that the boundaries did not prevent sediment from leaving the northern boundary when transported northwards along the shore.

4.3.6 Wave and Flow Fields

Over the 14 day simulation, the spectral wave and hydrodynamic models were used to produce wave and flow fields corresponding to the above specified wave conditions. These flow fields are an important aspect of the study as the currents developed in the hydrodynamic model are the main drivers of longshore sediment transport. Figure 4.10 presents the wave and flow fields produced by an average wave condition for Richards Bay that has a significant wave height of 1.5 m, period of 11.9 s and a south easterly incoming direction of 150 degrees. Wave fields have been plotted onto the flow grid for a better representation of how the wave field drives the nearshore currents.

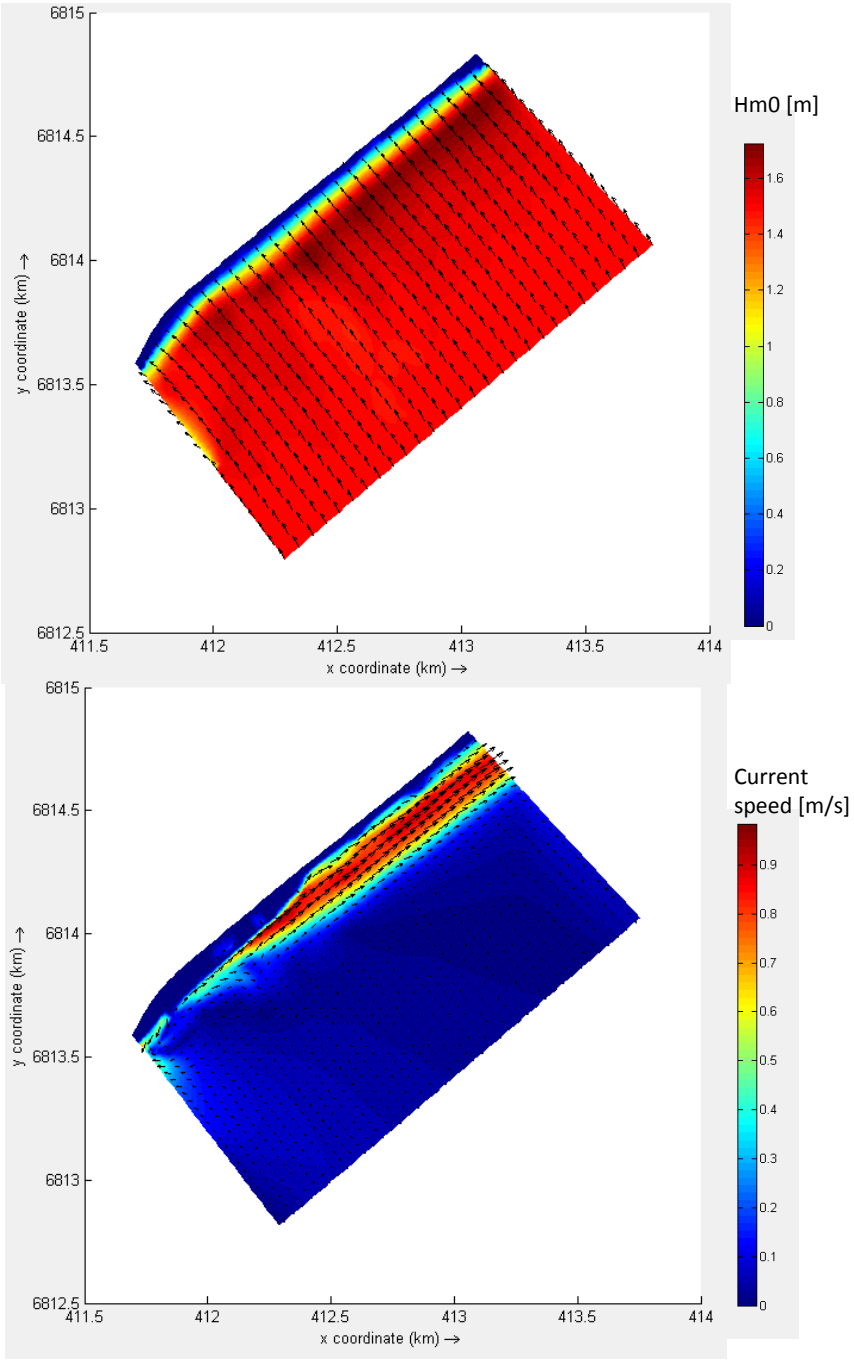

Figure 4.10: Wave field (top) and flow field (bottom) for an average wave condition: Hm0 = 1.5, T = 11.9 s, Dir = 150 deg

Large storm wave conditions are also important as the nearshore currents they produce are significantly larger than the currents produced by the average wave conditions throughout the year. This means large waves will significantly influence the longshore transport along the coastline.

Figure 4.11 presents the wave and flow fields for the storm wave event simulated which had a significant wave height of 3.5 m, a period of 13.1 s and a southerly incoming direction of 160 degrees.

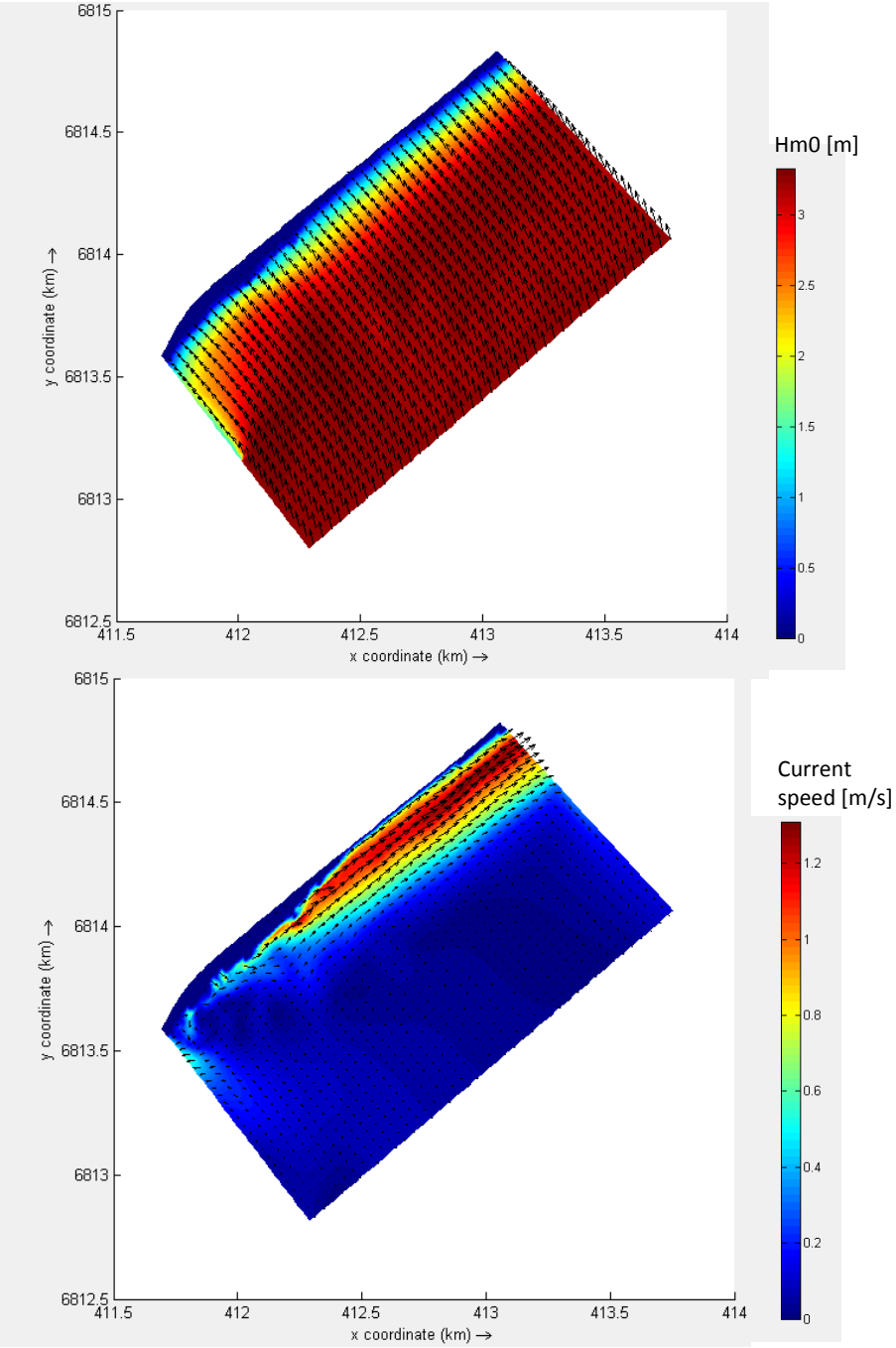

Figure 4.11: Wave field (top) and flow field (bottom) for a storm wave condition: Hm0 = 3.5, T = 13.1 s, Dir = 160 deg

It must be noted that due to the way the wave boundary was used to simulate the effect of the breakwater, the model is able to capture the dampening of the wave height behind the breakwater

but is not able to fully capture the circulation of the eddy and rip currents directly behind the breakwater as described by Pattiaratchi et al. (2009). This is a limitation of the study and may require further research to improve the simulated current patterns behind the breakwater.

4.3.7 Nourishment Schemes

This case study investigates three alternative beach nourishment schemes along the Richards Bay coastline. The sediment budget for each case was 1 000 000 m^3 for the year. Using the sediment nourishment function incorporated into the Delft3D morphological model, the budgeted sediment was added along the coastline 300m north of the harbour entrance during the simulation. The model reproduces a beach nourishment process by increasing the bathymetry of a defined dump area each time step to simulate the required nourishment rate. The three nourishment schemes evaluated were a continuous year round nourishment, a bulk nourishment and a bimonthly nourishment scheme.

1. Continuous Nourishment Scheme

The first scheme involves dumping 2740 m^3/day of sand onto the beach continuously for the entire year. This scheme is intended to be the most natural case feeding the system with a constant supply of sediment as if there was no disruption to the longshore transport. This scheme requires a single dredger to be station at a single port all year round or the construction of a fixed pipeline dredger that pumps the dredged sediment from the sand trap to the nourished beach continually year round.

2. Bulk Nourishment Scheme

The second scheme involves dumping all the budgeted sand onto the beach rapidly at a rate of 10 000 m^3/day. This means that within approximately 100 days, the entire 1 Mm^3 of sediment will have been dumped onto the beach.

3. Bimonthly Nourishment Scheme

The bimonthly scheme involves pumping approximately 166 500 m^3 every two months at a rate of 10 000 m^3/day. This schemes allows the dredger to service multiple ports but requires frequent travelling between the ports to ensure pumping at the same port every two months.

4.3.8 Morphology

Based on the Delft3D cross-shore sediment transport capability study, the van Rijn model was chosen to predict the movement of the nourished sediment and beach response for the sediment bypass case study. The calibration of the cross-shore component of the model was done in accordance with the previous Delft3D cross-shore capability study in Chapter 5 and the longshore transport was calibrated to the measured net northward transport of 850 000 m^3/year.

4.3.9 Simulation Output Monitoring

The predicted sediment nourishment and its influence on the case study beach was observed at four different points throughout the simulation for all three nourishment schemes. The results of the simulations were analysed 3 months, 6 months, 9 months and one year after the commencement of the nourishment schemes (morphological simulation time). The output of the models would include the bathymetric changes as well as the distribution of the nourished sediment throughout the morphological year.

Additional monitoring of the beach width changes of Alkantstrand was achieved by monitoring a cross-sectional profile (A-A) (Figure 4.12). The cross-section was taken 100m south of the discharge pipeline at the four time intervals stated above (beach width is defined as the distance from the coastal dunes to mean sea level).

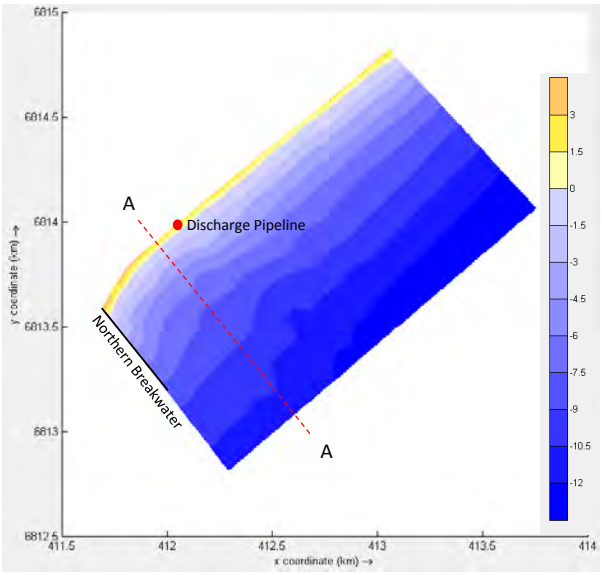

Figure 4.12: Plan view of model domain and position of cross-section A-A (m MSL).

This showed the predicted beach width of Alkanstrand throughout the year and how it differed with respect to the type of nourishment scheme implemented.

At these four observation times throughout the year for each nourishment scheme, the amount of sediment pumped into the model domain was determined. The amount of volume still within the system at each point was then compared to the amount lost through the boundaries.

CHAPTER 5

Delft3D Cross-shore Capability Results and Discussion

This chapter investigates three 2DH morphological models and whether they are capable of maintaining an equilibrium profile over a medium to long term simulation. A critical wave height of 1.6m that was predicted using Kraus' empirical model (1992). This means that wave heights above 1.6m should experience a net offshore movement of sediment and wave heights smaller than 1.6m should experience net onshore movement. The models were tested to investigated whether they can reproduce offshore sediment transport during a 3m erosion wave event and onshore sediment movement during a 1m accretion event using a single set of model parameters.

5.1 Van Rijn Model

The direction and magnitude of the cross-shore sediment transport predicted by the van Rijn model is directly influenced by the wave related suspended sediment transport factor (f_{sus}) which is an adjustable coefficient within the model. Figure 5.1 shows that varying f_{sus} from 0 to 0.2 has a significant influence on the cross-shore sediment transport rates for both the H_s = 1m (expected accretion) and H_s = 3m (expected erosion) wave events. These results revealed that the onshore movement of sediment increased linearly with increasing f_{sus} for both the H_s = 1m and H_s = 3m wave conditions (Figure 5.2).

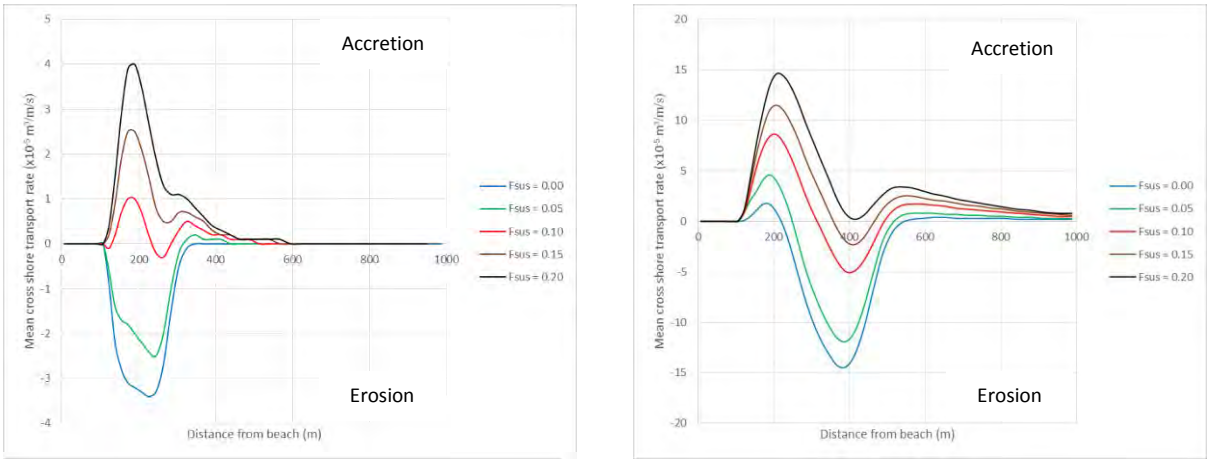

Figure 5.1: a) van Rijn cross-shore sediment transport rates for Hs = 1m and varying f_{sus}. b) van Rijn cross-shore sediment transport rates for Hs = 3m and varying f_{sus}.

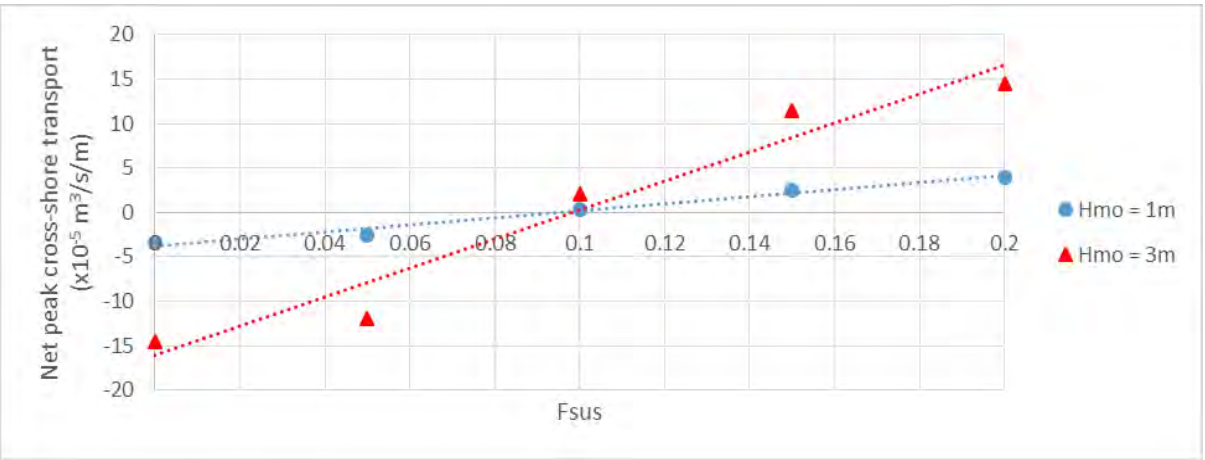

Figure 5.2: Net cross-shore transport rates varying as a function of f_{sus} (Positive rates represent onshore movement and negative rates represent offshore movement).

The van Rijn model predicted that for both wave conditions (regardless of whether erosion or accretion was empirically expected), net cross-shore accretion occurs where f_{sus} > 0.1 and net erosion occurs where f_{sus} < 0.1 (Figure 5.2). Therefore a single f_{sus} value cannot reproduce onshore movement for a 1m wave height and offshore movement for a 3m wave height. This means that a given f_{sus} value will reproduce either an erosion or accretion event independent of the wave height. These results also show that for all wave conditions, where f_{sus} is equal to 0.1 no net erosion or accretion is predicted by the van Rijn model (Table 5.1).

Table 5.1: Summary of van Rijn cross-shore calibration.

H_s (m)	Expected Cross-shore Movement	f_{sus}	Modelled Cross-shore Movement	Volume Moved (m^3/m beach width)
1	Onshore	0	Offshore	13.4
		0.05	Offshore	10.3
		0.1	None	-
		0.15	Onshore	10.1
		0.2	Onshore	13.9
3	Offshore	0	Offshore	53.7
		0.05	Offshore	50.23
		0.1	None	-
		0.15	Onshore	32.3
		0.2	Onshore	42.0

This shows that for a long term morphological simulation an equilibrium can be maintained using a f_{sus} = 0.1. It must be noted that this equilibrium is maintained due to a balance of erosion and accretion occurring at this f_{sus} value and is not due to expected seasonal erosion and accretion trends resulting in a balance of erosive and accretive wave forces.

In order to use the depth averaged van Rijn transport model to reproduce seasonal cross-shore erosion and accretion conditions associated with wave height changes, f_{sus} would need to vary as a function of wave height. Assuming a reference wave height (H_{ref}) was a condition at which no net accretion or erosion occurs (for this study using the average wave parameters along the east coast of KwaZulu-Natal, H_{ref} = 1.6m is given by Kraus's model (1992)), wave heights greater than H_{ref} should result in erosion and wave heights less than H_{ref} should result in accretion.

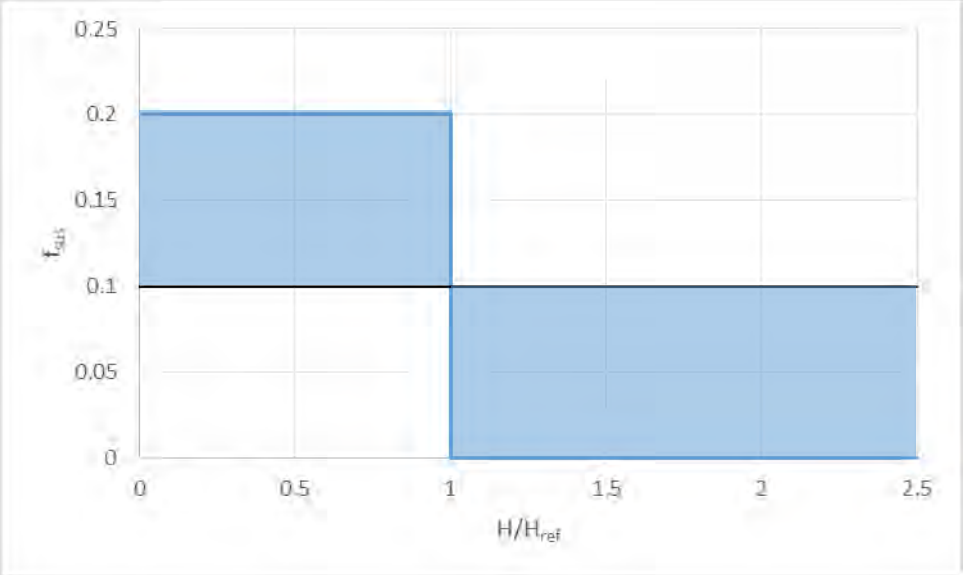

Figure 5.3: Range of f_{sus} values relative to H/H_{ref} to reproduce expected onshore/offshore sediment movement relative to wave height.

The shaded area of Figure 5.3 represents the feasible range of f_{sus} values that could be used to predict expected offshore or onshore sediment transport as a function of wave height. For a significant wave height less than the reference height onshore movement is expected and f_{sus} should be greater than 0.1. Alternatively with f_{sus} lower than 0.1, the model will predict offshore movement for wave heights greater than the reference height.

Using Figure 5.3, the f_{sus} value used within the van Rijn model is able to give a qualitative prediction of the cross-shore morphological evolution relative to wave height. Further studies would be required to be able to use this method to obtain an accurate quantitative prediction of the cross-shore

sediment transport using the van Rijn model. The model would need to be calibrated with a variable f_{sus} for different wave conditions to yield both the expected cross-shore transport direction and magnitude. This would allow a specification of how f_{sus} should vary as a function of wave height within the transport model to predict the correct cross-shore morphological evolution. This may be a viable approach to improve the cross-shore sediment transport predicted by the depth averaged van Rijn formula. Since Delft3D is open source software, this change can be implemented in the model. It must be noted that this calibration could also have an impact on the predicted longshore transport rates which should be taken into consideration if this issue is investigated further.

5.2 Bijker-Bailard Model

Similar to the van Rijn formula, the Bijker-Bailard formula allows for the incorporation of wave asymmetry effects on cross-shore transport through use of a calibration coefficient (A_{fac}). An increase in the wave asymmetry should in theory increase the amount of sediment transported towards the shore due to the wave forces. A range of A_{fac} values from 0.2 to 1 were tested on 1m (expected accretion) and 3m (expected erosion) wave conditions and the effect of this on the cross-shore transport for both wave events is shown in Figure 5.4.

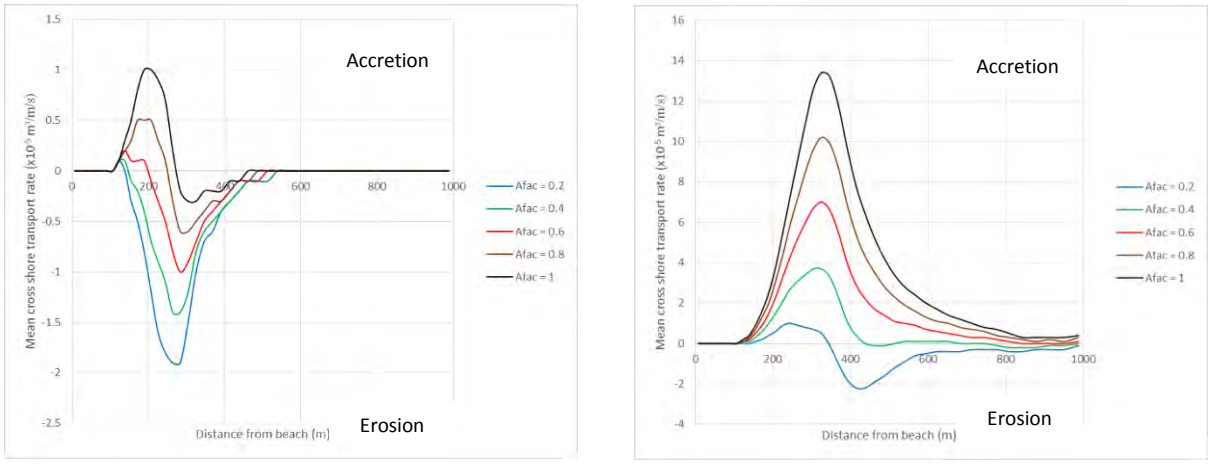

Figure 5.4: a) Bijker-Bailard cross-shore sediment transport rates for Hs = 1m and varying A_{fac}. b) Varying Bijker-Bailard cross-shore sediment transport rates for varying Hs = 3m and varying A_{fac}.

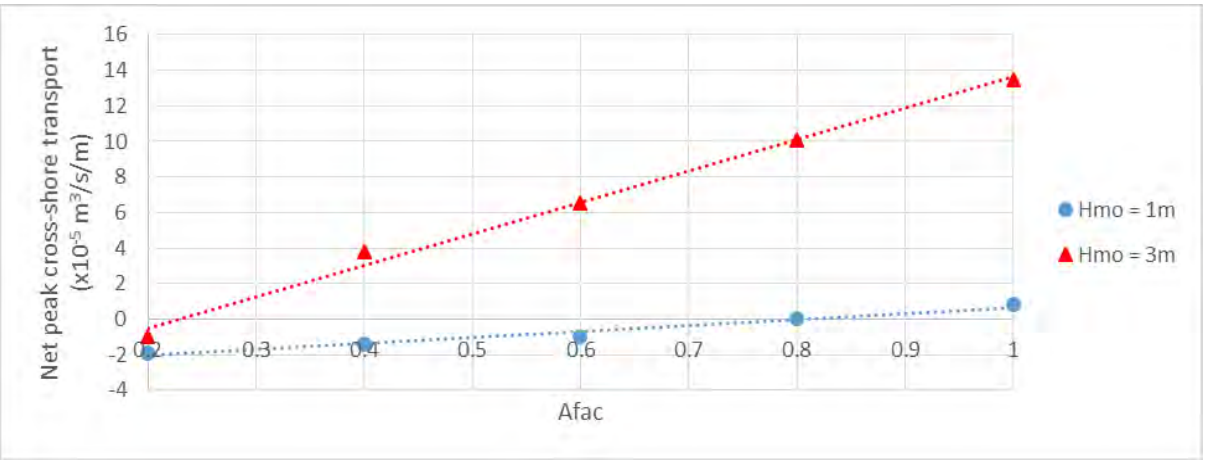

Figure 5.5: Net cross-shore transport rates varying as a function ofA_{fac} (Positive rates represent onshore movement and negative rates represent offshore movement)

For a wave height of 1m, the Bijker-Bailard formula predicts net onshore sediment movement for an A_{fac} > 0.8 and net offshore movement for an A_{fac} < 0.8 (Figure 5.5). Larger waves result in greater asymmetry. Therefore the influence A_{fac} has on cross-shore transport increases with wave height. Therefore for a wave height of 3m, net onshore sediment movement was predicted for an A_{fac} > 0.2 and net offshore movement was predicted for an A_{fac} < 0.2.

Table 5.2: Summary of Bijker-Bailard cross-shore calibration.

H_s (m)	Expected Cross-shore Movement	A_{fac}	Modelled Cross-shore Movement	Volume Moved (m^3/m beach width)
1	Onshore	0.2	Offshore	5.3
		0.4	Offshore	3.7
		0.6	Offshore	2.5
		0.8	None	-
		1.0	Onshore	4.6
3	Offshore	0.2	Offshore	0.82
		0.4	Onshore	14.9
		0.6	Onshore	24.8
		0.8	Onshore	34.9
		1.0	Onshore	45.4

Due to the A_{fac} value having a significant influence on the larger waves and the transport in the direction of wave propagation, the Bijker-Bailard formula does not produce significant erosion and offshore bar formation during large wave events with an A_{fac} > 0.2. However an A_{fac} < 0.2 results in net offshore sediment transport for smaller wave conditions and needs to be above 0.8 to reproduce the expected accretion for a wave height of 1m. Therefore no single A_{fac} value predicts erosion during

large wave events and accretion during smaller wave conditions. A single A_{fac} value may be able to reproduce a long term equilibrium profile through no net erosion or accretion but is not as easily predicted as was for the van Rijn model. This was because the A_{fac} value where no net erosion or accretion was predicted varied with the wave height.

It can be observed that varying just the A_{fac} as a function of wave height could not reproduce significant offshore transport during larger wave events and therefore would not be a viable solution to improve the Bijker-Bailards's cross-shore sediment transport model. The Bailard approach that incorporates a wave asymmetry factor to calibrate the cross-shore transport can also account for a bed slope correction factor which was not considered in this study. This calibration coefficient increases the offshore transport due to gravity and the bed slope gradient. It may be necessary to include this to accurately predict the significant erosion experienced along beaches during large wave events. This means that for the Bijker-Bailard model to reproduce expected onshore and offshore sediment transport, the wave asymmetry factor and the bed slope correction factor would need to vary as a function of wave height.

5.3 Soulsby-van Rijn Model

Unlike the van Rijn and Bijker-Bailard models, the Soulsby-van Rijn model does not allow the adjustment of any coefficient that directly influences the cross-shore sediment transport. Therefore the model was only run once with each wave condition to determine if it was capable of reproducing accretion for the small wave event and erosion for the large wave event. Figure 5.6 reveals that the Soulsby-van Rijn model predicted a net offshore movement of sediment for both the 1m and 3m wave height.

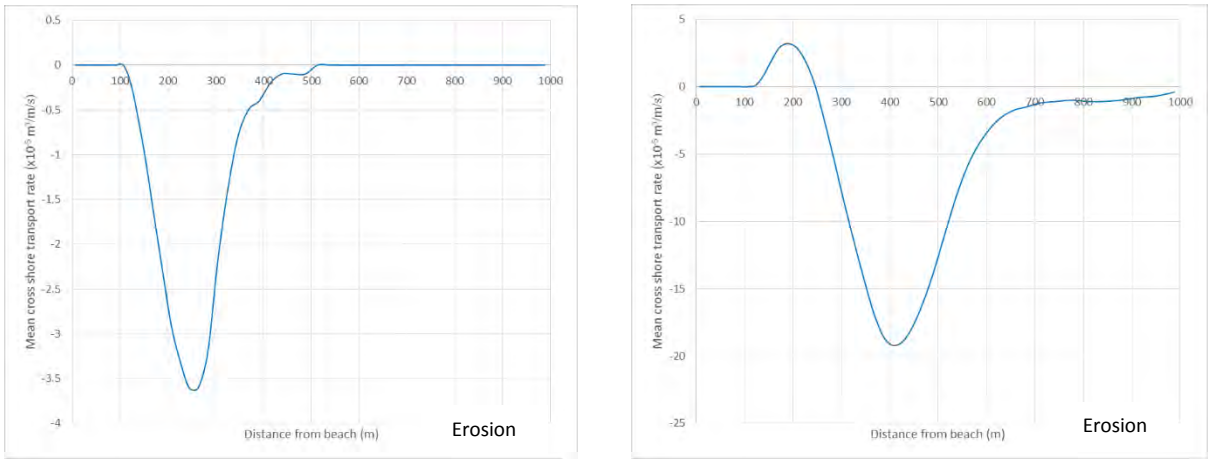

Figure 5.6: a) Soulsby-van Rijn cross-shore sediment transport rate for Hs = 1m. b) Soulsby-van Rijn cross-shore sediment transport rate for Hs = 3m.

This result reveals that the Soulsby-van Rijn was able to reproduce offshore sediment transport for large wave events but was unable to reproduce accretion expected from smaller waves. The small 1m wave height also caused a net offshore movement of sediment but at a lower rate than the larger wave event (Table 5.3).

Table 5.3: Summary of Soulsby-van Rijn cross-shore calibration.

H_s (m)	Expected Cross-shore Movement	Modelled Cross-shore Movement	Volume Moved (m^3/m beach width)
1	Onshore	Offshore	11.4
3	Offshore	Offshore	52.5

This net offshore transport is due to the method in which the Soulsby-van Rijn model incorporates the direction of the cross-shore sediment transport. The van Rijn and Bijker-Bailard models determine the magnitude of sediment transport in the direction of the propagating wave that counter acts the parameterized depth averaged return flow and sediment transport in the surf zone. Whereas the Soulsby-van Rijn assumes the sediment transport with the effects of waves is equal to the direction of the depth averaged flow (which is parameterized as a mean return flow in the cross-shore direction in the surf zone of the 2DH model).

This means that the model will constantly erode away the beach and is unable to predict beach recovery due to small waves. Therefore the Soulsby-van Rijn model is unable to maintain an equilibrium profile and is only applicable when used to reproduce short term erosion events.

5.4 Case Study Model Recommendation

As discussed in chapter 3, the beaches along the east coast of KwaZulu-Natal exhibit both beach erosion during storm events and recovery during smaller wave conditions that occur over longer periods. Therefore the chronic beach erosion along the beaches north of the Richards Bay harbour is due to northerly longshore transport of sediment and a lack of sediment supply caused by the harbour entrance. Therefore a sediment transport model is required that is able to reproduce an equilibrium profile over a medium to long term period as well as analyse the longshore transport accurately.

The Deflt3D cross-shore transport capability study revealed that none of the three sediment transport models tested could reproduce offshore movement during large waves and onshore movement during small waves with a single set of parameters which would maintain an equilibrium profile. However, the results did show that the van Rijn formula could be calibrated to maintain an equilibrium profile throughout the simulation by limiting the cross-shore sediment movement and preventing any net onshore or offshore sediment transport. This approach assumes that the longshore and cross-shore sediment transport act independently of one another which is not strictly correct. However, without long term cross-shore calibration data it is the only model that can maintain an equilibrium profile over a long term simulation.

For the Richards Bay sediment bypass case study, the van Rijn sediment transport model was chosen to model the beach response to three alternative nourishment schemes. The wave related transport factors were set to 0.1 which resulted in no net erosion or accretion during the simulation and no significant morphological changes occur due to cross-shore transport as shown in this study. Therefore the morphological changes to the modelled coast during the case study would be a result of the sediment pumped into the domain and the longshore transport (the primary cause of the chronic beach erosion north of the harbour entrance) causing the nourished sediment to spread and move up the coastline.

CHAPTER 6

Sediment Bypass Case Study Results and Discussion

This chapter presents the results of the Richards Bay sediment bypass case study. With a sediment budget of 1 Mm^3, Delft3D was used to model three alternative beach nourishment schemes and the beach response to the nourishment over the morphological period of one year. The results include a prediction of beach response to the nourishments, the distribution of the nourished sediment over the year and a quantitative analysis of the morphological evolution.

6.1 Initial Beach

All three morphological models started with the same initial bathymetry obtained from the hydrographic survey (Figure 6.1). The beach could be considered sand starved and had a nearly uniform beach width of 20 m. The three simulations started at the beginning of January which is considered the middle of summer and ran for a full morphological year until the end of December. This meant that the beach response due to the nourishment schemes were all relative to this initial bathymetry.

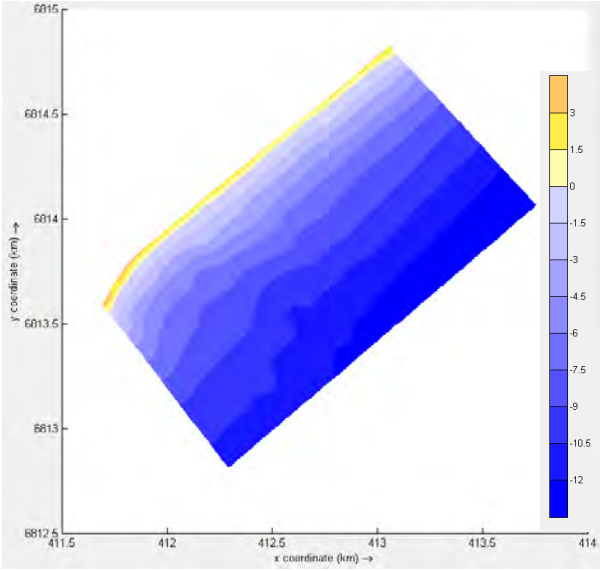

Figure 6.1: Initial Case Study Beach Bathymetry (m MSL).

6.2 Three Month Evaluation

After three simulated months the predicted morphological evolution for the three schemes was evaluated. It showed the beach response and nourished sediment distribution that had taken place for the three schemes between January and the beginning of April, which is also mid-Autumn. During this period, the wave climate was calm with no significant storm events occurring and the directional spread included both southerly and easterly incoming waves.

6.2.1 Continuous Nourishment Scheme

At the beginning of April 246600 m^3 of the budgeted sand had been dumped onto the beach at a continuous rate of 2740 m^3/day during the three months. Spreading of the sediment from the nourishment area can be observed, but very little sediment has been transported far northwards up the coastline. Due to the calmer easterly waves generally experienced during summer, the sediment gathered and nourished the beach directly in front of the sediment discharge pipeline and spread south to increase the beach width of the main recreational beach (Figure 6.2a). The calm southerly waves also spread the nourished sediment north, but no significant northern longshore transport occurred (Figure 6.2b)

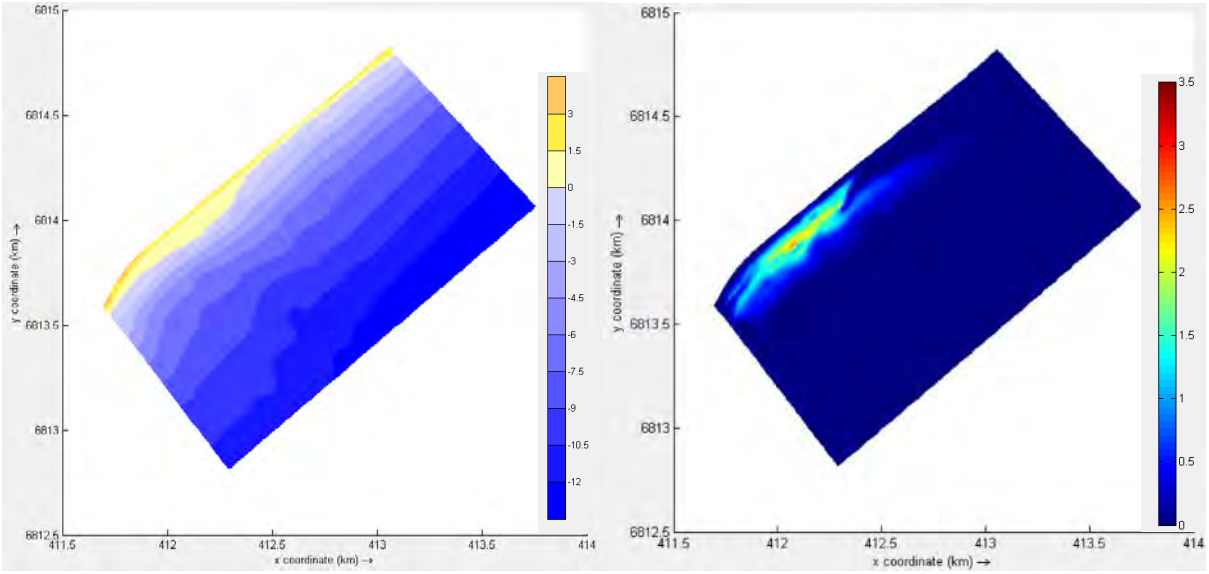

Figure 6.2: Results from the continuous nourishment after 3 months. a) Bathymetry (m MSL). b) Change in bathymetry relative to initial bathymetry (m).

Figure 6.3 shows the cross sectional bathymetry profile change for Alkantstrand immediately south of the discharge pipeline. It reveals that by the beginning of April the beach width of Alkantstrand will have increased by 90 m due to continuous daily beach nourishment.

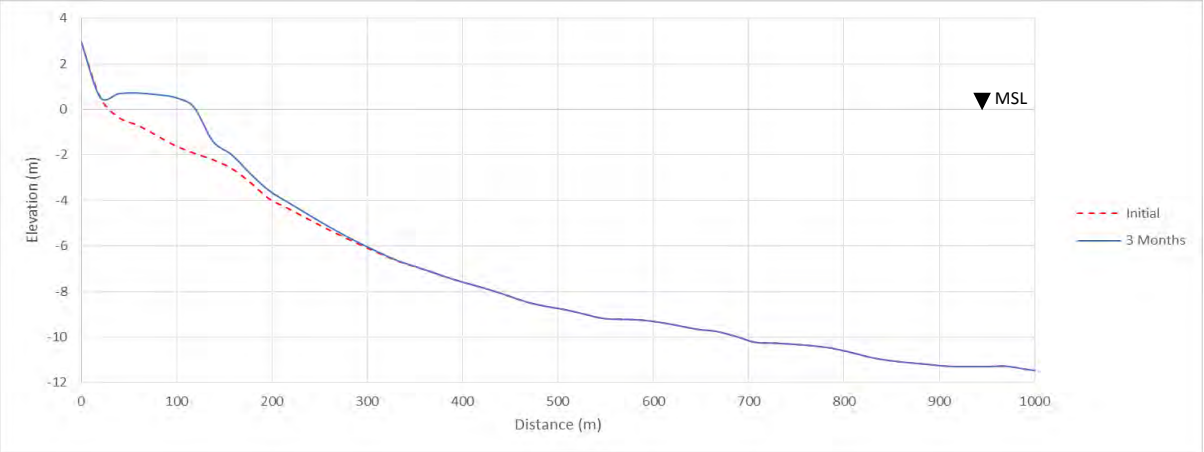

Figure 6.3: Cross sectional profile A-A after 3 months (Continuous nourishment scheme).

Even though there is no visible deposition of sediment along the northern beach within the model domain, nourished sediment has been transported and lost through the northern boundary of the model. This may have been a result of suspended sediment transported along the coast that did not settle and nourish the immediate coastline. Table 6.1 shows the volume of nourished sediment still within the model domain and the volume transported northwards out of the domain due to longshore transport.

Table 6.1: Nourished sediment distribution after 3 months (Continuous nourishment scheme).

Total percentage pumped (%)	Volume pumped (m^3)	Volume in model domain (m^3)	Volume lost through northern boundary (m^3)	Percentage lost through northern boundary (%)
25	246600	198420	48180	5

6.2.2 Bulk Nourishment Scheme

By the end of 3 months, 90% of the 1 Mm^3 (900000 m^3) of the budgeted sand had been dumped onto the beach which formed a large artificial sand island in front of the sediment discharge pipeline (Figure 6.4a). Significant spreading of the dumped sand both north and south of the discharge pipeline can be observed due to the large amount of sediment that was dumped onto the beach at a

rapid rate. Initial northward distribution can be observed as the nourished sand island begins to migrate northwards up the coast (Figure 6.4b). Only small longshore transport of the dumped sand is predicted along the coastline by the model during this period. This may be due to the calm wave conditions not being able to significantly erode the artificial sand island or that the beach change itself had an impact on the wave transformation which resulted in a reduction of the longshore transport.

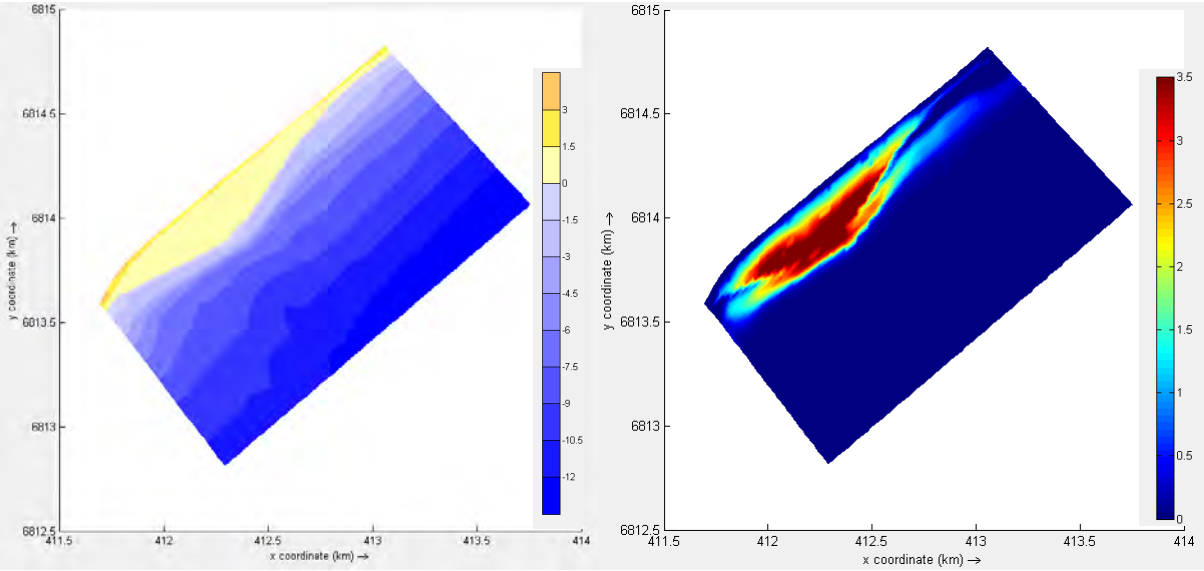

Figure 6.4: Results from the bulk nourishment after 3 months. a) Bathymetry (m MSL). b) Change in bathymetry relative to initial bathymetry (m).

The bulk nourishment resulted in a large increase of the recreational beach width south of the discharge pipeline. This part of the shoreline migrated 190 m seaward which is an additional 100 m of beach width than the continuous pumping scheme predicted at this point (Figure 6.5).

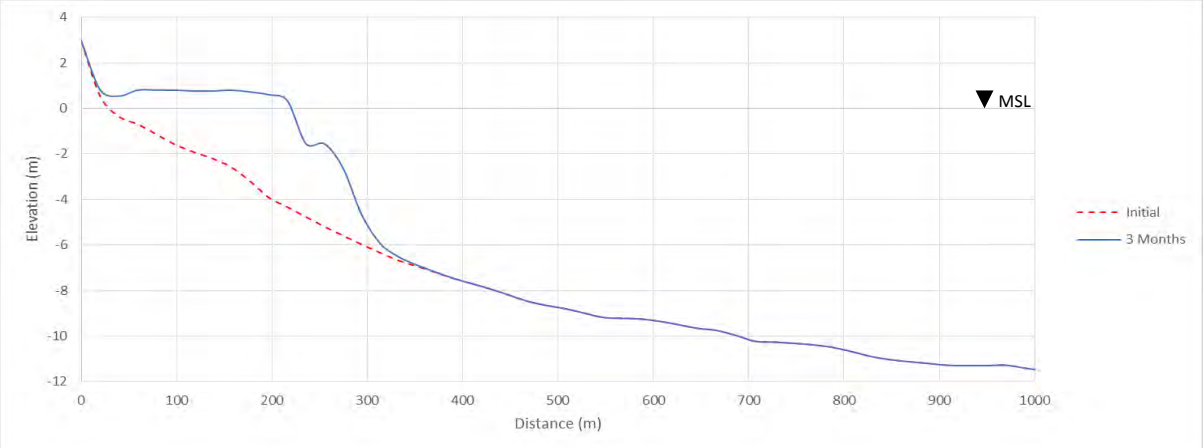

Figure 6.5: Cross sectional profile A-A after 3 months (Bulk nourishment scheme).

Due to the lateral spread of the rapidly dumped sediment and northerly longshore transport, some sand has been transported past the northern boundary after three months. However due to the calm wave climate, it does not erode the large artificial sand island and a significant amount of the nourished sediment is still within the model domain. Approximately only 14% of the 900000 m^3 has been lost through the northern boundary of the model.

Table 6.2: Nourished sediment distribution after 3 months (Bulk nourishment scheme).

Total percentage pumped (%)	Volume pumped (m^3)	Volume in model domain (m^3)	Volume lost through northern boundary (m^3)	Percentage lost through northern boundary (%)
90	900000	769100	130900	13

6.2.3 Bimonthly Nourishment Scheme

Two bimonthly bulk nourishments were simulated between January and April. Therefore 333300 m^3 of sand had been pumped onto the beach by the beginning of April. Due to the amount of nourished sediment being close to the continuous nourishment amount, the distribution of this scheme emulates the continuous nourishment scheme more closely than the bulk nourishment scheme. At this point, more sand has been dumped into the system than in the continuous scheme and therefore the beach north and south of the nourishment area have been more nourished than observed for the continuous case (Figure 6.6).

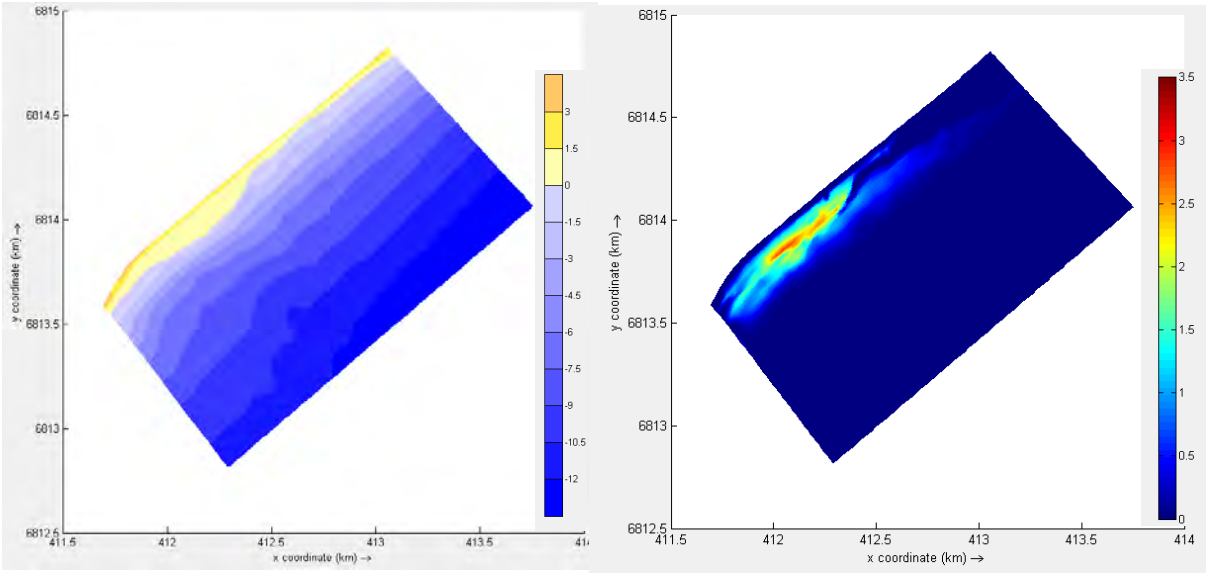

Figure 6.6: Results from the bimonthly nourishment after 3 months. a) Bathymetry (m MSL). b) Change in bathymetry relative to initial bathymetry (m).

The beach width increase of Alkantstrand due to the rapid nourishment of 333300 m^3 was approximately 120 m (Figure 6.7).

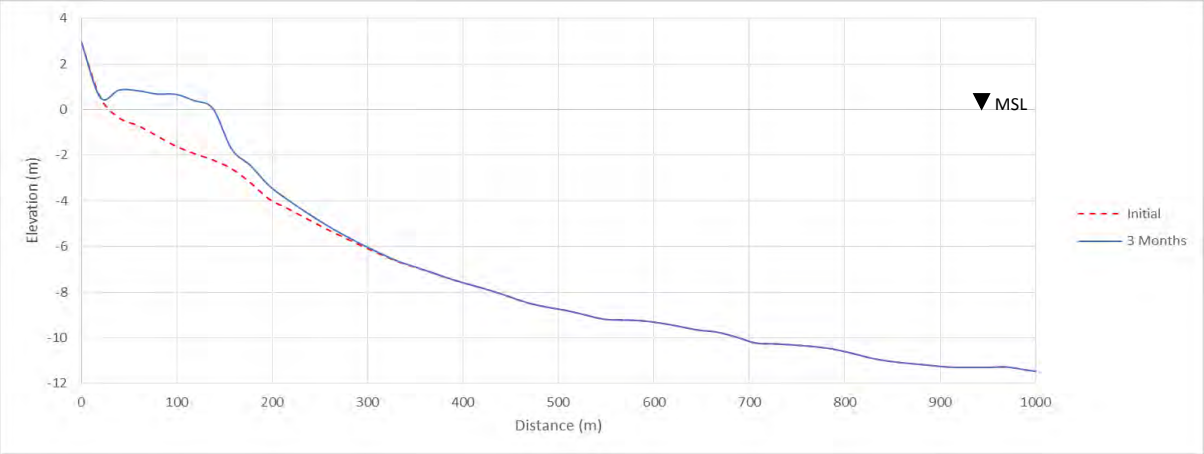

Figure 6.7: Cross sectional profile A-A after 3 months (Bimonthly nourishment scheme).

Table 6.3 represents the nourished sediment dumped onto the beach on a bimonthly basis, the amount of sand within the model domain after three months and the volume of sand lost through the northern lateral boundary due to longshore transport.

Table 6.3:Nourished sediment distribution after 3 months (Bimonthly nourishment scheme).

Total percentage pumped (%)	Volume pumped (m^3)	Volume in model domain (m^3)	Volume lost through northern boundary (m^3)	Percentage lost through northern boundary (%)
33	333300	264000	69300	7

6.3 Six Month Evaluation

The second evaluation was at the halfway point of the morphological year modelled for each nourishment case. The autumn to winter period between April and July experienced the roughest wave conditions with a predominant southerly wave direction. A storm event with wave heights exceeding 3.5 m also occurred during this period. It was observed that for all nourishment cases, most of the northward longshore occurred during this season due to the large southerly waves.

6.3.1 Continuous Nourishment Scheme

By the middle of the morphological year, half the budgeted sediment had been used to nourish the beach (500000 m^3). Due to the large southerly wave events during this period, approximately 416400 m^3 of the 500000 m^3 nourished sand has been transported northwards resulting in the beach almost returning to its initial sand starved state (Figure 6.8). Some sediment along Alkantstrand directly in front and south of the pipeline has remained and is attributed to the sheltering effect due to the harbour breakwaters and the very southerly direction of the large incoming waves during this period.

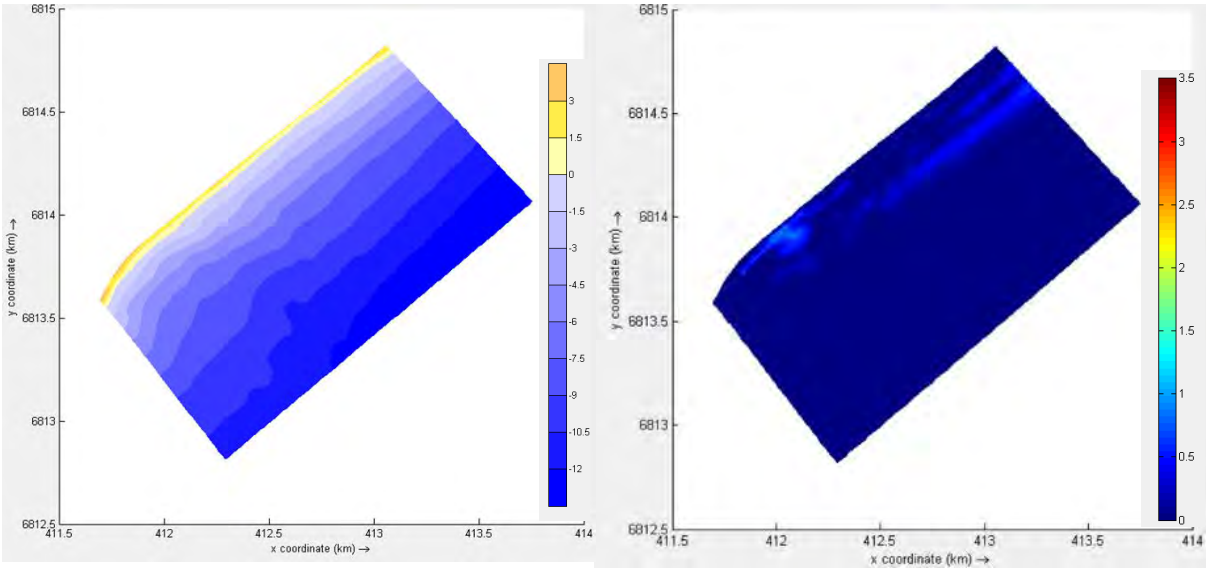

Figure 6.8: Results from the continuous nourishment after 6 months. a) Bathymetry (m MSL). b) Change in bathymetry relative to initial bathymetry (m).

Figure 6.9 shows the shoreline of Alkantstrand south of the discharge pipeline receded by 80 m due to the sediment inputs being insufficient to balance the high longshore transport rates during this period.

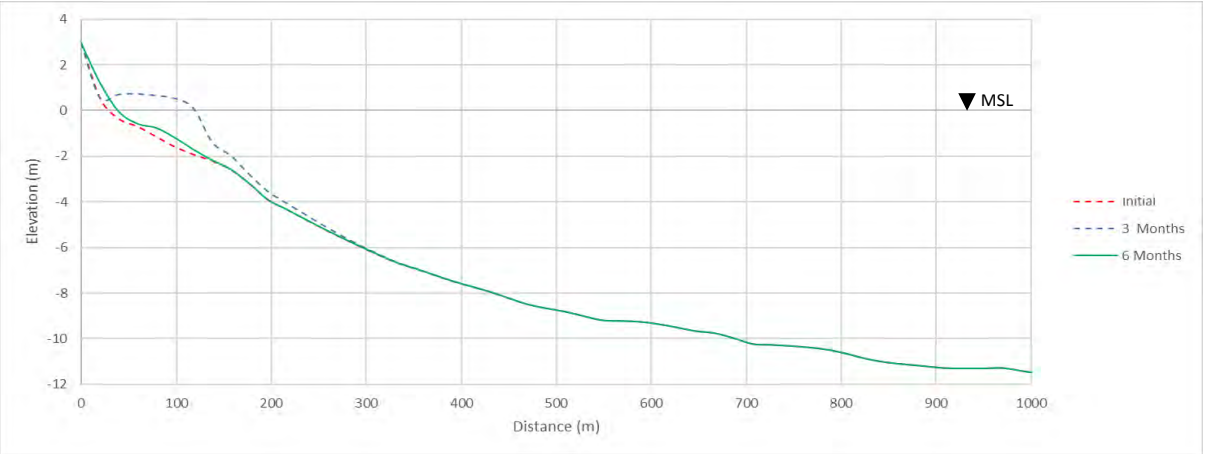

Figure 6.9: Cross sectional profile A-A after 6 months (Continuous nourishment scheme).

Table 6.4: Nourished sediment distribution after 6 months (Continuous nourishment scheme).

Total percentage pumped (%)	Volume pumped (m^3)	Volume in model domain (m^3)	Volume lost through northern boundary (m^3)	Percentage lost through northern boundary (%)
50	500000	83600	416400	42

6.3.2 Bulk Nourishment

It is immediately noticeable from Figure 6.10 that the storm event and large waves resulted in significant erosion and northward transport of the sand island created by the bulk nourishment scheme. The southern recreational beach has been protected from the large southerly waves to some degree by the sheltering effect of the harbour entrance but a significant amount of sand has been eroded and transported northwards. The large increase in beach width near the northern boundary and a decrease in beach width along Alkantstrand indicates that the storm event eroded the sand from the nourishment area and deposited in approximately 1.5km north of the breakwater after the storm. It can be seen that the sheltering effect of the breakwater ends approximately 1km north of the harbour entrance and the increase in wave energy at this point resulted in scour and reduction of beach width up to 180 m as seen in the middle of the model domain in Figure 6.10a. Unlike the continuous nourishment scheme, the beach for this scheme did not return to its initial sand starved state. The effects of the bulk nourishment after the storm are still evident along the southern and

northern sections of modelled coastline but the spreading of the nourished sediment northwards is not uniform as seen by the very narrow beach in the middle of the domain.

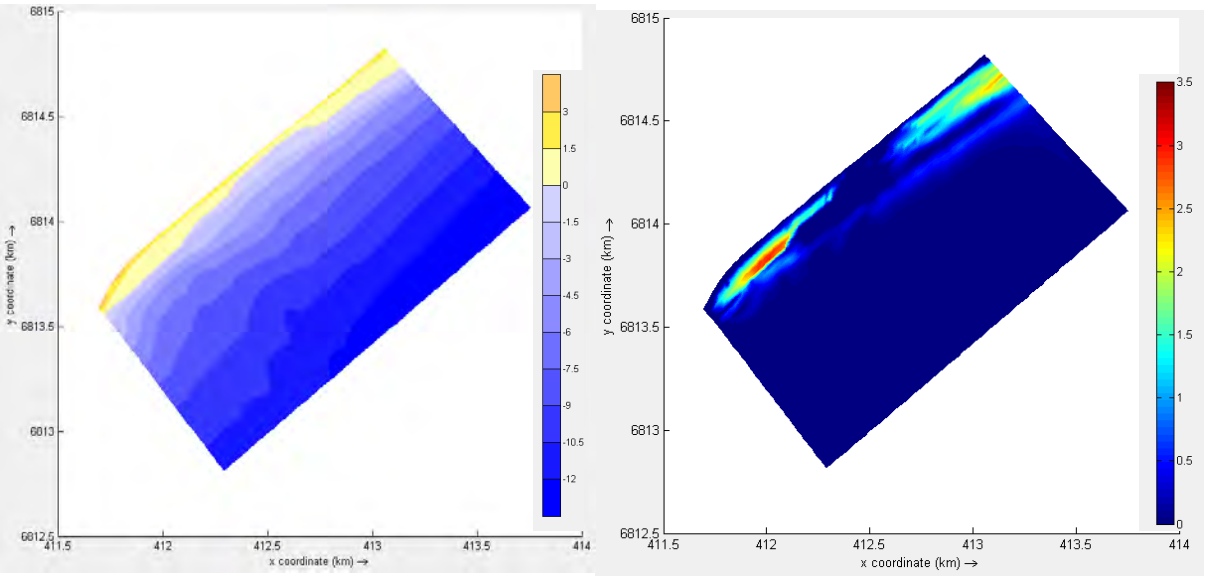

Figure 6.10: Results from the bulk nourishment after 6 months. a) Bathymetry (m MSL). b) Change in bathymetry relative to initial bathymetry (m).

Due to erosion and the large northward longshore transport of the bulk nourished sand, the beach width along the coast south of the discharge pipeline retreated 100 m towards the shore relative to its 3 month position (Figure 6.11).

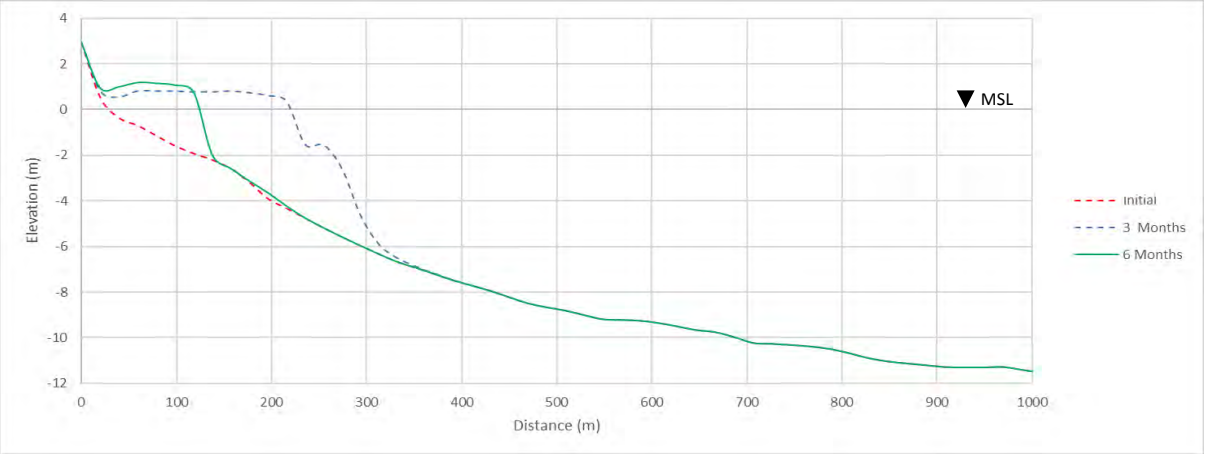

Figure 6.11: Cross sectional profile A-A after 6 months (Bulk nourishment scheme).

After 100 days, the full 1 Mm^3 of budgeted sand had been pumped onto the case study beach. After 6 months, over two thirds of the budgeted sand that was pumped onto the beach had been

transported northwards through the northern boundary of the model domain. The waves breaking onto the artificial sand island, especially for the large storm waves, moved a significant amount of the nourished sediment northwards.

Table 6.5: Nourished sediment distribution after 6 months (Bulk nourishment scheme).

Total percentage pumped (%)	Volume pumped (m^3)	Volume in model domain (m^3)	Volume lost through northern boundary (m^3)	Percentage lost through northern boundary (%)
100	1000000	315700	684300	68

6.3.3 Bimonthly Nourishment

After six months, three bimonthly nourishments have taken place resulting in 500000 m^3 of sand pumped onto the beach at this point. Similar to the continuous nourishment scheme, the large waves and storm event transported most of the nourished sediment north up the coastline and out of the northern boundary of the model. An overall reduction of beach width from the previous three month evaluation was observed but the sheltering effect of the harbour entrance did protect a section of coastline in front of the discharge pipeline. Due to this, even after the storm period Alkantstrand did not erode completely back to its initial state (Figure 6.12).

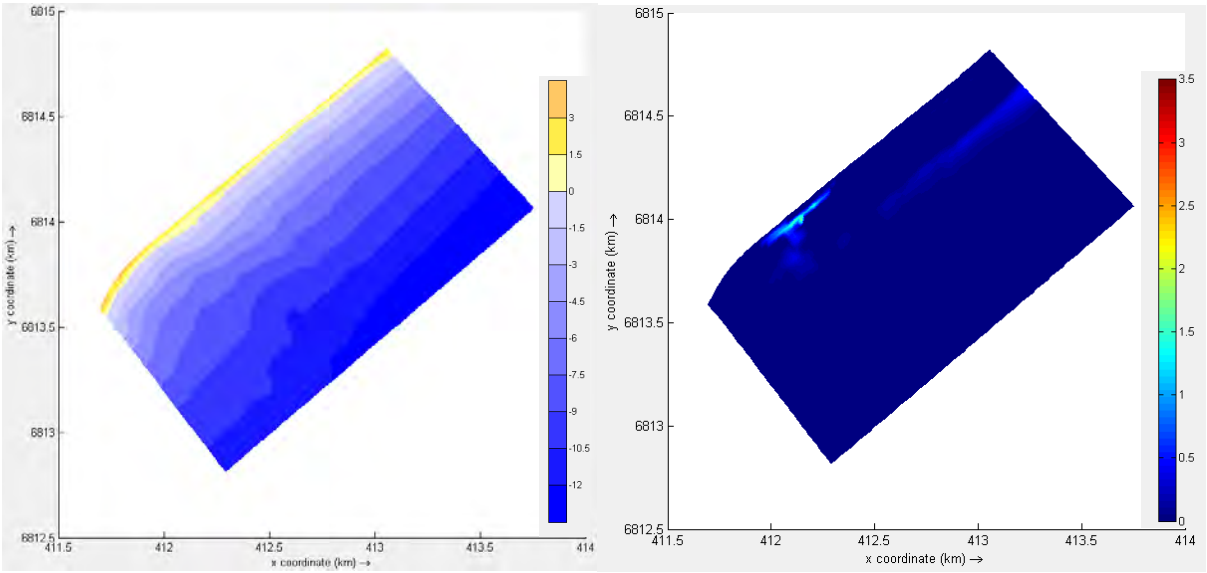

Figure 6.12: Results from the bimonthly nourishment after 6 months. a) Bathymetry (m MSL). b) Change in bathymetry relative to initial bathymetry (m).

After the winter/autumn period the beach width just south of the discharge pipeline eroded 80 m (Figure 6.13). This beach width after the storm season was still 10 m greater than the initial beach width at the beginning of the year.

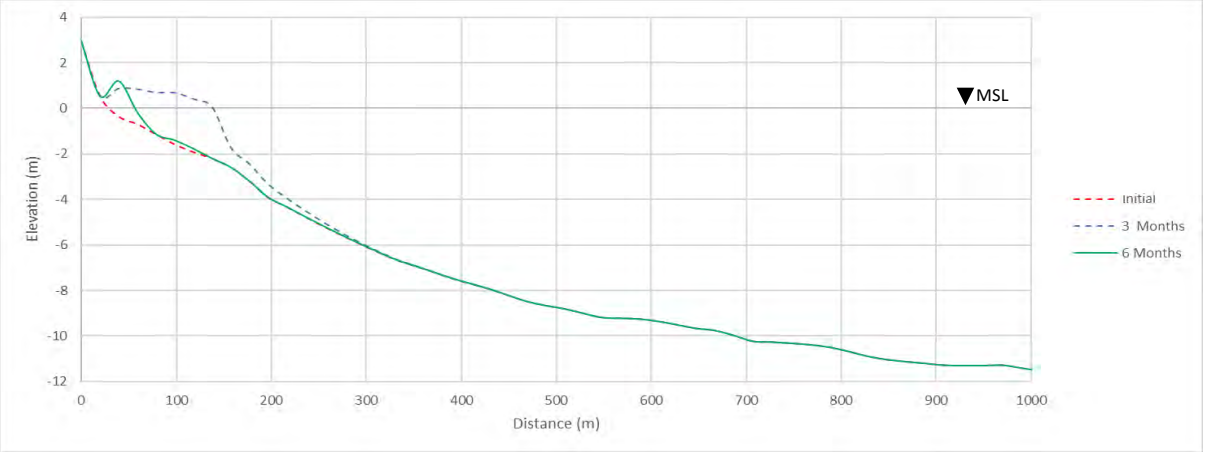

Figure 6.13: Cross sectional profile A-A after 6 months (Bimonthly nourishment scheme).

Due to the storm event, a majority of the sand pumped into the domain due to the nourishment scheme was transported northwards up the coastline through the northern boundary.

Table 6.6: Nourished sediment distribution after 6 months (Bimonthly nourishment scheme).

Total percentage pumped (%)	Volume pumped (m^3)	Volume in model domain (m^3)	Volume lost through northern boundary (m^3)	Percentage lost through northern boundary (%)
50	500000	45500	454500	45

6.4 Nine Month Evaluation

Moving into spring, the wave conditions typically calms after the rough autumn/winter period along the east coast of South Africa. Storm events are known to cause a significant loss of beach width as observed in the previous six month evaluation, but significant damage to coastal areas occurs when a second storm event happens before the beach has significantly recovered. Therefore effective beach recovery during this period is crucial to achieve before the next rough autumn/winter period, which experience large wave heights, to reduce coastal vulnerability.

6.4.1 Continuous Nourishment

The continuous pumping during this period caused a gradual seaward migration of the shore along the southern beach near the nourishment area by the end of September. There was no significant increase in beach width north of the outlet but the sediment distribution (Figure 6.14b) reveals than a net northward longshore transport can be observed as the nourished sediment begins to move up the coastline. After nine months of continuous pumping, 748000 m^3 of sand was dumped onto the beach of which 547700 m^3 had been transported through the northern boundary of the model and 20030 m^3 remains in the model domain (Table 6.7) causing a gradual increase in beach width.

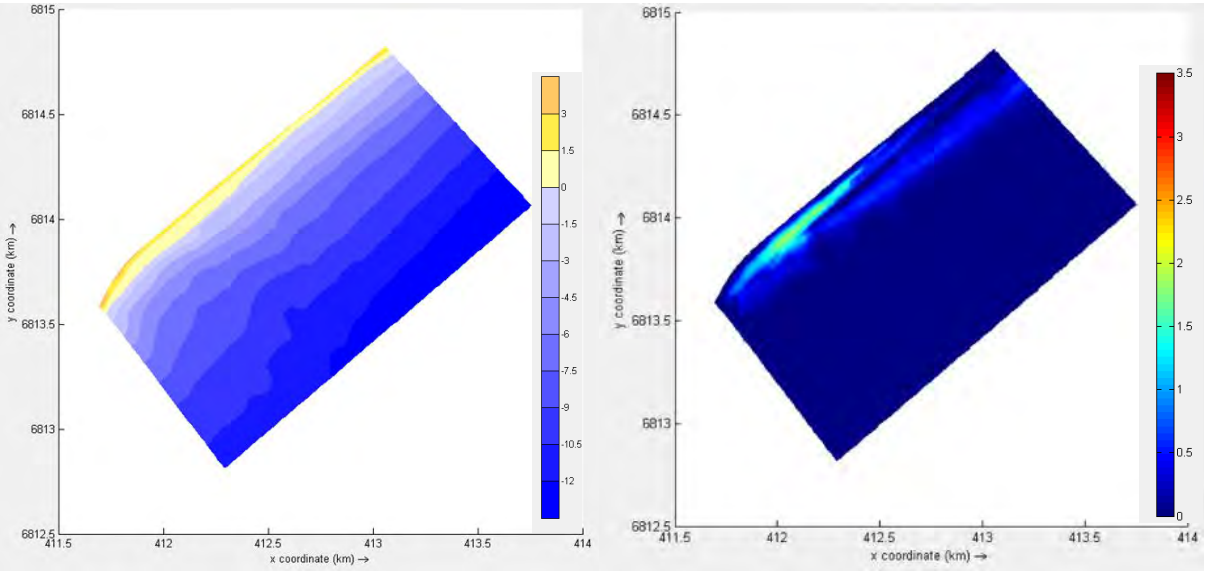

Figure 6.14: Results from the continuous nourishment after 9 months. a) Bathymetry (m MSL). b) Change in bathymetry relative to initial bathymetry (m).

By the end of September the depleted post storm Alkantstrand beach begins to recover due to the continuous nourishment, which aids in replenishing the sediment lost during the storm event. This results in a beach width increase of 40 m (Figure 6.15).

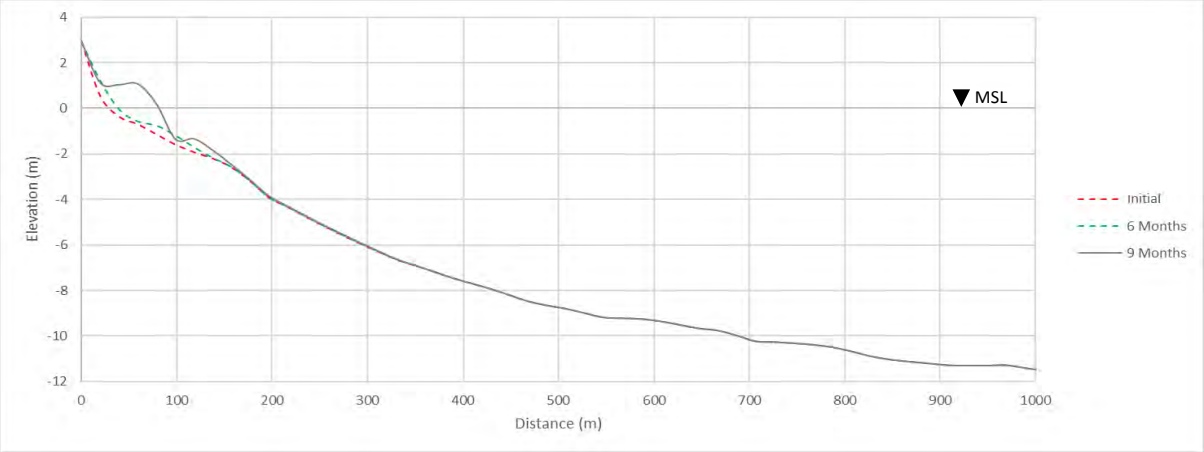

Figure 6.15: Cross sectional profile A-A after 9 months (Continuous nourishment scheme).

The sediment pumped into the model domain after the storm period begins moving gradually up the coastline due to the calmer waves. This gradual longshore transport begins to nourish the beaches north of Alkantstrand as the sand migrates up the coastline.

Table 6.7: Nourished sediment distribution after 9 months (Continuous nourishment scheme).

Total percentage pumped (%)	Volume pumped (m^3)	Volume in model domain (m^3)	Volume lost through northern boundary (m^3)	Percentage lost through northern boundary (%)
75	748000	200300	547700	55

6.4.2 Bulk Nourishment

In the three months between the last evaluation and the current nine month evaluation, no sediment was deposited into the system. Therefore the coastline retains a similar shape to the post storm profile but experienced an overall reduction of beach width due to constant northwards longshore transport and no additional nourishment to replenish the beach (Figure 6.16). The sheltering effect of the harbour entrance prevented significant longshore erosion of the artificial sand island that remained along Alkantstrand. The longshore transport along the coast unsheltered by the northern breakwater is evident in Figure 6.16b and a significant amount of the nourished sediment unsheltered was transported north up the coast and lost through the northern lateral boundary

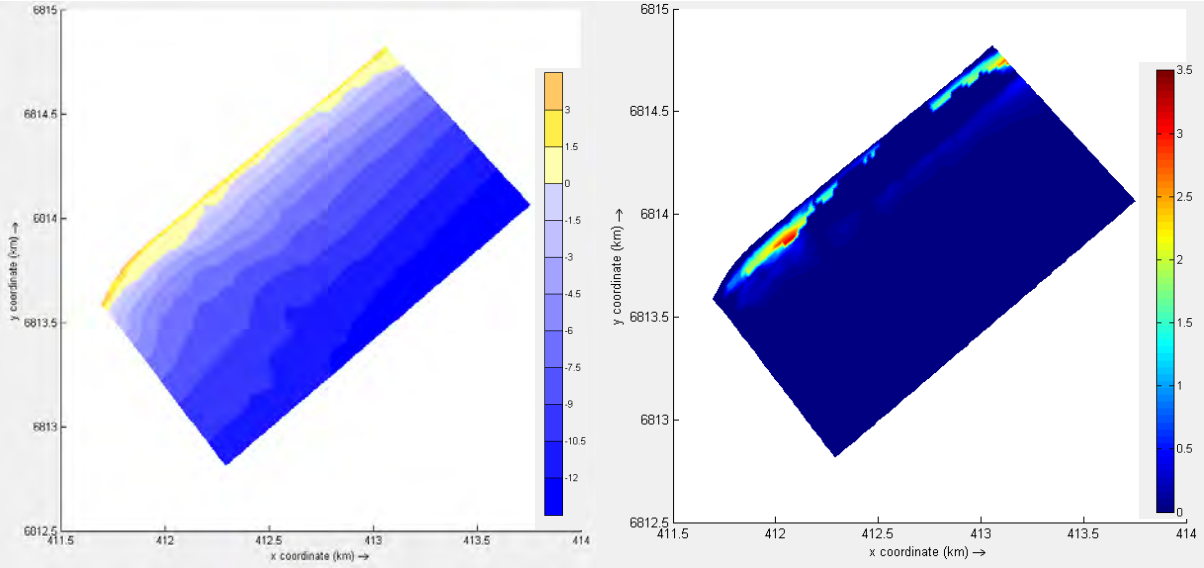

Figure 6.16: Results from the bulk nourishment after 9 months. a) Bathymetry (m MSL). b) Change in bathymetry relative to initial bathymetry (m).

Even though the sheltering effect of the breakwater significantly reduced the northern transport, it was still present and caused a beach width reduction along Alkantstrand of 40 m over this three month period (Figure 6.17).

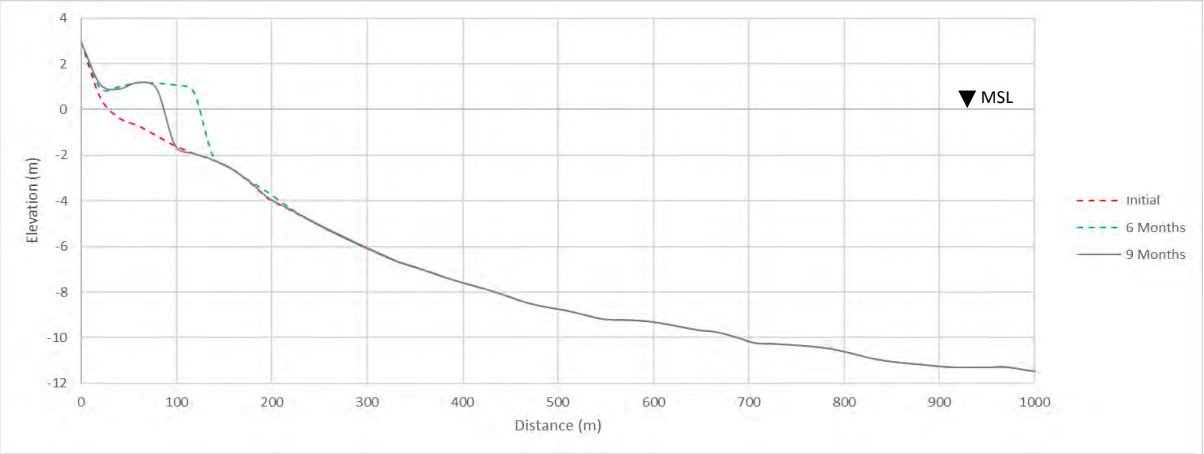

Figure 6.17: Cross sectional profile A-A after 9 months (Bulk nourishment scheme).

The northern beaches not sheltered by the breakwater had almost returned to a pre-nourished state due to the sediment being lost through the northern boundary and Table 6.8 shows that no additional sediment was pumped onto the beach to replace what was lost.

Table 6.8: Nourished sediment distribution after 9 months (Bulk nourishment scheme).

Total percentage pumped (%)	Volume pumped (m^3)	Volume in model domain (m^3)	Volume lost through northern boundary (m^3)	Percentage lost through northern boundary (%)
100	1000000	157800	842200	84

6.4.3 Bimonthly Nourishment

After the storm period an additional two bimonthly nourishments took place along the beach. This meant that 333300 m^3 of sand was dumped rapidly along the beach during this period to replenish the sediment lost during the winter/autumn period. Due to the rapid rate of nourishment implemented in the bimonthly scheme, the reclamation of the beach was not as uniform as observed in the continuous nourishment case. There is an evident bulge in front of the discharge pipeline where the sand has been deposited and settled (Figure 6.18a). It was also evident that the northwards longshore transport begins to erode the sand bulge as seen in Figure 6.18b and transports sediment up the coast resulting in an increase in beach width just north of the discharge pipeline.

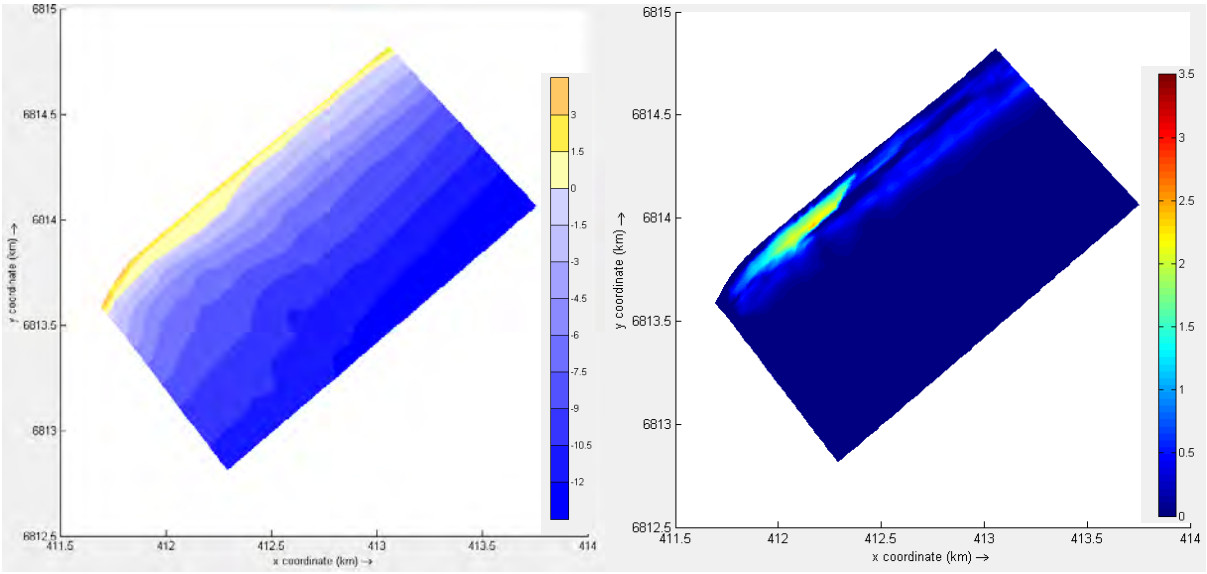

Figure 6.18: Results from the bimonthly nourishment after 9 months. a) Bathymetry (m MSL). b) Change in bathymetry relative to initial bathymetry (m).

This replenishment of the beach resulted in an increased beach width of 45 m along the main recreational beach of Richards Bay as seen in figure 6.19.

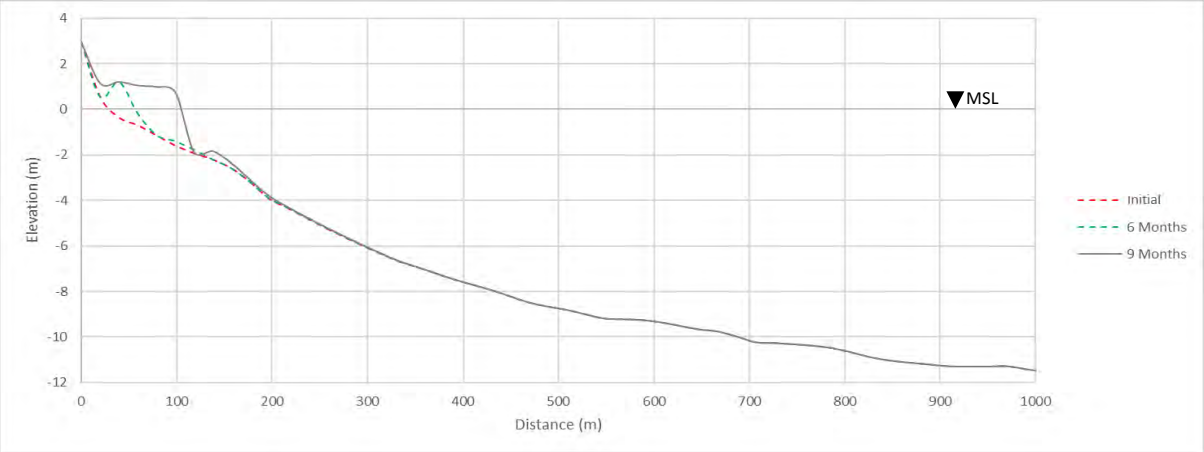

Figure 6.19: Cross sectional profile A-A after 9 months (Bimonthly nourishment scheme).

After nine months 833300 m^3 of the total 1 Mm^3 of sand had been pumped onto the beach at two month intervals. 61% of that had been transported up the coastline and through the northern lateral boundary of the model.

Table 6.9: Nourished sediment distribution after 9 months (Bimonthly nourishment scheme).

Total percentage pumped (%)	Volume pumped (m^3)	Volume in model domain (m^3)	Volume lost through northern boundary (m^3)	Percentage lost through northern boundary (%)
83	833300	221100	612200	61

6.5 One Year Evaluation

At the end of a full year of beach nourishment, the full budgeted 1 Mm^3 of sand for all three cases had been pumped onto the case study beach. This showed the beach response to the three different nourishment schemes over the case study period of one morphological year and allowed a comparison to be done on the performance of each scheme.

6.5.1 Continuous Nourishment

It can be observed that there was an overall seaward movement of the coastline along the entire case study beach due to continuous year round nourishment.

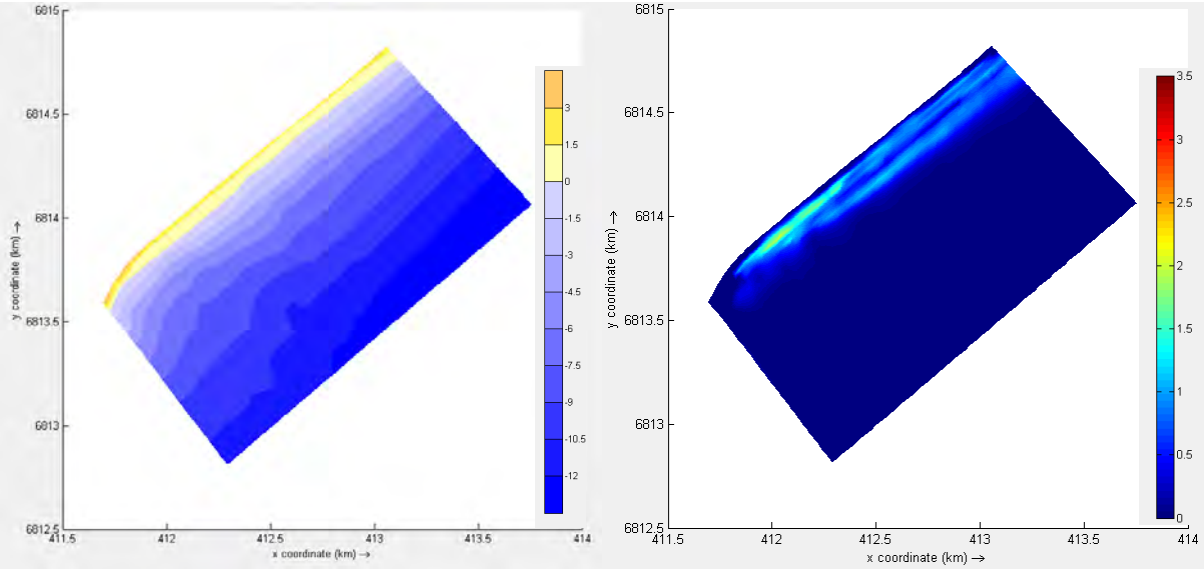

Figure 6.20: Results from the continuous nourishment after 1 year. a) Bathymetry (m MSL). b) Change in bathymetry relative to initial bathymetry (m).

During this period, the sediment pumped into the system approximately equalled the northward longshore transport resulting in little change of the beach width of Alkantstrand from the last evaluation at nine months. This increased the beach width north of the discharge pipeline resulted in a uniformly nourished coastline. The total beach width increase at the end of the year relative to the initial bathymetry was approximately 40 m along the entire modelled coastline north of the Richards Bay harbour entrance (Figure 6.21).

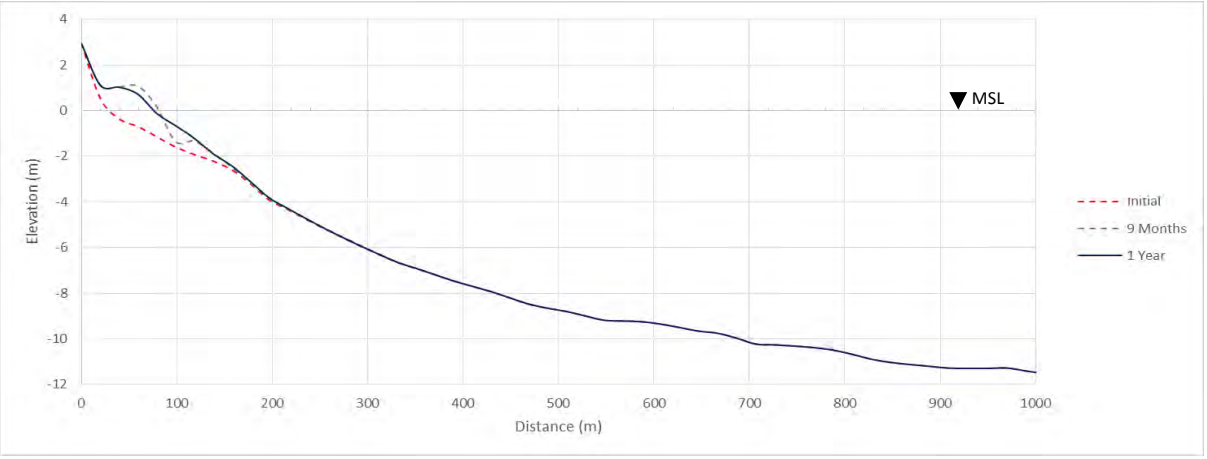

Figure 6.21: Cross sectional profile A-A after 1 year (Continuous nourishment scheme).

At the end of the continuous nourishment scheme, 27% of the sand pumped onto the beach throughout the year remained within the model domain. Therefore maintaining this nourishment rate the beach would grow at 27% per annum while there is available sediment in the sand trap. This remaining sediment results in the nourished coastline observed in Figure 6.20a while 74% of the nourished sediment was lost through the northern boundary due to longshore transport.

Table 6.10: Nourished sediment distribution after 1 year (Continuous nourishment scheme).

Total percentage pumped (%)	Volume pumped (m^3)	Volume in model domain (m^3)	Volume lost through northern boundary (m^3)	Percentage lost through northern boundary (%)
100	1000000	265000	735000	74

6.5.2 Bulk Nourishment

After a year, the majority of the 1 Mm^3 of sand dumped onto the beach in the beginning of the year has been transported north up the coastline. A small amount, approximately 13%, of the total budgeted sediment remained along Alkantstrand (Table 6.11). The sediment that remained along Alkantstrand was due to the harbour entrance decreasing the wave forces along the beach just north of the breakwater. This meant that the bulk nourishment left the main recreational beach in a nourished state after the period of a year but the beaches north of the discharge pipeline returned to their initial pre nourished state due to longshore transport as seen in Figure 6.22.

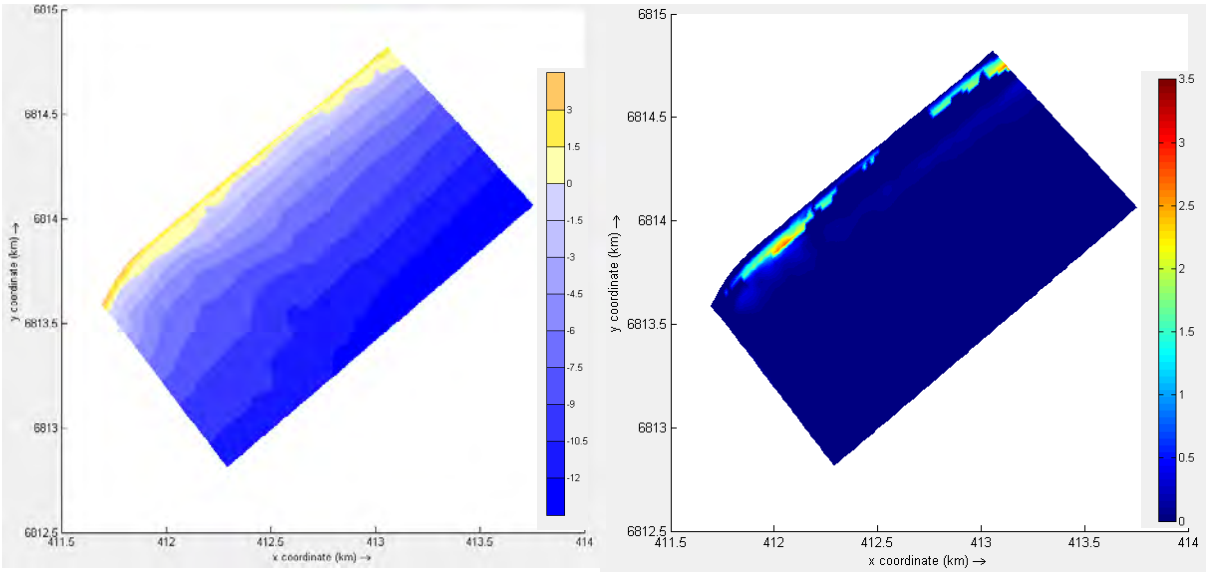

Figure 6.22: Results from the bulk nourishment after 1 year. a) Bathymetry (m MSL). b) Change in bathymetry relative to initial bathymetry (m).

After a year of morphological movement and allowing the bulk nourished sediment to move along the coastline naturally, a net increase of 40 m of beach width (Figure 6.23) from was observed from the initial bathymetry for the main beach south of the discharge pipeline.

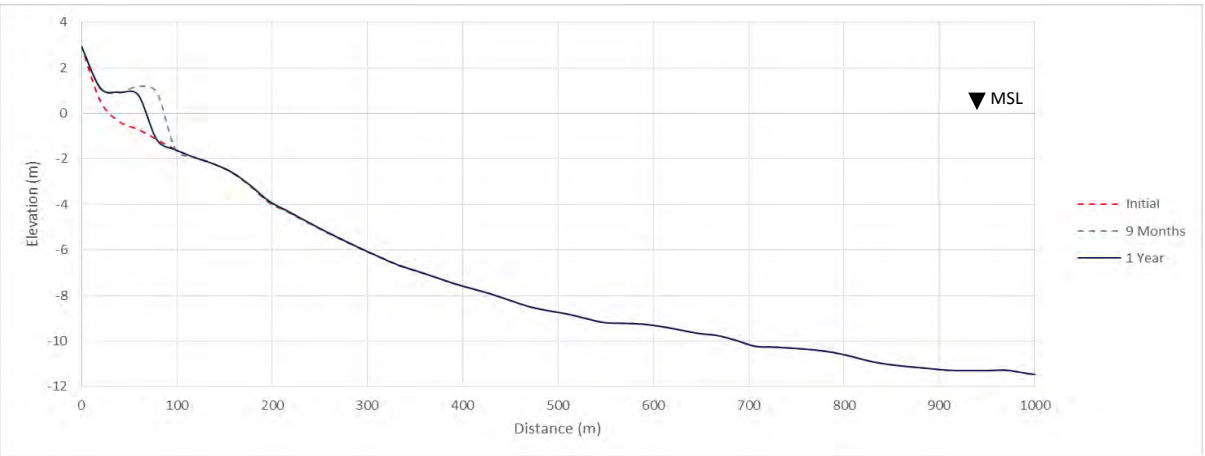

Figure 6.23: Cross sectional profile A-A after 1 year (Bulk nourishment scheme).

Table 6.11: Nourished sediment distribution after 1 year (Bulk nourishment scheme).

Total percentage pumped (%)	Volume pumped (m^3)	Volume in model domain (m^3)	Volume lost through northern boundary (m^3)	Percentage lost through northern boundary (%)
100	1000000	128700	871300	87

6.5.3 Bimonthly Nourishment

Figure 6.24 reveals that a bimonthly pumping scheme emulates a similar beach response to the continuous nourishment scheme with the entire modelled coastline showing an increase in beach width after the year of beach nourishment. The beach width increase was greater in the area in front of the discharge pipeline showing a slight bulge in the coastline and becomes more uniform up the coastline. This is because the sediment is dumped rapidly into the system and then moved up the coast due to longshore transport whereas the continuous nourished sediment was spread and transported as it was pumped onto the beach.

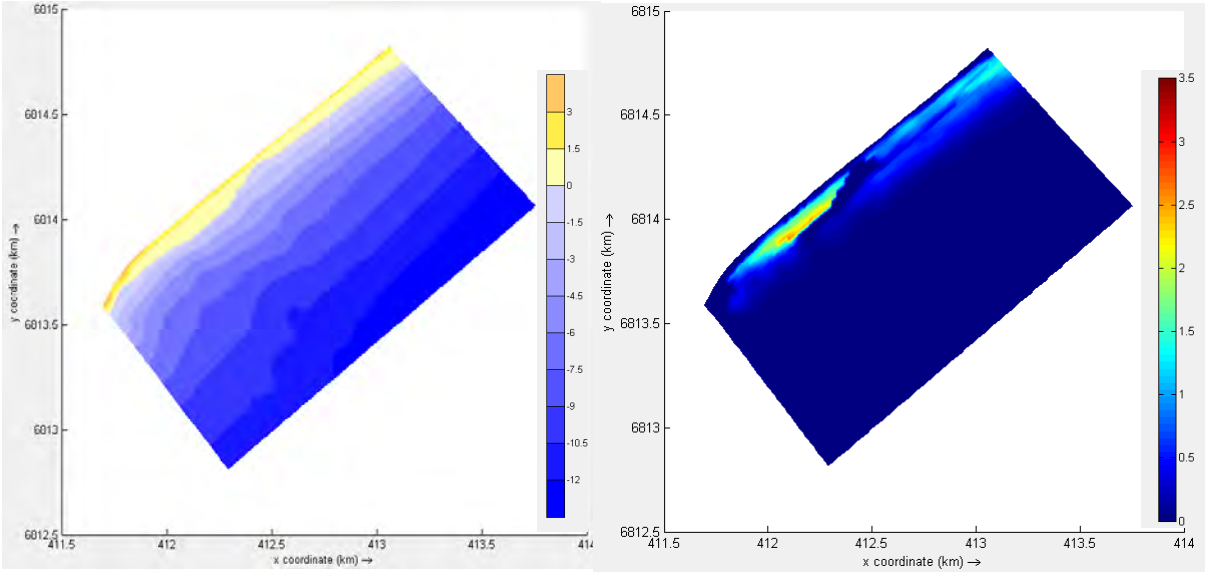

Figure 6.24: Results from the bimonthly nourishment after 1 year. a) Bathymetry (m MSL). b) Change in bathymetry relative to initial bathymetry (m).

There is little change in beach width along Alkantstrand beach between 9 months and 1 year. At the end of the morphological year, the bimonthly nourishment scheme resulted in an overall increase of beach width by 50 m along Alkantstrand relative to the initial shoreline (Figure 6.25). There was also a net increase in beach width approximately 40 m along the northern beaches due to longshore transport of the nourished sediment.

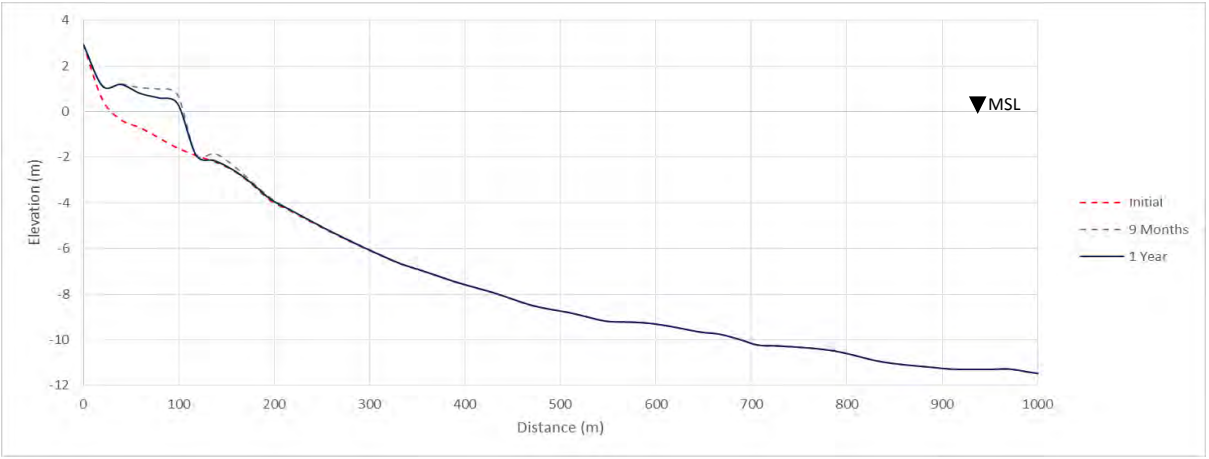

Figure 6.25: Cross sectional profile A-A after 1 year (Bimonthly nourishment scheme).

At the end of the bimonthly nourishment scheme, Table 6.12 shows 25% of the sand pumped onto the beach throughout the year remained within the model domain nourishing the main recreational

beach and the coastline north of Alkantstrand. 75% of the nourished sediment was lost through the northern boundary due to longshore transport.

Table 6.12: Nourished sediment distribution after 1 year (Bimonthly nourishment scheme).

Total percentage pumped (%)	Volume pumped (m^3)	Volume in model domain (m^3)	Volume lost through northern boundary (m^3)	Percentage lost through northern boundary (%)
100	1000000	253000	747000	75

6.6 Beach Response Analysis

Figure 6.26 shows the beach width increase after a year of nourishment for each beach nourishment scheme. The increase was recorded from the initial beach width at the beginning of the simulation starting directly alongside to the northern breakwater and extending 2km northwards along the coastline

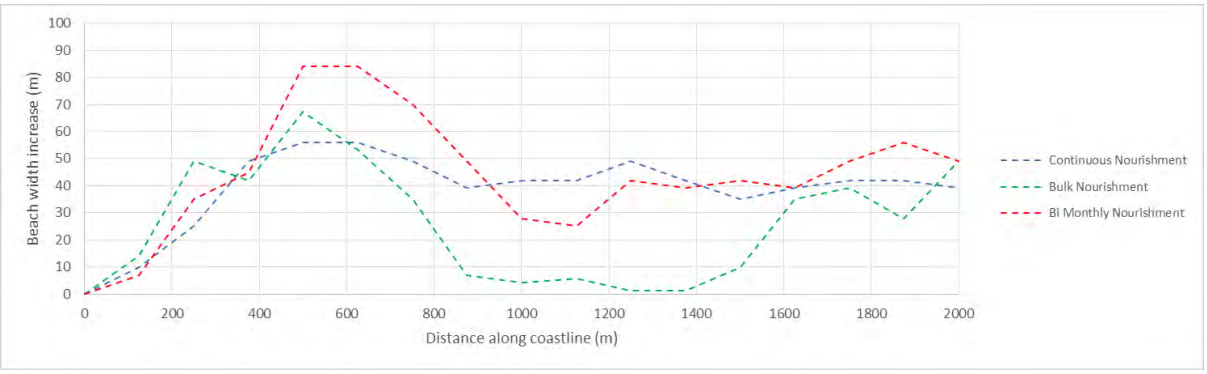

Figure 6.26: Modelled beach width increase due to beach nourishment schemes after one year.

The case study revealed that the predicted morphological evolution for the continuous and bimonthly nourishment schemes yield fairly similar results. For both schemes, the nourishment resulted in a net increase of beach width along the entire modelled coastline. The continuous nourishment scheme showed a uniform beach width increase of approximately 40m along the entire coastline. The bimonthly nourishment closely emulated a continuous nourishment scheme but small differences could be observed. The increase of beach width due to the continuous nourishment was uniform along the entire coastline (Figure 6.27a) and the bimonthly nourishment showed Alkantstrand experienced a greater beach width increase near the sediment discharge location than the northern beaches

(Figure 6.27b). The bimonthly nourishment showed a maximum beach width increase of 85m directly in front of the discharge pipeline. This peak reduces and shows a uniform increase of 40m along the northern beaches similar to the continuous nourishment. This was due to the sediment being dumped rapidly at intervals and took time for the longshore transport to move the dumped sediment from the recreational beach up the coast.

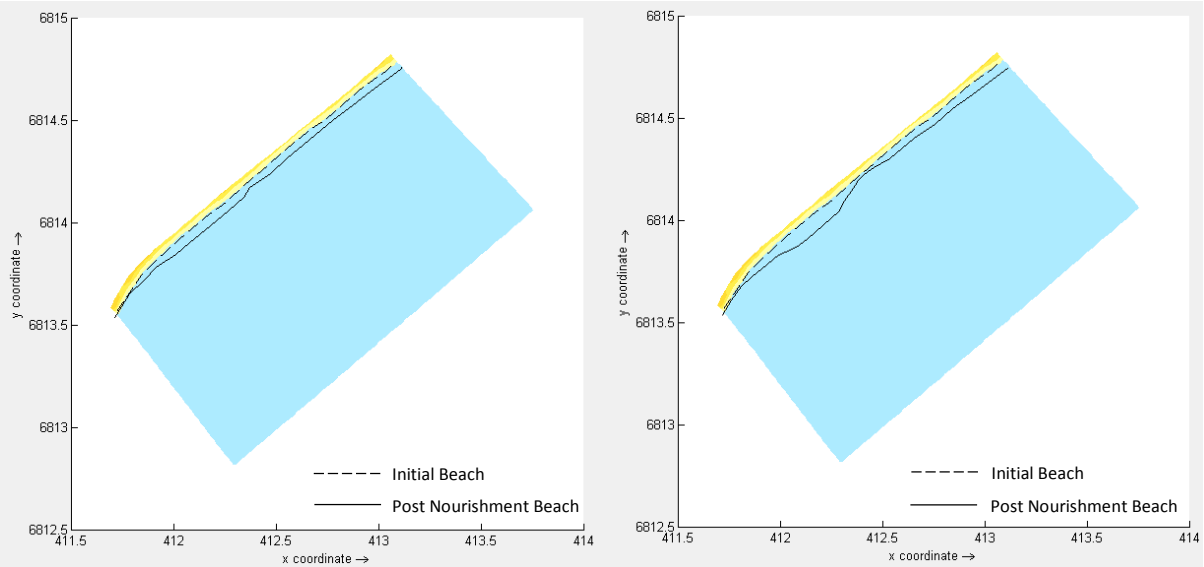

Figure 6.27: a) Beach width change after 1 year due to continuous nourishment. b) Beach width change after 1 year due to bimonthly nourishment (dashed line represents initial beach position and solid line represents beach position after 1 year).

The nourished sediment distribution for the bulk nourishment scheme was significantly different to both the continuous and bimonthly nourishment schemes. A majority of the nourished sediment that created an artificial sand island was transported up the coastline through the northern boundary after 1 year. Due to the sheltering effect of the harbour entrance, Alkantstrand was still sufficiently nourished at the end of the morphological year while the beaches north of the pipeline had almost returned to their initial sand starved state (Figure 6.28).

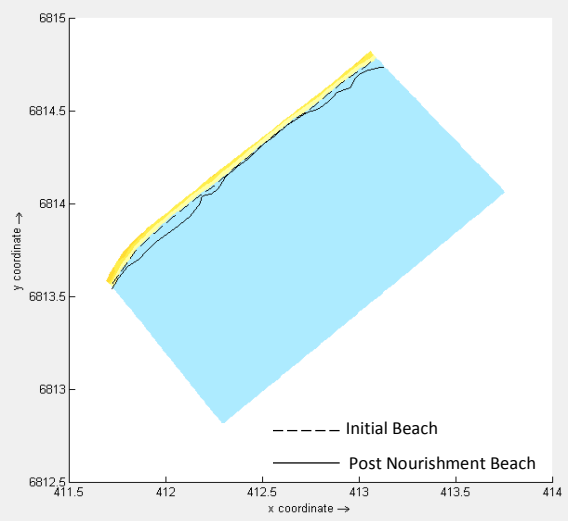

Figure 6.28: Beach width change after 1 year due to bulk nourishment (dashed line represents initial beach position and solid line represents beach position after 1 year).

Even though the bulk nourishment scheme did not uniformly nourish the entire modelled coastline as observed in the previous cases, the bulk nourishment did reduce coastal vulnerability and cause an overall increase of beach width along the main recreational beach (Figure 6.28). Therefore this scheme also was able to address the immediate problem concerning the loss of recreational beach width and coastal structure damage to the lifeguard tower just north of the harbour entrance.

Table 6.13 presents a summary of the sediment dumped onto the beach throughout the year for each scheme. It also shows how much of the sediment moved up the coastline and out of the lateral model boundaries. These results show that implementing a continuous bypass scheme moving 1 Mm^3 of sediment per annum would result in Alkantstrand growing at a rate of approximately 27% per annum. This growth is due to the availability of sediment from the sand trap allowing 1 Mm^3 of sand to be added instead of the predicted average net longshore transport of 850 000 m^3 resulting in nourishment of the beach down-drift of the harbour entrance. Similarly, a bimonthly scheme would result in Alkantstrand growing 25% per annum. The bulk scheme would cause a growth of only 13% which would be focused immediately north of the harbour entrance (Figure 6.28).

Table 6.13: Summary of nourished distribution for three alternative bypass schemes

Bypass Scheme	Morphological Time	Total percentage pumped (%)	Volume pumped (m^3)	Volume in model domain (m^3)	Volume lost through northern boundary (m^3)
Continuous	3 Months	25	246600	198420	48180
	6 Months	50	500000	83600	416400
	9 Months	75	748000	200300	547700
	1 Year	100	1000000	265000	735000
Bulk	3 Months	90	900000	769100	130900
	6 Months	100	1000000	315700	684300
	9 Months	100	1000000	157800	842200
	1 Year	100	1000000	128700	871300
Bimonthly	3 Months	33	333300	264000	69300
	6 Months	50	500000	45500	454500
	9 Months	83	833300	221100	612200
	1 Year	100	1000000	253000	747000

6.7 Economic Considerations

The implementation of alternative nourishment schemes involves different dredging methods and infrastructure. These have an impact on the cost and viability of implementing a specific sediment bypass scheme. The following section discusses the economic considerations that should be investigated to determine the economic viability of implementing each beach nourishment scheme. It must be noted that this study does not consider the dredger for harbour maintenance operations and only considers the dredger in terms of implementing sediment bypass schemes.

6.7.1 Continuous Bypass Economic Considerations

There are two methods in which a continuous nourishment scheme could be implemented at the port of Richards Bay. The first would be to base a single dredger permanently in the port. The Isandlwana hopper dredger currently servicing the port of Richards Bay has a hopper capacity of 4300 m^3. The daily nourishment rate required for this scheme is only 2740 m^3 per day. This means that the current dredger would not be required to supply a full hopper load of dredged sediment per day. Due to the fact that the Isandlwana is required to service more ports than just Richards Bay and would not be used efficiently if based permanently in a single port, it would not be an economically viable option to keep the Isandlwana hopper dredger permanently in the port of Richards Bay.

A smaller more cost effective hopper dredger could be purchased with a smaller capacity with the sole purpose of operating constantly and maintaining a continuous sediment bypass scheme along the coast of Richards Bay. The second alternative to purchasing a second hopper dredger would be to construct a fixed pipeline dredger near the sand trap and a booster pump that pumps the sediment from the sand trap directly onto Alkantstrand via submerged pipelines. If a continuous nourishment scheme was implemented, a cost analysis comparing the purchase of a new hopper dredger to the cost of constructing a fixed pipeline dredger would need to be undertaken.

6.7.2 Bulk Bypass Economic Considerations

Regarding current infrastructure and nourishment capability, the bulk nourishment scheme is an economically viable sand bypass scheme. This is because no additional infrastructure or resources are needed to implement this scheme. A single dredger is able to service multiple ports including meeting the Richards Bay bypass volume requirements.

Regarding the capacity at which the current dredger can implement a bulk nourishment scheme, it would take 100 days for it to dump the required sediment onto the case study beach. Therefore, this scheme could be implemented at three ports with equivalent sediment nourishment requirements to the Richards Bay bypass within a year and still have a sufficient period of the year (approximately 60 days) available for repairs and maintenance to the dredger and inclement weather. Therefore maintenance and dredger repairs would not result in delays or compromise the bypass schemes. The travel costs associated with the dredger moving between the ports will also be low compared to a bimonthly scheme because the dredger would only be required to travel between the ports once a year.

The risk must be taken into account that the dredger may be needed at a different location in a case of emergency. Therefore unforeseen events such as flooding and storms may result in the disruption of a bulk nourishment scheme. Theoretically, the Isandlwana can efficiently undertake a bulk nourishment scheme which would service multiple ports but realistically a smaller capacity hopper dredger may be required to undertake emergency dredging projects not scheduled in the bulk bypass scheme.

6.7.3 Bimonthly Bypass Considerations

The bimonthly scheme requires the dredger to be in the port of Richards bay for only 17 days every two months. A bimonthly nourishment emulates a continuous nourishment performance resulting in a uniformly nourished coastline and it is possible for a single dredger to service multiple ports by operating on a bimonthly cycle. Based on the dredging and dumping time as well as the travel time between ports, it is possible that using this scheme, the current Isandlwana dredger would be able to successfully service the ports of Richards Bay, Durban and Port Elizabeth.

However, economic considerations relating to the increased travel costs associated with this scheme need to be taken into account. This nourishment scheme will require the dredger to travel between the three ports on a bimonthly basis (six annual trips between the ports) which will significantly increase both travel and maintenance costs compared to the bulk nourishment scheme. Due to the dredger being required to constantly move between ports to keep up with the required sediment bypass volumes, it must be noted that this scheme does not allow long periods during the year for the dredger to be idle. This means that if the dredger experiences technical problems or has to undergo maintenance where it is unable to dredge for an extended period of time, the bimonthly nourishment scheme cannot be successfully maintained.

6.7.4 Summation of Economic Considerations

Table 6.14 presents a summary of aspects that influence the viability of implementing a specific sediment bypass scheme as discussed above. It must be noted that economics is a major factor and it is important to identify these factors but this dissertation does not quantify them. Further cost analysing should be undertaken as further research to provide an accurate cost comparison of the alternative bypass schemes.

Table 6.14: Summary of economic considerations associated with alternative bypass schemes.

Bypass Scheme	Additional infrastructure required	Long distance travel between ports
Continuous	• Purchase new smaller capacity dredger to be permanently stationed at port. or • Construction of a fixed bypass pipeline and booster pump.	Negligible
Bulk	• Can be implemented using current infrastructure and bypass capabilities.	Approximately 1750 km per annum (1 trip between ports per annum)
Bimonthly	• Can be implemented using current infrastructure and bypass capabilities. • In reality an additional backup dredger may be required in the event of an emergency.	Approximately 10500 km per annum (Travels between ports every 2 months)

6.8 Environmental Analysis Considerations

Although sediment bypass schemes are put in place to mitigate the effects breakwaters have on longshore transport, there are environmental implications associated with these schemes. This includes the implementation of the bypass schemes as well as their effect on the beaches down-drift of the coastal structures. Two of the main factors that required consideration when analysing the environmental impact of alternative bypass schemes are carbon emissions from the dredger and the effect of the bypass on the ecosystem. Eisted et al. (2009) predicts that a hopper dredger the weight of the Isandlwana will produce an average carbon emission of 16 gCO_2/tonne-km when travelling long distances and is used in the following section to quantify the carbon emissions produced due to the dredger travelling between ports.

6.8.1 Continuous Bypass Environmental Impact Considerations

With regard to implementing the nourishment scheme, it will be dependent on whether the continuous nourishment will be done by a small hopper dredger permanently situated at the port or if a fixed pump dredger is constructed near the sand trap where the sediment is taken from for the nourishment scheme. A dredger based permanently in the port of Richards Bay would not have a significant impact on the environment regarding carbon emissions compared to a case where it had to travel long distances between many ports. However the economic implications of a dredger servicing just one port may not be viable as discussed above. The other option of constructing a dredger pump south of the harbour entrance near the sand trap where the sediment accumulates may introduce additional environmental concerns. The construction of this additional infrastructure may have negative environmental impacts as carbon emissions would arise during the construction process and the construction may disrupt natural ecosystems along the coastline south of the harbour entrance.

The purpose of a bypass nourishment scheme is to negate or mitigate the effect anthropogenic coastal structures have on the disruption of longshore transport along the coastline. In this regard, the continuous nourishment scheme is an effective nourishment scheme that emulates a natural longshore transport as if there were no disruption to the sediment moving northwards. After a year of continuous nourishment the entire beach was in a state of accretion and increased in beach width. It must be considered that a continuous nourishment scheme would result in a constant sediment plume and constant sediment in suspension near the discharge area and main recreational beach. Even though the beach is being effectively nourished, the water visibility and quality along Alkantstrand will be poor throughout the year as the dumped sediment will not have time to settle. The sediment plumes created by this scheme would be relatively small and not have a large impact on the sea life and ecosystem along the beach. It must also be noted that there would be safety risks posed to beach visitors due to the sediment being discharged onto the beach continuously through an outlet pipe. This may require the closure of the section of beach in the vicinity of the discharge over the pumping period, which would be the entire year for a continuous scheme.

6.8.2 Bulk Bypass Environmental Impact Considerations

Eisted et al's. (2009) carbon emission model predicts that for a round trip done by the Isandlwana between the ports of Richards Bay and Port Elizabeth, the carbon travel emissions as a result of

implementing a yearly bulk nourishment scheme would produce approximately 137 tonnes of CO_2/year. Therefore the operation of a bulk nourishment would have a low impact on the environment with regards to carbon emissions. It can be implemented with the infrastructure and dredger used to currently service the Richards Bay bypass scheme. Therefore this nourishment scheme involves no negative environmental implications associated with the construction of additional infrastructure such as a pipeline dredge. This scheme only requires the dredger to travel between the ports it services once a year.

A large scale bulk nourishment and the plume caused by it could have significant environmental impacts along the coastline. The rapid nourishment of 1 Mm^3 of sediment would result in the development of a large sand island near the discharge pipeline as seen in the above results. The bulk nourishment changes the shape of the coastline rapidly, therefore the existing ecosystem may be significantly affected as it does not have enough time to adapt to the rapid changes. Studies by Courtenay et al. (1980) reveal that rapid alterations to habitat as a result of beach nourishment have adverse effects on fish populations. This can also extend to other nearshore organisms such as crabs and coastal birds. The fine large sediment plumes caused by this nourishment can also lead to asphyxiating fish and other fauna along the Richards Bay coastline. The decomposition of the dead organisms would raise the hydrogen sulphide levels making it difficult for the ecosystem along the case study beach to revive (PIANC, 2010).

6.8.3 Bimonthly Bypass Environmental Impact Considerations

The carbon emissions produced from the dredging process would be similar to the bulk nourishment but the significant amount of travelling required for the dredger to implement a bimonthly nourishment scheme would have substantial negative impact on the environment. This scheme requires the dredger to travel between the ports it services up to six times a year. This would increase the carbon emissions produced by travelling from 137 tonnes of CO_2/year as predicted for the bulk nourishment scheme to 822 tonnes of CO_2/year.

The bimonthly nourishment also efficiently mitigates the disruption to the longshore transport caused by the harbour entrance. The smaller bulk nourishments that happen periodically over the year are dispersed along the coastline by the tide and wave energy resulting in the entire beach being significantly nourished. Fine sediment plumes would occur near the discharge pipeline but would not be present continuously. Further investigations would need to be done to determine whether

sediment plumes generated on a bimonthly basis would result in asphyxiating fish along the coast and other adverse effects on the ecosystem associated with a continuous beach nourishment scheme. Fish asphyxiation would be relatively unlikely in comparison to the bulk nourishment which can be considered as a benefit of the bimonthly scheme.

6.8.4 Summation of Carbon Emissions

The carbon emissions produced during the dredging process will be similar for all three schemes as the same volume of sediment is dredged and dumped per annum. The carbon emission difference arises due to the travelling of the dredger between the different ports during the year. Table 6.15 presents a summary of the carbon emissions produced by the hopper dredger travelling long distances between ports to implement a specific sediment bypass scheme:

Table 6.15: Summary of predicted carbon emissions produced by dredger travelling between ports.

Bypass Scheme	**Predicted carbon emissions due to travel (tonnes of CO_2/year)**
Continuous	-
Bulk	137
Bimonthly	822

CHAPTER 7

Conclusion

The over-arching aim of this research is to contribute to developing morphological modelling in a local South African context. Particularly with respect to applications concerning sustainable coastal management practices. The focus is on sediment bypass schemes and beach management through nourishment. To achieve this aim the research addressed two questions. The first investigated whether the depth averaged Delft3D morphological model was capable of reproducing an equilibrium profile over a long term simulation. This was achieved by investigating and calibrating three sediment transport models within Delft3D and testing their capability of reproducing offshore sediment transport during large wave conditions and onshore movement during smaller wave conditions. The second was achieved by numerically modelling alternative sand nourishment schemes along Alkantstrand which is currently in a sand starved state due to a lack of recent beach nourishment.

7.1 Cross-shore Sediment Model Calibration

The three sediment transport models tested were the van Rijn, Bijker_Bailard and the Soulsby-van Rijn that are incorporated within the Delft3D software. Accretion and erosion wave conditions were predicted using Kraus's (1992) empirical model and used to test the predicted cross-shore sediment movement relative to the selected wave and sediment parameters.

7.1.1 Capability Results

The calibration study revealed that for all three sediment transport models, a single set of fixed parameters could not reproduce a combination of offshore movement during large wave events and onshore movement during smaller wave events as is observed in reality.

The study further revealed that a single wave related transport factor governs the direction of cross-shore movement within the van Rijn model and is not influenced by wave height. It was possible to define a cross-shore suspended load factor (f_{sus} = 0.1) within the van Rijn transport model that balanced the onshore and offshore sediment transport.

The Bijker-Bailard model cross-shore sediment movement was strongly influenced by the wave asymmetry factor applied to the sediment transported in the direction of wave propagation. An increase in the wave asymmetry factor resulted in an increase of onshore transport.

The Soulsby-van Rijn model did not allow the calibration of any coefficients that directly influence the direction of cross-shore sediment transport and predicted only net offshore movement of sediment for both wave conditions. This result meant that the Soulsbly-van Rijn model would not be able to maintain an equilibrium profile and could only produce persistent beach erosion independent of wave height.

7.1.2 Delft3D Cross-shore Sediment Transport Recommendations

The following recommendations first discuss the capability of the tested depth averaged morphological models and advise how the current models can be calibrated. Secondly recommendations are given on further research and possible methods required to improve the cross-shore morphology predicted by the models.

7.1.2.1 Application of current depth averaged models

The van Rijn sediment transport model is recommended in terms of its current cross-shore sediment transport capability prediction. Even though it is unable to predict both offshore movement for large waves and onshore movement during smaller waves in a single long term simulation, it is possible to predict either an erosion or an accretion event by adjusting just the suspended wave related transport factor accordingly. To analyse only longshore transport and its influence on the coastal morphology the suspended wave related transport factor can be set to 0.1 which will result in no net offshore or onshore movement influencing the morphology. This setup was used for the case study model where longshore transport and a lack of sediment supply was the focus of the investigation. However, it must be noted that there is an interdependence between longshore and cross-shore transport and both need to predict accurate transports to accurately model coastal morphodynamic evolution.

7.1.2.2 Further research to improve cross-shore morphological modelling

One method to improve the depth averaged van Rijn model would be to vary the suspended wave related transport factor as a function of wave height. Therefore small wave conditions would require f_{sus} > 0.1 to reproduce accretion. Large wave conditions require a f_{sus} < 0.1 to reproduce beach erosion. Delft3D is open source software which can be modified to vary f_{sus} as a function of wave height. It must be noted that this approach would reproduce qualitative expected cross-shore transport directions related to wave heights. This would mean that for larger waves, the parameterised hydrodynamic undertow would be the dominant driver of sediment transport and for smaller waves the onshore near-bed orbital velocities would drive the onshore sediment transport. Therefore throughout the simulation, the suspended wave related transport factor can be made to vary as a function of wave height to reproduced accurate cross-shore sediment transport.

The depth averaged morphological models parametrize the three dimensional processes that occur within the water column in the surf zone. Therefore, to better capture the surf zone hydrodynamics that drive the sediment transport, it would be beneficial to investigate the cross-shore capability of three dimensional morphological models. Since a full 3D model captures the vertical structure of wave induced flows such as undertow instead of parameterizing them, it should predict the observed offshore movement during large waves and onshore movement during smaller waves. However, extensive calibration associated with 3D hydrodynamic models is required to accurately analyse the turbulence in the vertical water column as well as being computationally demanding and therefore impractical for long term morphodynamic simulations.

7.2 Beach Nourishment Case Study

After a one year simulation, the continuous beach nourishment of 2740 m^3/day resulted in a uniform beach width increase of approximately 40m along the entire case study beach. Therefore this nourishment scheme effectively mitigates the disruption of longshore transport due to the Richards Bay harbour entrance and recovers the beaches north of the entrance from their sand starved state.

The bimonthly nourishment scheme closely emulates the continuous nourishment scheme in terms of beach response. The significant difference between the two schemes is that the current dredging infrastructure can support a bimonthly nourishment scheme if implemented efficiently while a

continuous scheme would require either the construction of a new fixed bypass scheme or the purchase of a smaller capacity hopper dredge to be permanently stationed at the port.

The bulk nourishment scheme effectively nourishes the main recreational beach however the beaches that are unprotected by the sheltering effect of the harbour breakwater had almost returned to their initial sand starved state after 1 year. This bypass method could be a site specific solution to the coast of Richards Bay as it can operate using the current infrastructure and dredging capabilities of the port and addresses the immediate issue along the main recreational beach where erosion is causing damage to structures and tourism.

7.3 Recommendations

7.3.1 Sediment Bypass Scheme Recommendation

The bulk nourishment scheme would be more cost effective than the other schemes and an adequate solution to the Alkantstrand chronic beach erosion but would be a site specific solution to Richards Bay beaches where the coastal infrastructure is located directly north of the harbour breakwater. In general, coastal structures, wetlands and property may be located further down-drift of harbour entrances which would require a uniform beach width increase along the coastline. Therefore in terms of mitigating the longshore sediment disruption and uniformly nourishing the coastline from the breakwater northwards, a continuous or bimonthly beach nourishment is recommended.

Based on the current infrastructure and performance, a bimonthly beach nourishment scheme would be the most effective method of implementing a sediment bypass along the east coast of South Africa. It is a scheme that can be implemented without the additional costs of building new dredging infrastructure and provides a continuous nourishment of the entire beach down-drift of the harbour entrance.

In theory, the bimonthly scheme does not require the assistance of a second dredger to service multiple ports along the east coast of South Africa. In reality, the risk of a single dredger implementing this scheme is effectively high and would require a second smaller capacity hopper dredger. This second dredger would be required as a backup to avoid costly delays in the event of emergency repairs or maintenance to the main dredger Isandlwana.

7.3.2 Further Research Recommendations

This research is a relative comparison of alternative beach nourishment schemes over the period of a year and how the different schemes alter the beach response. In order to better understand and model the movement of sediment during a beach nourishment, physical monitoring of a beach nourishment should be done to compare with the modelled results and further calibrate the model.

This study could also be expanded by increasing the case study period and area. Over a longer period of years the bulk nourishment scheme may emulate a continuous nourishment on larger spatial and time scales. This is similar to how the bimonthly bulk nourishment emulated the continuous nourishment over the period of a year.

Conditions may not always allow the start of a dredging scheme to commence at the beginning of the year. Further research could be done concerning how the beach response changes with regard to sequencing. Temporal sequencing of reduced wave climates was investigated by Olij (2015) and can be applied to expand the sand bypass case study.

This research evaluates the performance of alternative schemes and only deals superficially with economic and environmental considerations associated with the different schemes. Further in depth research should be done regarding an economic analysis and environmental impact assessment for the three beach nourishment schemes.

REFERENCES

Ataei, S., Adjami, M., Lashteh Neshaei, M. A. & Haghighifar, M., 2014. *Classification of equilibrium beach profile in the Caspian Sea.* Iran, ICOPMAS.

Bailard, J. A., 1981. An Energetics Total Load Sediment Transport Model for Plane Sloping. *Journal of Geophysical Research ,* 86(11), p. 10938–10954..

Battjes, J. A., 1987. *Surf Similarity.* Hamburg, ASCE.

Battjies , J. A. & Janssen, J. P., 1978. *Energy loss and set-up due to breaking random waves.* Hamburg, Germany, Proceedings of 16th Conference on Coastal Engineering.

Bosboom, J. & Stive, M., 2012. *Coastal Dynamics 1.* 3rd ed. Delft: Delft University of Technology.

Bowen, A. J., 1969. The Generation of Long Shore Currents on a Plane Beach. *Marine Res.,* Volume 37, pp. 206-215.

Bruun, J., 1954. Coastal Erosion and the Developement of Beach Profiles. *U.S. Army Corps of Engineers, Beach Erosion Board,* Volume 54.

Bruun, P. & Willekes, G., 1992. Bypassing and Backpassing at Harbours, Navigation Channels and Tidal Entrances: Use of Shallow-water Hopper Dredges with Pump-out Capabilities. *Coastal Research,* 8(4), pp. 972-977.

Corbella, S. & Stertch, D., 2014. Directional wave spectra on the east coast of South Africa. *Journal of the South African Institution of Civil Engineering,* 56(3), pp. 53-64.

Corbella, S. & Stretch, D., 2012. Predicting coastal erosion trends using non-stationary statistics and process-based models. *Coastal Engineering,* Volume 70, pp. 40-49.

Corbella, S. & Stretch, D., 2012. Shoreline recovery fromstorms on the east coast of Southern Africa. *Natural Hazards and Earth System Science,* 12(1), pp. 11-22.

Corbella, S. & Stretch, D., 2012. The wave climate on the KwaZulu-Natal coast of South Africa. *South African Institution of Civil Engineering,* 54(2), pp. 45-54.

Corbella, S. & Stretch, D. D., 2012. The wave climate on the KwaZulu-Natal coast of South Africa. *South African Institute of Civil Engineering,* 54(2), pp. 45-54.

Courtenay, W. R., Hartig, B. C. & Loisel, G. R., 1980. *Ecological Evaluation of a Beach Nourishment Project, Hallandale, Florida,* s.l.: U.S. Army Corps of Engineers, Coastal Engineering Research Center.

Dean, R. & Dalrymple, R., 2004. *Coastal Processes with Engineering Applications.* . ed. Cambridge: The Press Syndicate of the University of Cambridge.

Dean, R. G., 1988. *Realistic Economic Benefits from Beach Nourishment.* Malaga, Spain, ASCE.

Dean, R. G., 2002. *Beach Nourishment, Theory and Practice.* 1 ed. Singapore: World Scientific Publishing.

Dean, R. G., Kriebel, D. L. & Walton, T. L., 2001. *Cross-shore Sediment Transport.* s.l.:U.S. Army Coastal and Hydraulics Laboratory.

Dingemans, M. W., Radder, A. C. & De Vriend, H. J., 1987. Computation of the driving forces of wave-induced currents. *Coastal Engineering,* Volume 11, pp. 539-563.

Eisted, R., Larsen, A. & Christensen, T., 2009. *Collection, transfer and transport of waste: accounting of greenhouse gases and global warming contribution,* Denmark: SAGE.

Inman, D. L. & Bagnold, R. A., 1963. *Littoral Processes in the Sea.* 3 ed. New York: Interscience.

IPCC, 1990. *Strategies for Adaptation to Sea Level Rise,* s.l.: Intergovernmental Panel on Climate Change.

Kamphuis, J. W., 1991. Alongshore Sediement Transport Rate. *Coastal Engineering,* 117(6), pp. 624-640.

Keulegan, G. H. & Krumbein, W. C., 1919. Stable Configuration of Bottom Slope in a Shallow Sea and its Bearing on Geological Processes. *Amrican Geophysical Union,* 60(6), pp. 855-861.

Komar, P. D. & Inman, D. L., 1970. Loingshore Sand Transport on Beaches. *Geophysics,* 75(30), pp. 5914-5927.

Kraus, N. C., 1992. *Engineering approaches to cross-shore sediment transport processes.* Venice, Italy, 23rd International Conference on Coastal Engineering.

Longuet-Higgins, M. S., 1970. Longshore Currents Generated by Obliquely Incident Sea Waves. *Geophys. Res.,* 75(33), pp. 6778-6801.

Mather, A. & Stretch, D. D., 2012. A Perspective on Sea Level Rise and Coastal Storm Surge from. *Water,* Volume 4, pp. 237-259.

Mulder, J. P. & Tonnon, P. K., 2011. *Sand Engine: Background and Design of a Mega-Nourishment Pilot in the Netherlands. Proceedings of the 32nd International Conference on Coastal Engineering.* Shanghai, China, ICCE.

Olij, D. J., 2015. *Wave climate reduction for medium term process based morphodynamic simulations,* Delft: Delft University of Technology.

Pattiaratchi, C., Olsson, D., Hetzel, Y. & Lowe, R., 2009. Continental Shelf Research. *Wave-driven circulation patterns in the lee of groynes,* Volume 29, pp. 1961-1964.

PIANC, 2010. *Dredging and port construction around coral reefs,* s.l.: EnviCom Working Group.

Ponce, V. M., 1989. *Engineering Hydrology, Principles and Practices.* New Jersey: Prentice Hall.

Roelvink, D. & Reniers, A., 2012. *A Guide to Modelling Coastal Morphology.* London: World Scientific Publishing.

Schoonees, J. S., 2000. Annual variation in the net longshore sediment transport rate. *Coastal Engineering,* 40(2), pp. 141-160.

Schoonees, J. S., 2000. Annual variation in the net lonhshore sediment transport rate. *Coastal Engineering,* Volume 40, pp. 141-160.

Schoonees, J. S. & Theron, A. K., 1993. Review of field data base fore longshore sediment transport. *Coastal Engineering,* Volume 19, pp. 1-25.

Soulsby, R. L., 1987. Calculating bottom orbital velocity beneath waves. *Coastal Engineering,* Volume 11, pp. 371-380.

Stronge, W. B., 1995. The Economics of Government Funding for Beach Nourishment Projects. *Shore and Beach,* 63(3), pp. 4-6.

Thomson, R., 1981. *Oceanography of the British Columbia Coast.* 1st ed. Ottawa: Department of Fisheries and Oceans.

Thornton, E. B., 1970. Variations of Longshore Current Across the Surf Zone. *Proc. 12th Intl. Conf. CoastalEng.,* pp. 291-308.

Trouw, K. et al., 2012. *Numerical modelling of hydrodynamics and sediment transport in the surf zone: A sensitivity analysis study with different types of numerical models.* Santander, Spain, Coastal Engineering.

U.S. Army Corps of Engineers, C. E. R. C., 1986. *Shoreline Protection Manual.* s.l.:s.n.

van Son, S. T., 2009. *Monitoring and modeling nearshore morphodynamic,* Deflt, Netherlands: TU Delft.

Walstra, D. J., Hoekstra, R., Tonnon , P. K. & Ruessink, B. G., 2013. Input reduction for long-term morphodynamic simulations in wave dominated coastal settings. *Coastal Engineering,* Volume 77, pp. 57-70.

Wright, J. et al., 1999. *Waves, Tides and Shallow-Water Processes.* 2nd ed. Oxford: Butterworth-Heinemann.

APPENDICES

APPENDIX A

DELFT3D – Sediment Transport Models

The following sediment transport model description has been extracted directly from the Delft3D-FLOW User Manual (2011).

A1. van Rijn Formula

Bed-load transport rate:

The magnitude and direction of the bed load transport are calculated using an approximation method:

$$|S_b| = 0.006\rho_s w_s D_{50} M^{0.5} M_e^{0.7} \quad \text{(A-1)}$$

where:

S_b bedload transport [kg/m/s]

M sediment mobility number due to waves and currents [-]

M_e excess sediment mobility number [-]

w_s particle settling velocity [m/s]

$$M = \frac{v_{eff}^2}{(s-1)gD_{50}} \quad \text{(A-2)}$$

$$M_e = \frac{(v_{eff}-v_{cr})^2}{(s-1)gD_{50}} \quad \text{(A-3)}$$

$$v_{eff} = \sqrt{v_R^2 + U_{on}^2} \quad \text{(A-3)}$$

In which:

v_{cr} critical depth averaged velocity for initiation of motion (based on a parameterisation of the Shields curve) [m/s]

v_R magnitude of an equivalent depth-averaged velocity computed from the velocity in the bottom computational layer, assuming a logarithmic velocity profile [m/s]

U_{on} near-bed peak orbital velocity [m/s] in onshore direction (in the direction on wave propagation) based on the significant wave height

The direction of the bedload transport vector is determined by two parts: part due to current ($S_{b,c}$) which acts in the direction of the near-bed current, and part due to waves ($S_{b,w}$) which acts in the direction of wave propagation:

$$S_{b,c} = \frac{S_b}{\sqrt{1+r^2+2|r|cos\varphi}} \quad \text{(A-4)}$$

$$|S_{b,w}| = r|S_{b,c}| \quad \text{(A-5)}$$

where:

$$r = \frac{(|U_{on}|-v_{cr})^3}{(|v_R|-v_{cr})^3} \quad \text{(A-6)}$$

$S_{b,w}$ = 0 if r < 0:01, $S_{b,c}$ = 0 if r > 100, and φ = angle between current and wave direction for which Van Rijn (2003) suggests a constant value of 90 degrees.

The wave-related suspended sediment transport is modelled using an approximation method:

$$S_{s,w} = f_{sus}\gamma U_A L_T \quad \text{(A-7)}$$

where:

$S_{s,w}$ wave-related suspended transport [kg/(ms)]

f_{sus} user-defined tuning parameter

γ phase lag coefficient (= 0.2)

U_A velocity asymmetry value [m/s] = $\frac{U_{on}^4-U_{off}^4}{U_{3n}^4-U_{off}^3}$

L_T suspended sediment load [kg/m2] = $0.007\rho_s D_{50} M_e$

The three separate transport modes are imposed separately. The direction of the bedload due to currents $S_{b,c}$ is assumed to be equal to the direction of the current, whereas the two wave related transport components $S_{b,w}$ and $S_{s,w}$ take on the wave propagation direction.

A2. Bijker Formula

The basic formulation of the sediment transport formula according to Bijker is given by:

$$S_b = bD_{50}\frac{q}{C}\sqrt{g}(1-\emptyset)\exp(A_r) \quad \text{(A-8)}$$

$$S_s = 1.83S_b(I_1 \ln\left(\frac{33h}{r_c}\right) + I_2) \quad \text{(A-9)}$$

where:

C Chezy coefficient (as specified in input of Delft3D-FLOW module)

h water depth

q flow velocity magnitude

Ø porosity

and:

$$A_r = \max(-50, \min(100, A_{ra})) \quad \text{(A-10)}$$

$$b = BD + \max(0, \min\left(1, \frac{(h_w/h)-C_d}{C_s-C_d}\right))(BS - BD) \quad \text{(A-11)}$$

$$I_1 = 0.216\frac{(\frac{r_c}{h})^{z-1}}{(1-\frac{r_c}{h})^z}\ \int_{r_c/h}^{1} \ln\ (\frac{1-y}{y})^z dy \quad \text{(A-12)}$$

$$I_2 = 0.216\frac{(\frac{r_c}{h})^{z-1}}{(1-\frac{r_c}{h})^z}\ \int_{r_c/h}^{1} \ln y\ (\frac{1-y}{y})^z dy \quad \text{(A-13)}$$

where:

BS Coefficient b for shallow water (default value 5)

BD Coefficient b for deep water (default value 2)

C_s Shallow water criterion (Hs=h) (default value 0.05)

C_d Deep water criterion (default value 0.4)

r_c Roughness height for currents [m]

and:

$$A_{ra} = \frac{-0.27\Delta D_{50} C^2}{\mu q^2 (1+0.5\left(\psi\frac{U_b}{q}\right)^2)} \quad \text{(A-14)}$$

$$\mu = \left(\frac{C}{18\ \log(\frac{12h}{D_{90}})}\right)^{1.5} \quad \text{(A-15)}$$

$$z = \frac{w}{\frac{0.41q\sqrt{g}}{C}\sqrt{1+0.5\left(\psi\frac{U_b}{q}\right)^2}} \quad \text{(A-16)}$$

$$U_b = \frac{wh_w}{2\sinh(k_w h)} \quad \text{(A-17)}$$

$$w = \frac{2\pi}{T} \quad \text{(A-18)}$$

$$\psi = C\sqrt{\frac{f_w}{2g}} \quad \text{(A-19)}$$

$$f_w = \exp(-5.977 + \frac{5.123}{a_0^{0.194}}) \quad \text{(A-20)}$$

$$a_0 = \max(2,\ \frac{U_b}{wr_c}) \quad \text{(A-21)}$$

where:

C Chezy coefficient (as specified in input of Delft3D-FLOW module)

h_w wave height (Hrms)

k_w wave number

T wave period computed by the waves model or specified by you as T user.

U_b wave velocity

w sediment fall velocity [m/s]

Δ relative density

Within the Bijker formula it is possible to include sediment transport in the wave direction due to wave asymmetry following the Bailard approach (1981).

$$S_{b,asymm}(t) = \frac{\rho c_f \varepsilon_b}{(\rho_s - \rho) g (1-\phi) \tan(\varphi)} |u(t)|^2 u(t) \quad \text{(A-22)}$$

$$S_{s,asymm}(t) = \frac{\rho c_f \varepsilon_s}{(\rho_s - \rho) g (1-\phi) \mathrm{w}} |u(t)|^3 u(t) \quad \text{(A-23)}$$

where:

$u(t)$ near bed velocity signal [m/s]

ρ density of water [kg/m3]

ρ_s density of the sediment [kg/m3]

c_f coefficient of the bottom shear stress [-] (constant value of 0.005)

ϕ porosity [-] (constant value of 0.4)

φ natural angle of repose [-] (constant value of tan φ = 0:63)

w sediment fall velocity [m/s]

ε_b efficiency factor of bedload transport [-] (constant value of 0.10)

ε_s efficiency factor of suspended transport [-] (constant value of 0.02

The (short wave) averaged sediment transport due to wave asymmetry, Equations A.22 and A.23, is determined by using the following averaging expressions of the near bed velocity signal (calibration coefficients included):

$$\langle u|u|^2 \rangle = A_{fac} \langle \tilde{u}|\tilde{u}|^2 \rangle + 3 U_{fac} \bar{u} \langle \tilde{u}^2 \rangle \quad \text{(A-24)}$$

$$\langle u|u|^3 \rangle = A_{fac} \langle \tilde{u}|\tilde{u}|^3 \rangle + 3 U_{fac} \bar{u} \langle \tilde{u}^3 \rangle \quad \text{(A-25)}$$

in which:

$\tilde{u}$ orbital velocity signal

u averaged flow velocity (due to tide, undertow, wind, etc.)

A_{fac} user-defined calibration coefficient for the wave asymmetry

U_{fac} user-defined calibration coefficient for the averaged flow

A3. Soulsby van Rijn Formula

The sediment transport is split into a bedload and suspended load fraction. The direction of the bedload transport is assumed to be equal to the direction of the depth-averaged velocity (u = cross-shore velocity and v = longshore velocity) in a 2D simulation.

$$S_{bx} = A_{cal} A_{sb} u \xi \quad \text{(A-26)}$$

$$S_{by} = A_{cal} A_{sb} v \xi \quad \text{(A-27)}$$

and the suspended transport magnitude is given by the following formula:

$$S_s = A_{cal} A_{ss} \xi \sqrt{u^2 + v^2} \quad \text{(A-28)}$$

where:

A_{cal} a user defined calibration scale factor

A_{sb} bed-load multiplication factor

$$A_{sb} = 0.05H \left(\frac{D_{50/H}}{\Delta g D_{50}} \right)^{1.2} \quad \text{(A-29)}$$

A_{ss} suspended load multiplication factor

$$A_{ss} = 0.012 D_{50} \frac{D_*^{-0.6}}{(\Delta g D_{50})^{1.2}} \quad \text{(A-30)}$$

ξ a general multiplication factor

$$\xi = \left(\sqrt{U^2 + \frac{0.018}{C_D} U_{rms}^2} - U_{cr} \right)^{2.4} \quad \text{(A-31)}$$

where U is the total depth-averaged velocity and C_D is the drag coefficient due to currents, defined by:

$$C_D = \left(\frac{\kappa}{\ln\left(\frac{H}{z_0}\right)-1}\right)^2 \tag{A-32}$$

The root-mean-square orbital velocity is computed as:

$$U_{rms} = \sqrt{2}\frac{\pi H_{rms}}{T_p \sinh(kH)} \tag{A-33}$$

$$D_* = \left(\frac{g\Delta}{\nu^2}\right)^{1/3} D_{50} \tag{A-34}$$

Using the critical bed shear velocity according to Van Rijn:

$$U_{cr} = \begin{cases} 0.19 D_{50}^{0.1} \log\left(\frac{4H}{D_{90}}\right) & if\ D_{50} < 0.5mm \\ 8.5 D_{50}^{0.6} \log\left(\frac{4H}{D_{90}}\right) & if\ 0.5mm < D_{50} < 2mm \end{cases} \tag{A-35}$$

APPENDIX B

Durban Profile Data

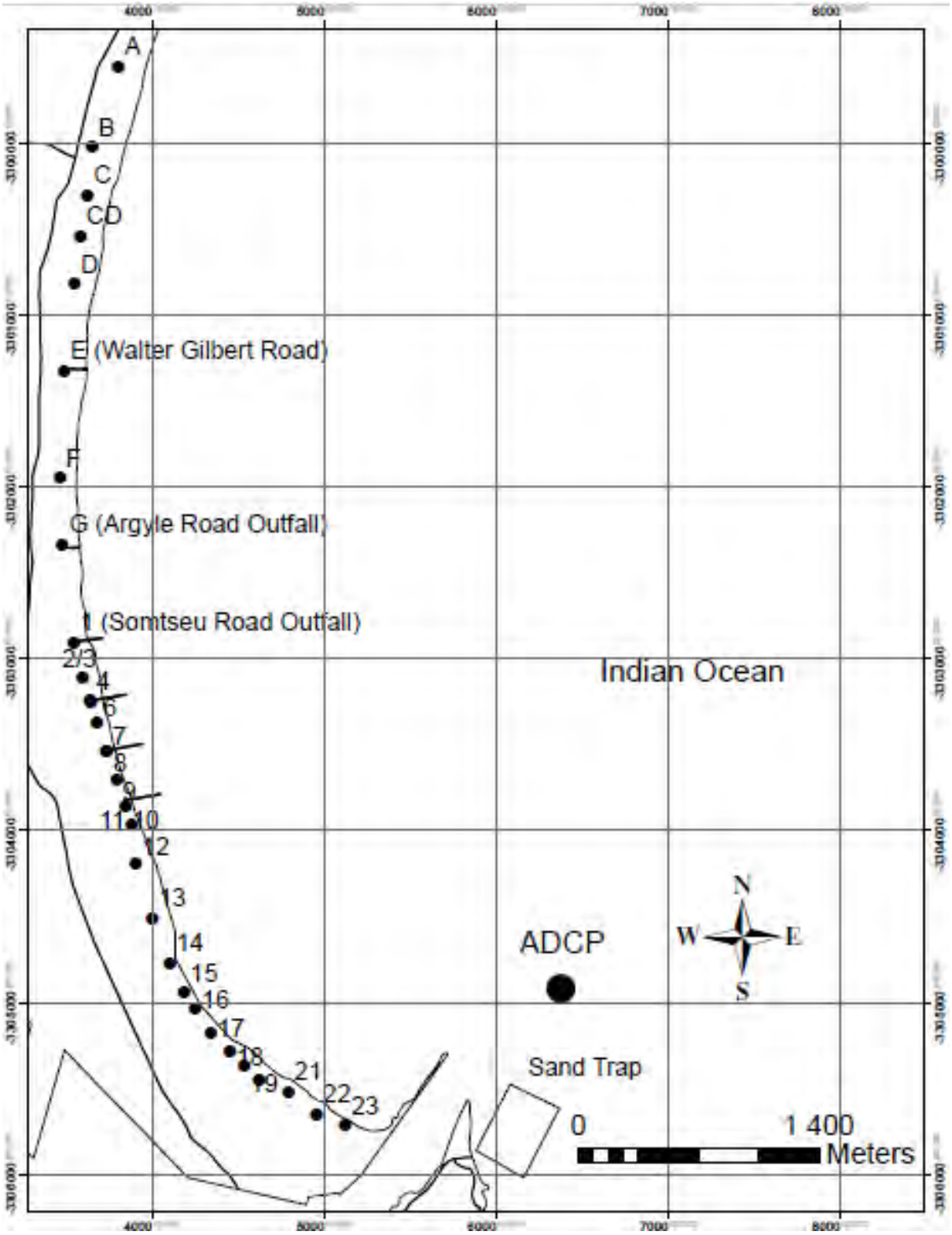

Figure B-1: Plan of survey station locations (Durban, South Africa).

APPENDIX C

Delft3D Sediment Transport Model Input Files

Cross-shore capability study sediment transport and morphology input files:

cross_shore_input.sed

```
[SedimentFileInformation]
  FileCreatedBy   = Delft3D FLOW-GUI, Version: 3.56.29165
 [SedimentOverall]
  Cref          =  1.6000000e+003     [kg/m3]
  IopSus        = 0
[Sediment]
  Name          = #Sediment_sand#
  SedTyp        = sand
  RhoSol        =  2.6500000e+003
  SedDia        =  3.5000000e-004     [m]
  CDryB         =  1.6000000e+003     [kg/m3]
  IniSedThick     =  4.0000000e+001     [m]
  FacDSS        =  1.0000000e+000
```

cross_shore_input.mor

```
[MorphologyFileInformation]
  FileCreatedBy   = Delft3D FLOW-GUI, Version: 3.56.29165
 [Morphology]
  EpsPar        = false
  IopKCW        = 1                   Flag for determining Rc and Rw
  RDC           = 0.01          [m]   Current related roughness height (only used if IopKCW <> 1)
  RDW           = 0.02          [m]   Wave related roughness height (only used if IopKCW <> 1)
  MorFac        =  1.0000000e+000     [-]   Morphological scale factor
  MorStt        =  1.8000000e+002     [min]   Spin-up interval from TStart till start of morphological
changes
  Thresh        =  9.0000000e-001     [m]   Threshold sediment thickness for transport and erosion
reduction
  MorUpd        = true                Update bathymetry during FLOW simulation
  EqmBc         = true                Equilibrium sand concentration profile at inflow boundaries
  DensIn        = false               Include effect of sediment concentration on fluid density
  AksFac        =  1.0000000e+000     [-]   van Rijn's reference height = AKSFAC * KS
  RWave         =  2.0000000e+000     [-]   Wave related roughness = RWAVE * estimated ripple
height. Van Rijn Recommends range 1-3
  AlfaBs        =  1.0000000e+000     [-]   Streamwise bed gradient factor for bed load transport
  AlfaBn        =  1.5000000e+000     [-]   Transverse bed gradient factor for bed load transport
  Sus           =  1.0000000e+000     [-]   Multiplication factor for suspended sediment reference
concentration
  Bed           =  1.0000000e+000     [-]   Multiplication factor for bed-load transport vector
magnitude
  SusW          =  3.0000000e-001     [-]   Wave-related suspended sed. transport factor
  BedW          =  1.0000000e-001     [-]   Wave-related bed-load sed. transport factor
  SedThr        =  1.0000000e-001     [m]   Minimum water depth for sediment computations
  ThetSD        =  1.0000000e-001     [-]   Factor for erosion of adjacent dry cells
  HMaxTH        =  1.5000000e+000     [m]   Max depth for variable THETSD. Set < SEDTHR to use
global value only
  FWFac         =  1.0000000e+000     [-]   Vertical mixing distribution according to van Rijn
(overrules k-epsilon model)
  NeuBcSand     = TRUE
```

Nourishment case study sediment transport and morphology input files:

nourishment_sand.sed

```
[SedimentFileInformation]
  FileCreatedBy    = Delft3D FLOW-GUI, Version: 3.56.29165
 [SedimentOverall]
  Cref          =  1.6000000e+003     [kg/m3]
  IopSus        = 0
[Sediment]
  Name          = #Sediment_sand#
  SedTyp        = sand
  RhoSol        =  2.6500000e+003     [kg/m3]
  SedDia        =  3.5000000e-004     [m]
  CDryB         =  1.6000000e+003     [kg/m3]
  IniSedThick     = 4.0000000e+000     [m]
  FacDSS        =  1.0000000e+000     [-]
```

nourishment_sand.mor

```
[MorphologyFileInformation]
  FileCreatedBy    = Delft3D FLOW-GUI, Version: 3.56.29165
  [Morphology]
  EpsPar        = false
  IopKCW         = 1                    Flag for determining Rc and Rw
  RDC           = 0.01            [m]    Current related roughness height (only used if IopKCW <> 1)
  RDW           = 0.02            [m]    Wave related roughness height (only used if IopKCW <> 1)
  MorFac         =  2.6000000e+001     [-]    Morphological scale factor
  MorStt         =  6.0000000e+001     [min]   Spin-up interval from TStart till start of morphological
changes
  Thresh         =  9.0000000e-001     [m]    Threshold sediment thickness for transport and erosion
reduction
  MorUpd          = true                 Update bathymetry during FLOW simulation
  EqmBc          = true                 Equilibrium sand concentration profile at inflow boundaries
  DensIn         = false                Include effect of sediment concentration on fluid density
  AksFac         =  1.0000000e+000     [-]    van Rijn's reference height = AKSFAC * KS
  RWave          =  2.0000000e+000     [-]    Wave related roughness = RWAVE * estimated ripple
height. Van Rijn Recommends range 1-3
  AlfaBs         = 1.0000000e+000     [-]    Streamwise bed gradient factor for bed load transport
  AlfaBn         = 1.5000000e+000     [-]    Transverse bed gradient factor for bed load transport
  Sus           = 1.0000000e+000     [-]    Multiplication factor for suspended sediment reference
concentration
  Bed           = 1.0000000e+000     [-]    Multiplication factor for bed-load transport vector
magnitude
  SusW          = 1.0000000e-001     [-]    Wave-related suspended sed. transport factor
  BedW          = 1.0000000e-001     [-]    Wave-related bed-load sed. transport factor
  SedThr         =  1.0000000e-001     [m]    Minimum water depth for sediment computations
  ThetSD         =  1.0000000e-001     [-]    Factor for erosion of adjacent dry cells
  HMaxTH          = 1.5000000e+000     [m]    Max depth for variable THETSD. Set < SEDTHR to use
global value only
  FWFac          = 1.0000000e+000     [-]    Vertical mixing distribution according to van Rijn
(overrules k-epsilon model)
  NeuBcSand       = TRUE
```

Nourishment case study nourishment input files:

monthly_nourishment.dad

```
[DredgeFileInformation]
[General]
  PolygonFile = dadareas.pol
  TimeSeries = Dump.ddt
  DredgeDistr = 1
  DumpDistr = 1
  DumpWhenDry = false
  DredgeWhenDry = true
[Nourishment]
  Name = Dump
  Volume = 1000000
  MaxVolRate = 1000000
  Sediment = Sediment_sand
  SedPercentage = 100
  Dump = Dump 001
  Percentage = 100
```

bulk_nourishment.dad

```
[DredgeFileInformation]
 [General]
  PolygonFile = dadareas.pol
  TimeSeries = Dump.ddt
  DredgeDistr = 1   DumpDistr = 1
  DumpWhenDry = false
  DredgeWhenDry = true
[Nourishment]
  Name = Dump
  Volume = 1000000

  MaxVolRate = 3650000
  Sediment = Sediment_sand
  SedPercentage = 100
  Dump = Dump 001
  Percentage = 100
```

bimonthly_nourishment.dad

```
[DredgeFileInformation]
[General]
  PolygonFile = dadareas.pol
  TimeSeries = Dump.ddt
  DredgeDistr = 1   DumpDistr = 1
  DumpWhenDry = false
  DredgeWhenDry = true
[Nourishment]
  Name = Dump
  Volume = 1000000
  MaxVolRate = 3650000
  Sediment = Sediment_sand
  SedPercentage = 100
  Dump = Dump 001
```

APPENDIX D

Case Study Model Setup and Calibration

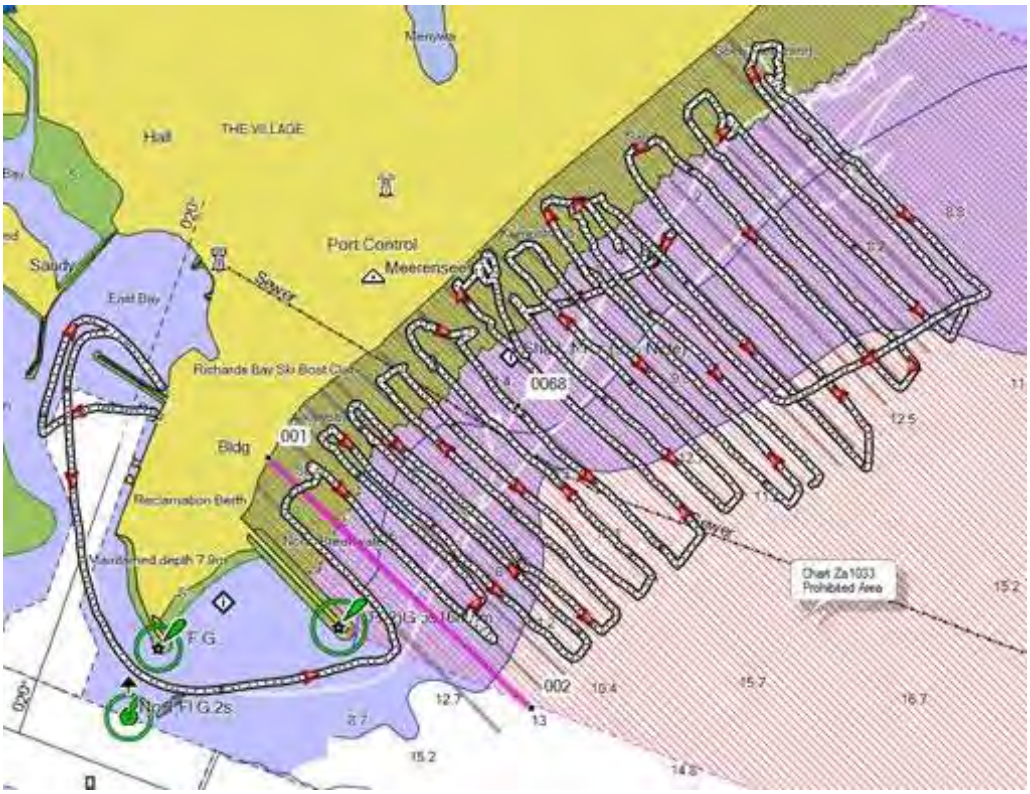

Figure D-1: Path travelled during bathymetric survey (09/07/2015).

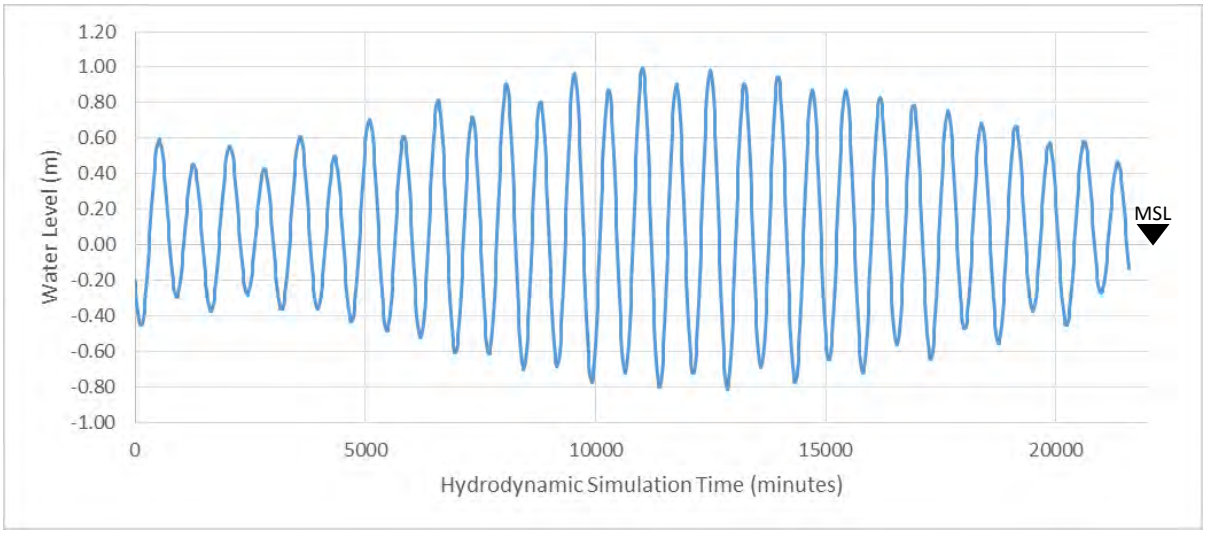

Figure D-2: Tidal level imposed on eastern sea boundary during case study hydrodynamic simulation.

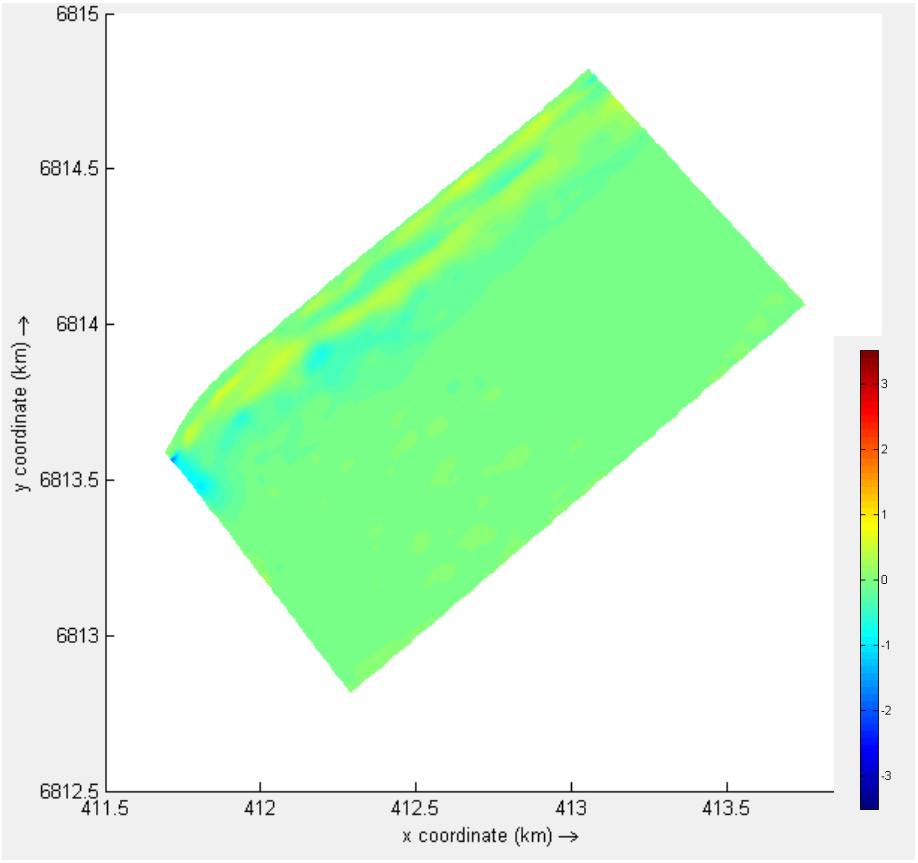

Figure D-3: Annual cross-shore cumulative sedimentation and erosion (m) predicted during case study model calibration (van Rijn model).

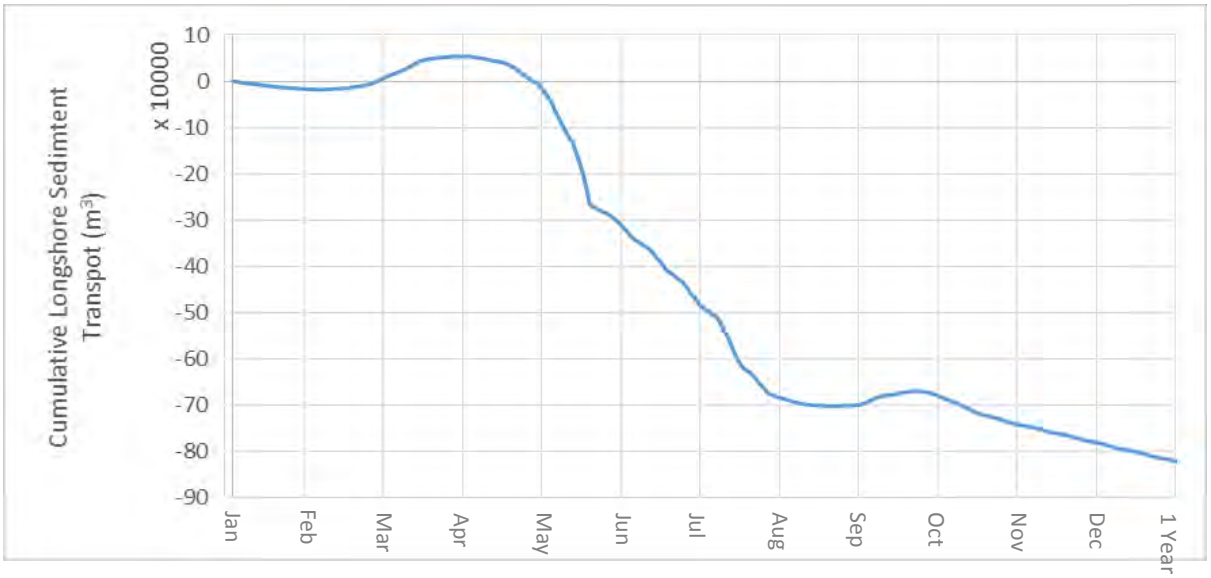

Figure D-4: Annual longshore sediment transport predicted during case study model calibration (van Rijn model).